

**Rietveld method and texture, microstructure,
stresses, phase, structure, reflectivity...
Combined Analysis**

Daniel Chateigner
IUT-Univ. Caen Basse-Normandie
CRISMAT-ENSICAEN (Caen-France)

The Rietveld method: XN-Ray Workshop, Aachen, 26th – 30th Sept. 2011

Structure determination on real (textured) samples

Dilemma 1

Structure and QTA: correlations: $f(g)$ and $|F_h|^2$ are different !

$f(g)$:

- Angularly constrained: $[h_1k_1l_1]^*$ and $[h_2k_2l_2]^*$ make a given angle: more determined if F^2 high
- lot of data (spectra) needed

$|F_h|^2$:

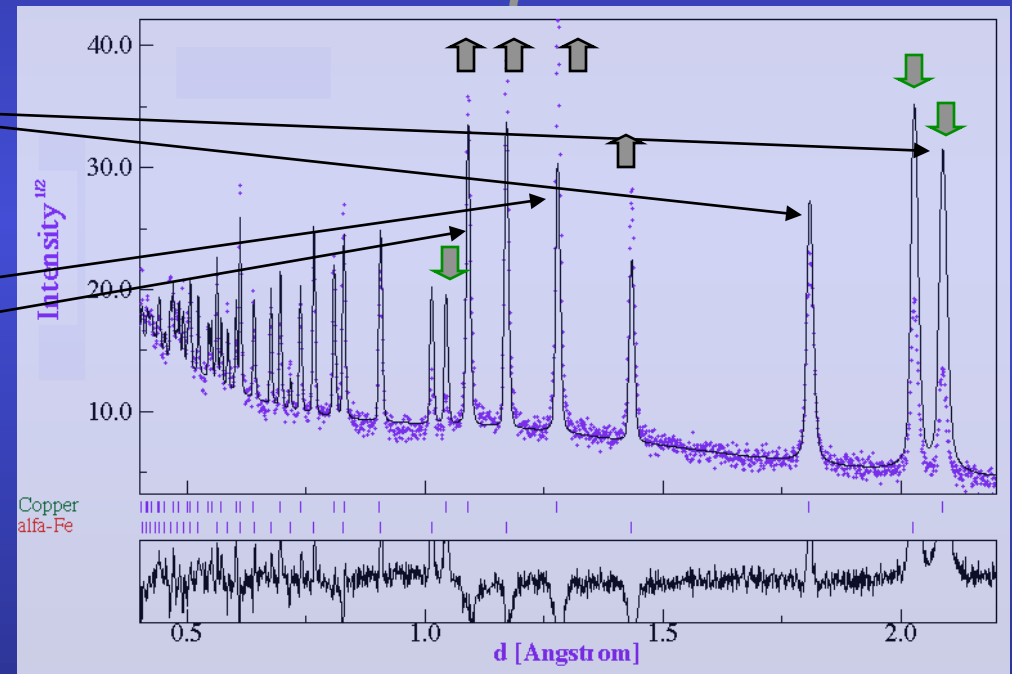
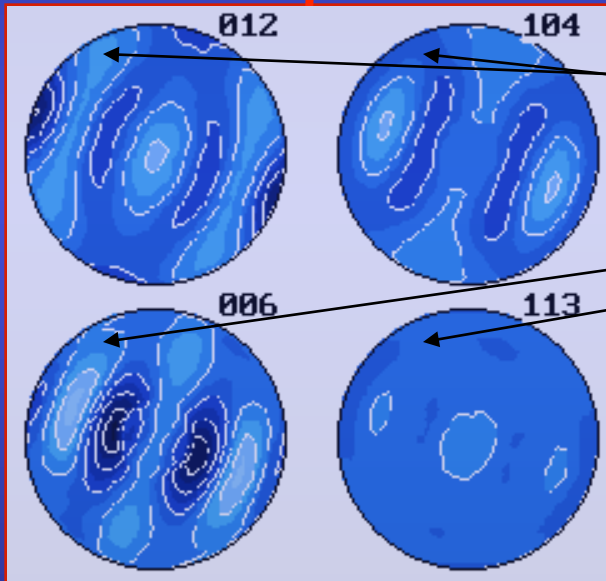
- Position, f_i , and Debye-Waller constrained
- work on the sum of all diagrams on average

Texture from Spectra

Orientation Distribution Function (ODF)

From pole figures

From spectra



Le Bail extraction + ODF: WMV, E-WIMV, Generalized spherical harmonics, components, ADC, entropy maximisation ...

Why not benefit of texture in Structure determination ?

Perfect powders:

- overlaps (intra- and inter- τ)
- no angular constrain
- anisotropy difficult to resc

Single pattern

Single crystals:

- reduced overlaps
 - max angular constrains
- Perfect texture: max anisotropy

Many individual diffracted peaks

Textured powders:

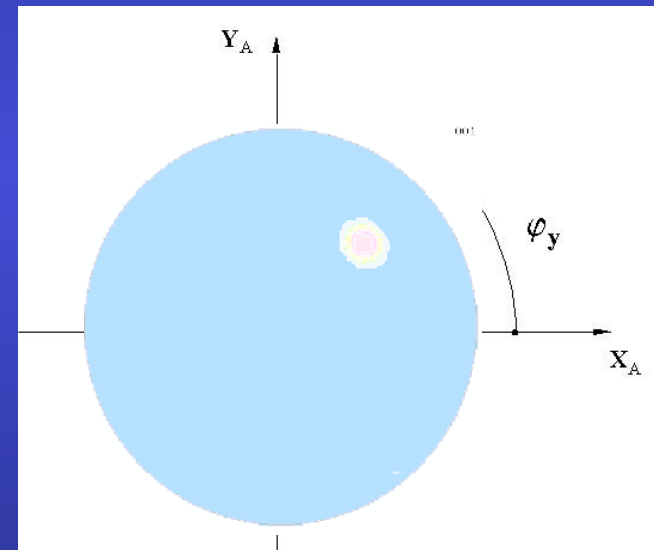
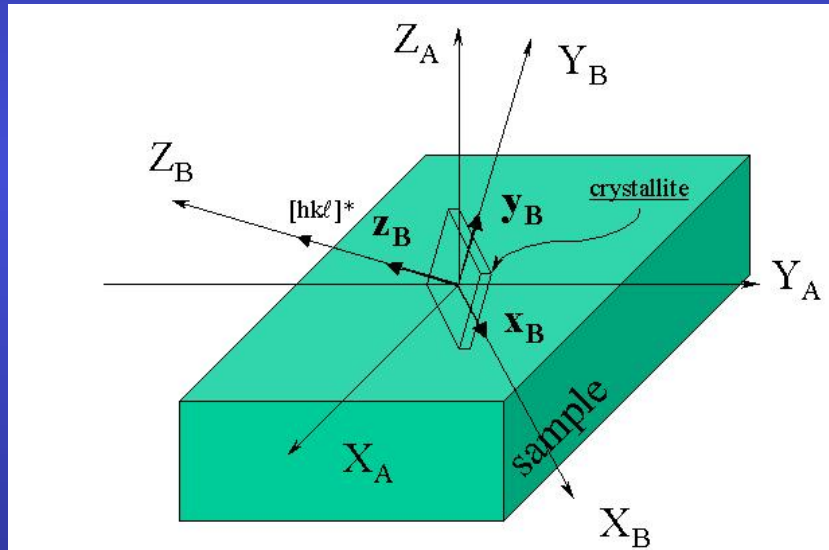
- reduced overlaps
- angular constrain = $f(\text{texture strength})$
- Intermediate anisotropy

Many patterns to measure and analyse

Pole figures

$\{hkl\}$ -Pole figure: location of distribution densities, for the $\{hkl\}$ diffracting plane, defined in the crystallite frame K_B , relative to the sample frame K_A .

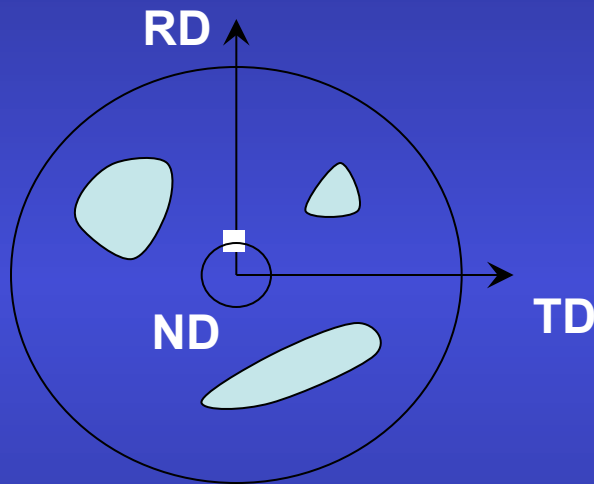
Pole figures space: \mathbb{S}^2 , with $\mathbf{y} = (\vartheta_y, \varphi_y) = [hkl]^*$



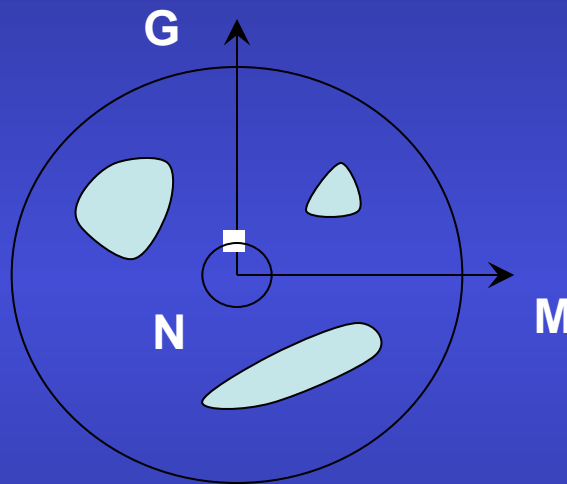
Direct Pole Figure: built on diffracted intensities $I_h(\mathbf{y})$, $\mathbf{h} = \langle hkl \rangle^*$
Normalised Pole Figure: built on distribution densities $P_h(\mathbf{y})$

Density unit: the "multiple of a random distribution", or "m.r.d."

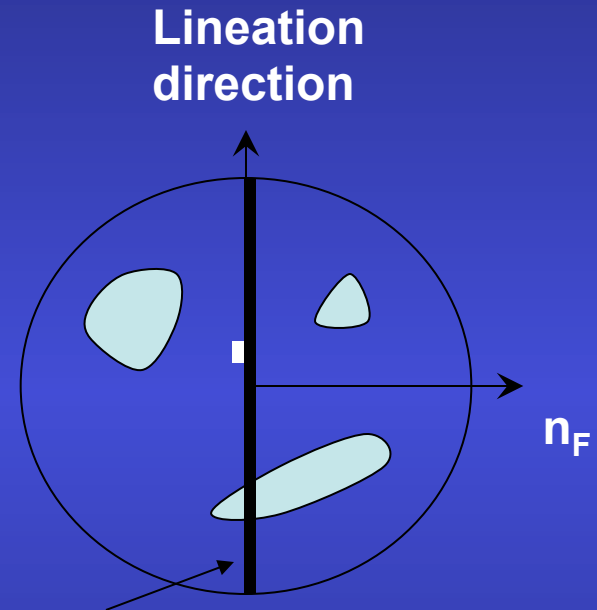
Usual pole figure frames K_A



metallurgy



malacology

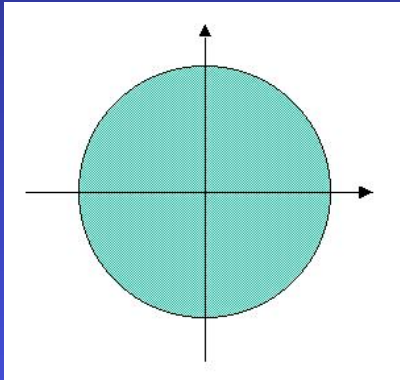


geophysics

Thin films: substrate directions ...

X_A, Y_A, Z_A

Texture types

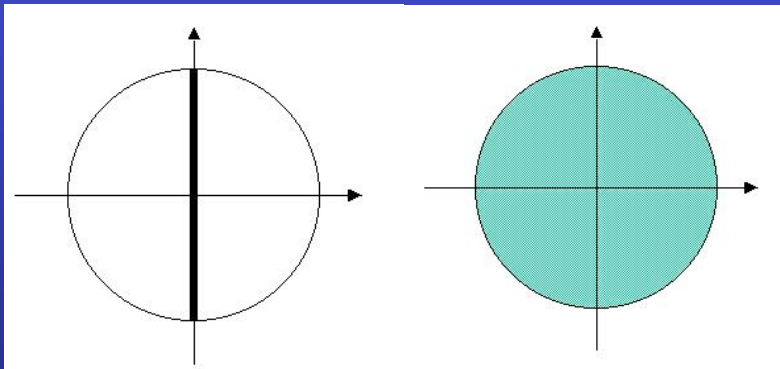


Random texture

3 degrees of freedom

All $P_h(\mathbf{y})$ homogeneous

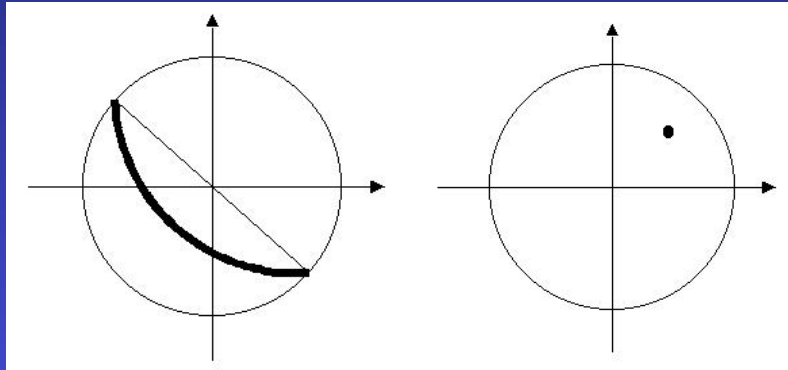
1 m.r.d. density whatever \mathbf{y}



Planar texture

2 degrees of freedom

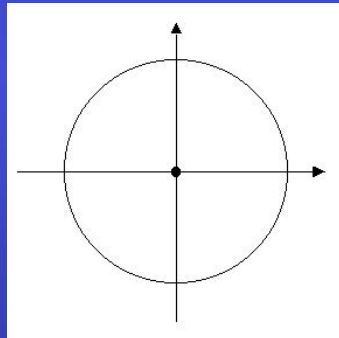
1 $[hkl]$ at random in a plane



Fibre texture

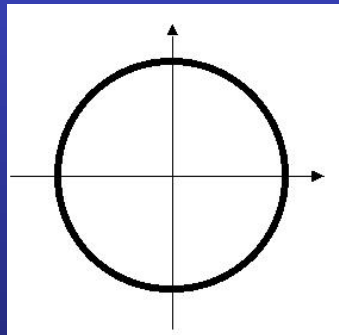
1 degree of freedom

1 $[hkl]$ along 1 y direction



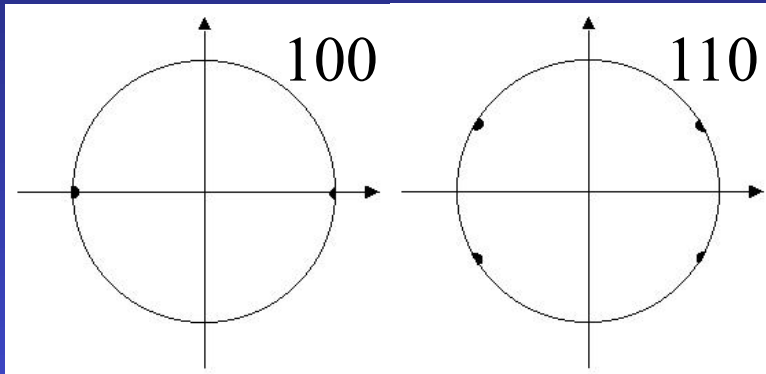
Cyclic-Fibre texture

$$\mathbf{c} // Z_A$$



Cyclic-Planar texture

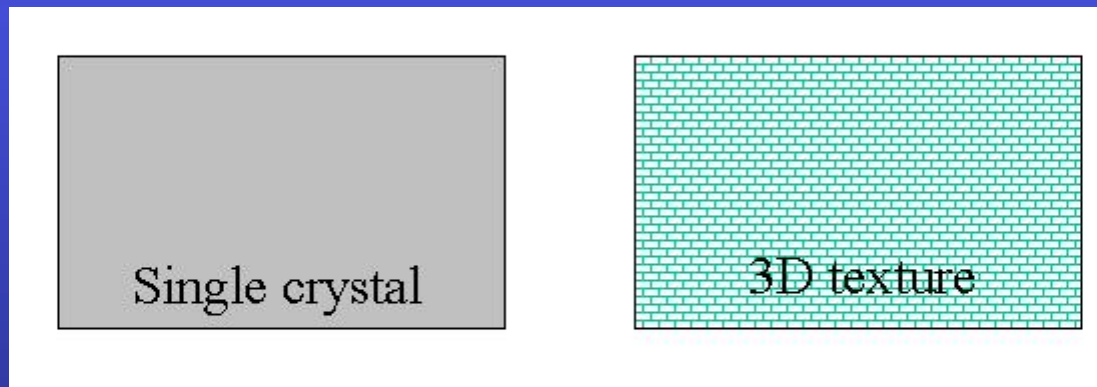
$$\mathbf{c} // (X_A, Y_A)$$



Single crystal-like texture

0 degree of freedom

2 $[hkl]$'s along 2 y directions



Single-crystal and perfect 3D orientation not distinguished

Pole figure and Orientation spaces

Pole figure expression:

$$\frac{dV(\mathbf{y})}{V} = \frac{1}{4\pi} P_h(\mathbf{y}) d\mathbf{y}$$

$$d\mathbf{y} = \sin\vartheta_y d\vartheta_y d\varphi_y$$

$$\int_{\varphi_y=0}^{2\pi} \int_{\vartheta_y=0}^{\pi/2} P_h(\vartheta_y, \varphi_y) \sin\vartheta_y d\vartheta_y d\varphi_y = 4\pi$$

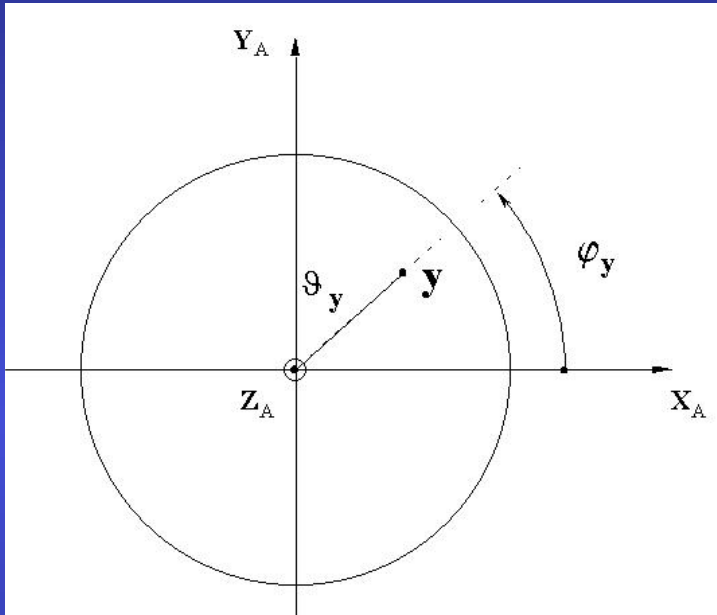
Orientation Distribution Function $f(\mathbf{g})$:

$$\frac{dV(\mathbf{g})}{V} = \frac{1}{8\pi^2} f(\mathbf{g}) d\mathbf{g}$$

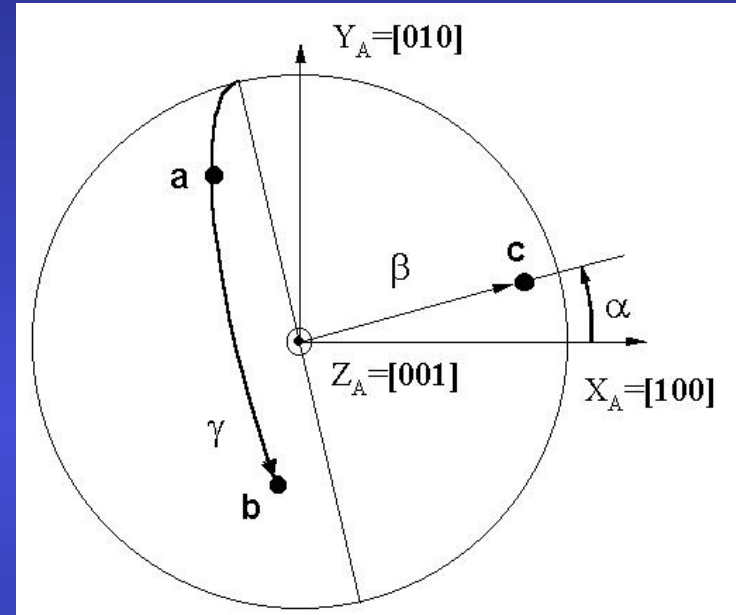
$$d\mathbf{g} = \sin(\beta) d\beta d\alpha d\gamma$$

$$\int_{\alpha=0}^{2\pi} \int_{\beta=0}^{\pi/2} \int_{\gamma=0}^{2\pi} f(\mathbf{g}) d\mathbf{g} = 8\pi^2$$

From Pole figures to the ODF



Pole figure: one direction fixed in K_A



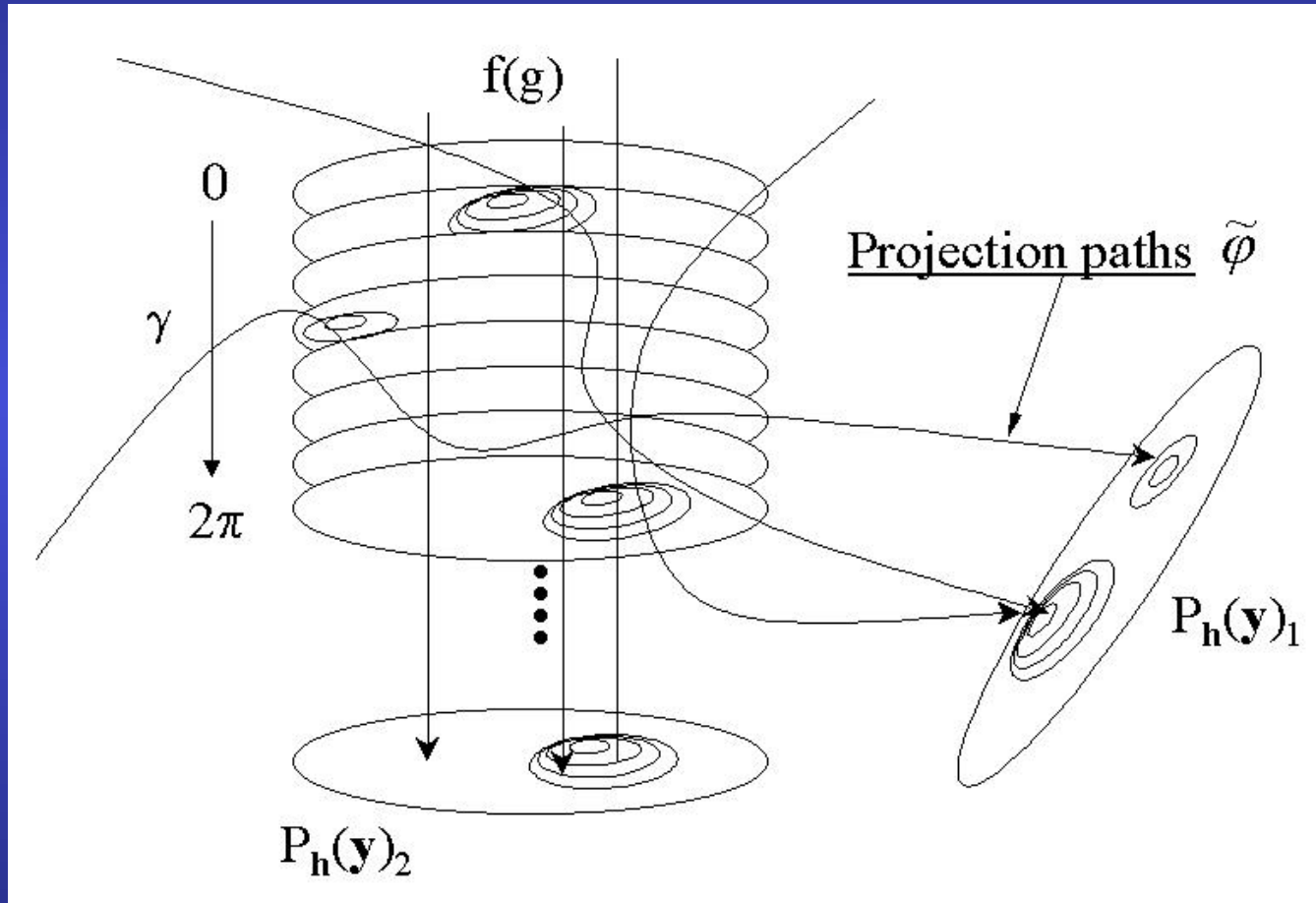
Orientation: two directions fixed in K_A

Fundamental Equation of QTA

$$P_h(\mathbf{y}) = \frac{1}{2\pi} \int_{h//y} f(\mathbf{g}) d\tilde{\varphi}$$

Needs several pole figures to construct $f(\mathbf{g})$

From $f(g)$ to the pole figures



Rietveld-Structure

$$I_i^{\text{calc}}(\chi, \phi) = \sum_{n=1}^{\text{Nphases}} S_n \sum_k L_k |F_{k;n}|^2 S(2\theta_i - 2\theta_{k;n}) P_{k;n}(\chi, \phi) A + bkg_i$$

Texture

$$P_k(\chi, \phi) = \int_{\varphi} f(g, \varphi) d\varphi$$

- Generalized Spherical Harmonics (Bunge):

$$P_k(\chi, \phi) = \sum_{l=0}^{\infty} \frac{1}{2l+1} \sum_{n=-l}^l k_l^n(\chi, \phi) \sum_{m=-l}^l C_l^{mn} k_n^{*m}(\Theta_k \phi_k) \quad f(g) = \sum_{l=0}^{\infty} \sum_{m,n=-l}^l C_l^{mn} T_l^{mn}(g)$$

- Components (Helming):

$$f(g) = F + \sum_c I^c f^c(g)$$

- WIMV (William, Imhof, Matthies, Vinel) iterative process:

$$f^{n+1}(\mathbf{g}) = N_n \frac{f^n(\mathbf{g})f^0(\mathbf{g})}{\left(\prod_{\mathbf{h}=1}^I \prod_{m=1}^{M_h} P_{\mathbf{h}}^n(\mathbf{y}) \right)^{\frac{1}{IM_h}}}$$

$$f^0(\mathbf{g}) = N_0 \left(\prod_{\mathbf{h}=1}^I \prod_{m=1}^{M_h} P_{\mathbf{h}}^{\text{exp}}(\mathbf{y}) \right)^{\frac{1}{IM_h}}$$

E-WIMV (Rietveld only):

with $0 < r_n < 1$, relaxation parameter,
 M_h number of division points of the integral
 around k ,
 w_h reflection weight

$$f^{n+1}(\mathbf{g}) = f^n(\mathbf{g}) \prod_{m=1}^{M_h} \left(\frac{P_{\mathbf{h}}(\mathbf{y})}{P_{\mathbf{h}}^n(\mathbf{y})} \right)^{r_n \frac{w_h}{M_h}}$$

- Entropy maximisation (Schaeben):

$$f^{n+1}(\mathbf{g}) = f^n(\mathbf{g}) \prod_{m=1}^{M_h} \left(\frac{P_{\mathbf{h}}(\mathbf{y})}{P_{\mathbf{h}}^n(\mathbf{y})} \right)^{\frac{r_n}{M_h}}$$

- arbitrarily defined cells (ADC, Pawlik): Very similar to E-WIMV, with integrals along path tubes

Residual Stresses shift peaks with y

Dilemma 2

Stress and QTA: correlations: $f(g)$ and C_{ijkl}

$f(g)$:

- Moves the $\sin^2\Psi$ law away from linear relationship
- Needs the integrated peak (full spectra)

strains:

- Measured with pole figures
- needs the mean peak position

Isotropic samples: triaxial, biaxial, uniaxial stress states

Textured samples: Reuss, Voigt, Hill, Bulk geometric mean approaches

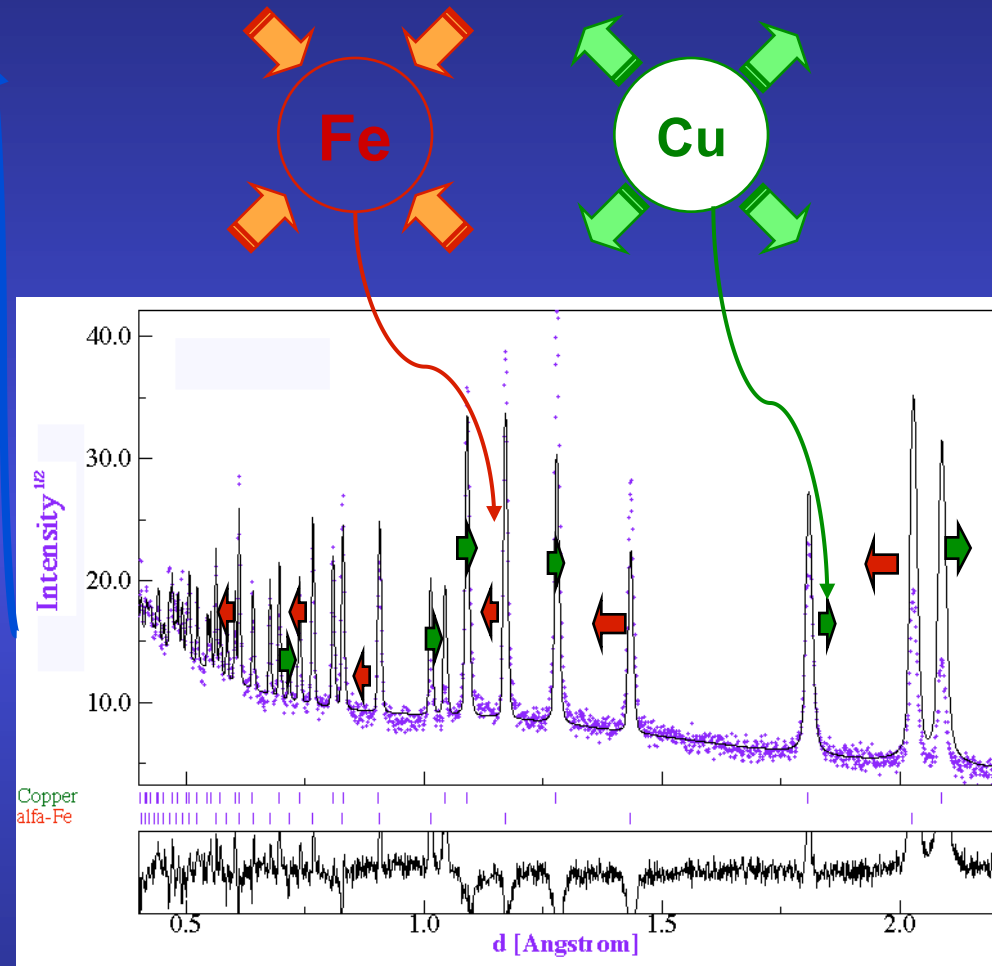
Residual Stresses and Rietveld

- Macro elastic strain tensor (I kind)
- Crystal anisotropic strains (II kind)

C

Macro and micro stresses

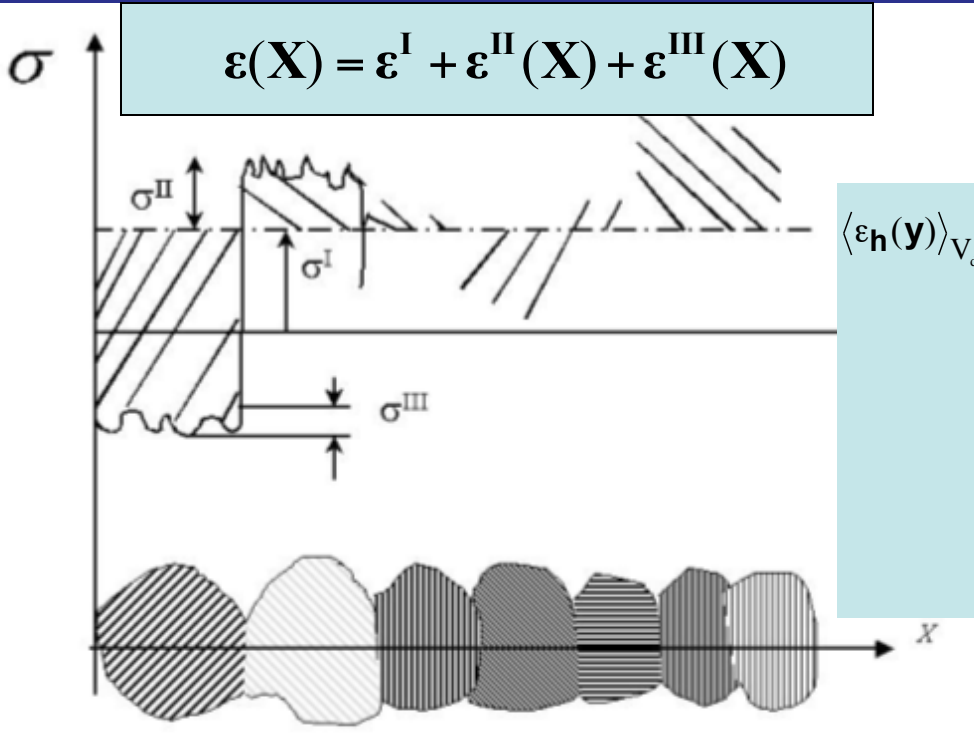
Applied macro stresses



Isotropic samples: triaxial, biaxial, uniaxial stress states

Textured samples: Reuss, Voigt, Hill, Bulk geometric mean approaches

Strain-Stress



Isotropic samples:
triaxial, biaxial uniaxial stress state

$$\begin{aligned} \langle \varepsilon_{\mathbf{h}(\mathbf{y})} \rangle_{V_d} &= \frac{1}{V_d} \int_{V_d} (\varepsilon_{33}^I + \varepsilon_{33}^{II} + \varepsilon_{33}^{III}) dV \\ &= (\varepsilon_{11}^I \cos^2 \phi + \varepsilon_{12}^I \sin 2\phi + \varepsilon_{22}^I \sin^2 \phi - \varepsilon_{33}^I) \sin^2 \psi + \varepsilon_{33}^I + \\ &\quad (\varepsilon_{13}^I \cos \phi + \varepsilon_{23}^I \sin \phi) \sin 2\psi + \frac{1}{V_d} \int_{V_d} (\varepsilon_{33}^{IIe} + \varepsilon_{33}^{IIIi} + \varepsilon_{33}^{IIIpi}) dV \\ &= \frac{\langle d(\mathbf{hkl}, \phi, \psi) \rangle_{V_d} - d_0(\mathbf{hkl})}{d_0(\mathbf{hkl})} \end{aligned}$$

Textured samples:
triaxial, biaxial uniaxial stress state
+ ODF + SDF + model

$$\begin{aligned} \langle E(\mathbf{g}) \rangle_{V_d} &= \frac{1}{V_d} \int_{V_d} E^{SC}(\mathbf{g}) f(\mathbf{g}) d\mathbf{g} \\ &= \left(\int_{V_d} E^{SC}(\mathbf{g}) f(\mathbf{g}) d\mathbf{g} \right) \frac{1}{V_d} \end{aligned}$$

$$\chi^2 = \sum_i w_i^2 \left[\varepsilon_i^{calc}(S_{ijkl}^M, \mathbf{h}, \mathbf{y}) - \varepsilon_i^{meas}(S_{ijkl}^M, \mathbf{h}, \mathbf{y}) \right]^2$$

Non-linear least-square fit

Layered systems

Dilemma 3

Layer, Rietveld and QTA: correlations: $f(g)$, thicknesses and structure

$f(g)$:

- Pole figures need corrections for abs-vol
- Rietveld also to correct intensities

layers:

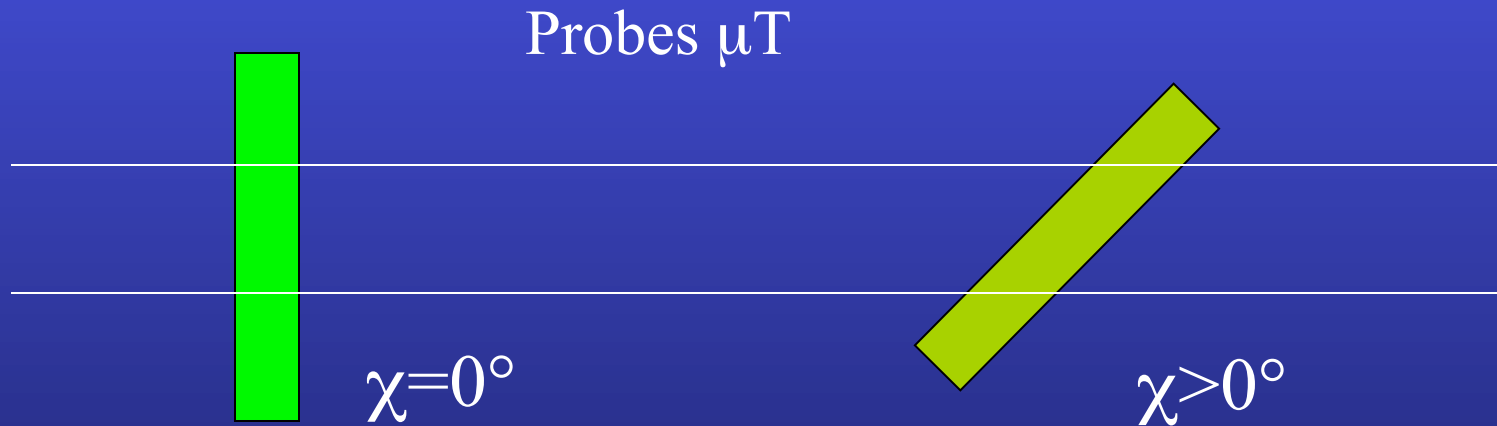
- unknown sample true absorption coefficient μ
- unknown effective thickness (porosity)

Layering

Asymmetric Bragg-Brentano

$$C_{\chi}^{\text{top film}} = g_1 (1 - \exp(-\mu T g_2 / \cos \chi)) / (1 - \exp(-2\mu T / \sin \omega \cos \chi))$$

$$C_{\chi}^{\text{cov. layer}} = C_{\chi}^{\text{top film}} \left(\exp(-g_2 \sum \mu'_i T'_i / \cos \chi) \right) / \left(\exp(-2 \sum \mu'_i T'_i / \sin \omega \cos \chi) \right)$$



Phase and Texture

Dilemma 4

Phase and QTA: correlations: $f(g)$, S_{Φ}

$f(g)$:

- angular relationships
- plays on individual spectra
- essential to operate on textured sample

S_{Φ} :

- plays on overall scale factor (sum diagram)

Phase analysis

- Volume fraction

$$V_{\Phi} = \frac{S_{\Phi} V_{uc\Phi}^2}{\sum_{\Phi} (S_{\Phi} V_{uc\Phi}^2)_{\Phi}}$$

- Weight fraction

$$m_{\Phi} = \frac{S_{\Phi} Z_{\Phi} M_{\Phi} V_{uc\Phi}^2}{\sum_{\Phi} (S_{\Phi} Z_{\Phi} M_{\Phi} V_{uc\Phi}^2)_{\Phi}}$$

Z = number of formula units

M = mass of the formula unit

V = cell volume

How it works

Le Bail extraction

$$T_{hkl}^k = T_{hkl}^{k-1} \frac{\sum_i I_i^{\text{exp}} S_{hkl}^i}{\sum_i I_i^{\text{calc}} S_{hkl}^i}$$

- Starts with nominal intensities (T_{hkl})
 - Computes the full pattern (I^{calc})
 - Uses the formula to compute next T_{hkl}
 - Cycle the last two steps until convergence
-
- In Maud, options:
 - Only few cycles for texture (3-5) necessary
 - The range for the weighting of the profile can be reduced
 - Background subtracted or not

Structure and Residual Stresses (shift peaks with \mathbf{y})

Dilemma 5

Stress and cell parameters: correlations: peak positions and C_{ijkl}

Cell parameters:

- Measured at high angles
- Bragg law evolution

strains:

- Measured precisely at high angles
- stiffness-based variation, also with Ψ

Shapes, microstrains, defaults, distributions

Dilemma 6

Shapes and stress-texture-structure: correlations ?

Shapes:

- line broadening problem
- average positions modified
- if anisotropic: modification changes with y

Stress-texture-structure:

- need “true” peak positions and intensities
- need deconvoluted signals

Scherrer, Integral breadth, Williamson-Hall ...

$$\langle D \rangle_v = \frac{K\lambda}{\beta_s(2\theta) \cos\theta}$$

More elegant, mandatory for whole-pattern: Stokes deconvolution
Bertaut-Warren-Averbach treatment, e.g. for a 00l peak:

$$\Omega_{\mathbf{h}} = \sum_{L_{\mathbf{h}}} C_{L_{\mathbf{h}}} e^{-2i\pi L_{\mathbf{h}}(s-s_0)}$$

$$C_L = C_L^{\langle R_{\mathbf{h}} \rangle} C_L^{\langle \varepsilon_{\mathbf{h}}^{\text{III}} \rangle} = C_L^S C_L^D$$

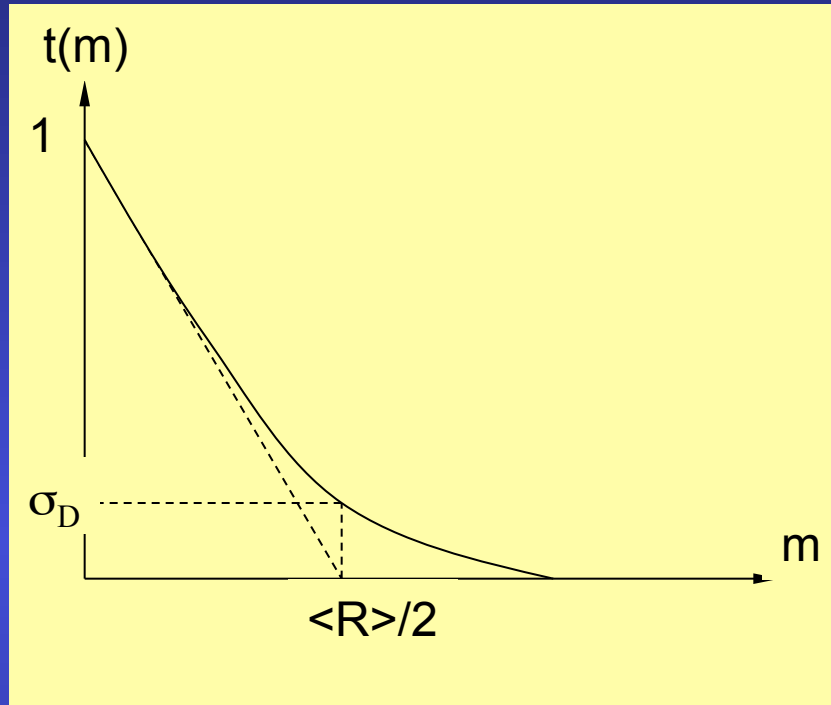
$$C_L^S = A_L^S$$

$$C_L^D = A_L^D + iB_L^D$$

$$A_{L,p} = A_L^{\langle R_{\mathbf{h}} \rangle} - A_L^{\langle R_{\mathbf{h}} \rangle} 2\pi^2 L^2 p^2 \left\langle \left(\varepsilon_{\mathbf{h}}^{\text{III}} \right)_L^2 \right\rangle \text{ or}$$

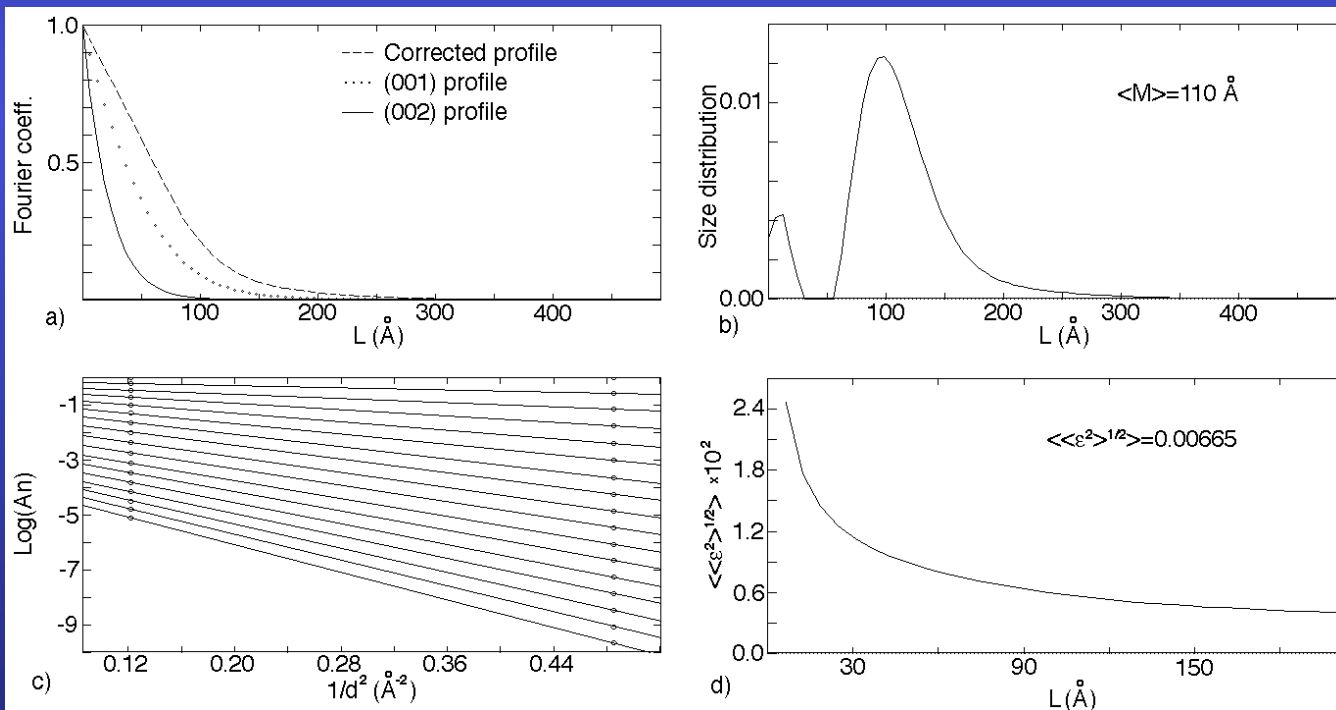
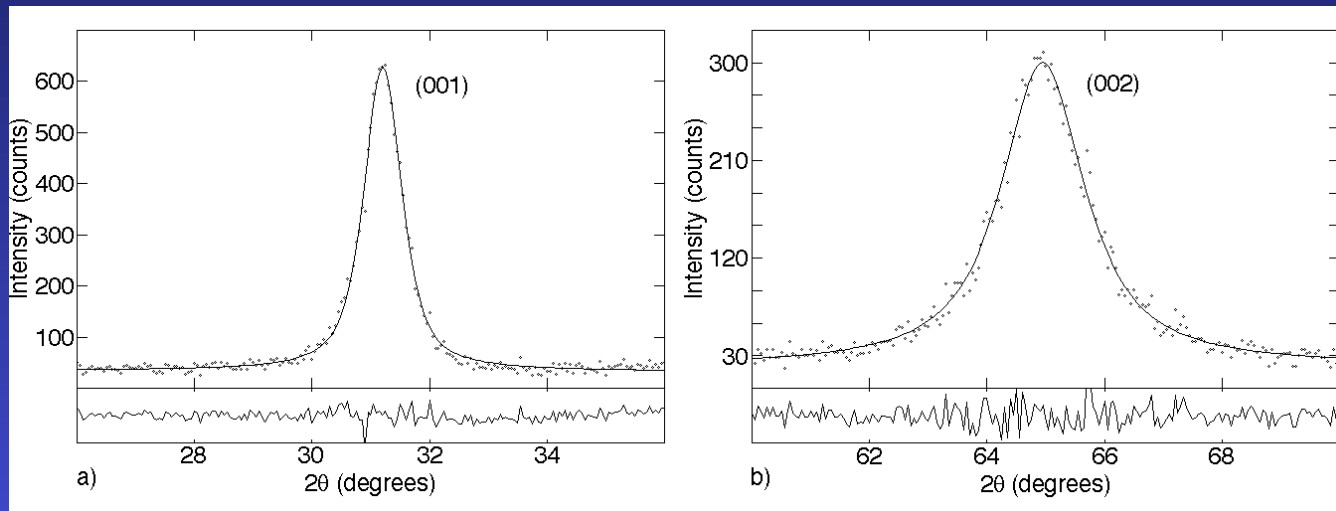
$$\ln A_{L,p} = \ln A_L^{\langle R_{\mathbf{h}} \rangle} - 2\pi^2 L^2 p^2 \left\langle \left(\varepsilon_{\mathbf{h}}^{\text{III}} \right)_L^2 \right\rangle$$

Second derivative: distribution of column lengths

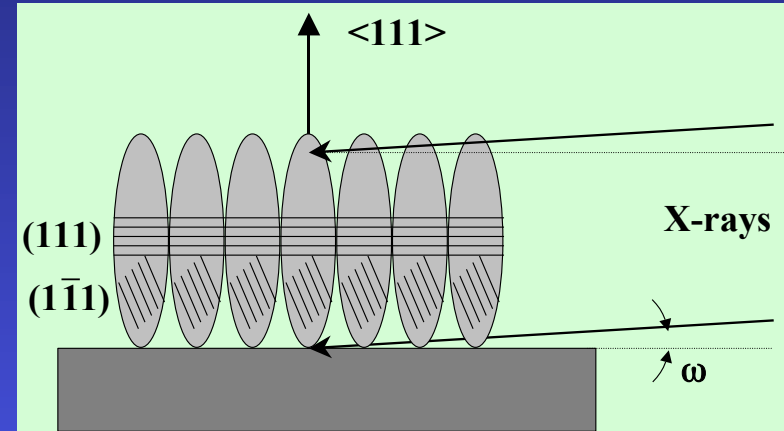
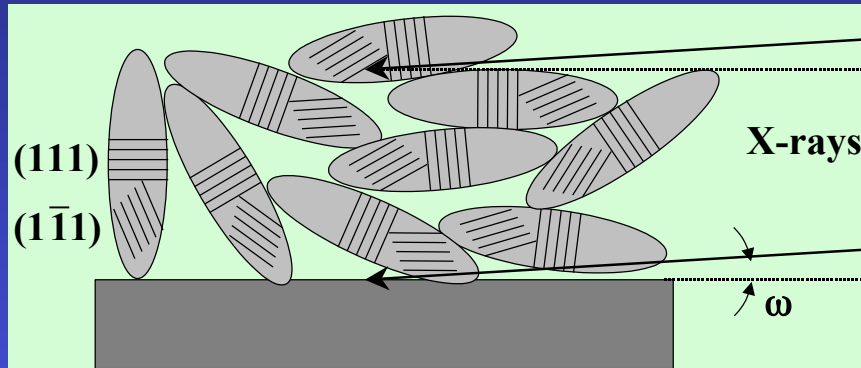


$$\left(\frac{dA_L^S}{dL} \right)_{L \rightarrow 0} = \frac{1}{\langle R_F \rangle}$$

$$\frac{d^2 A_L^S}{dL^2} = \mathcal{D}_A^S(L) \quad \text{and} \quad L \frac{d^2 A_L^S}{dL^2} = \mathcal{D}_V^S(L)$$



Anisotropic sizes and microstrains

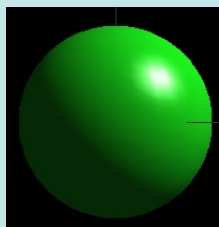


- Texture helps the "real" mean shape determination
- Determination by peak deconvolution + Popa formalism

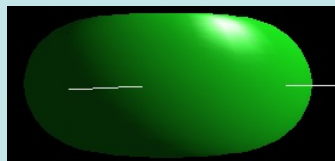
$$\langle R_h \rangle = R_0 + R_1 P_2^0(x) + R_2 P_2^1(x) \cos \varphi + R_3 P_2^1(x) \sin \varphi + R_4 P_2^2(x) \cos 2\varphi + R_5 P_2^2(x) \sin 2\varphi + \dots$$

$$\langle \varepsilon_h^2 \rangle E_h^4 = E_1 h^4 + E_2 k^4 + E_3 \ell^4 + 2E_4 h^2 k^2 + 2E_5 \ell^2 k^2 + 2E_6 h^2 \ell^2 + 4E_7 h^3 k + 4E_8 h^3 \ell + 4E_9 k^3 h + 4E_{10} k^3 \ell + 4E_{11} \ell^3 h + 4E_{12} \ell^3 k + 4E_{13} h^2 k \ell + 4E_{14} k^2 h \ell + 4E_{15} \ell^2 k h$$

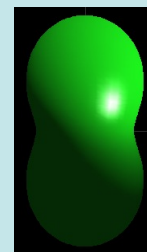
$\bar{1}$



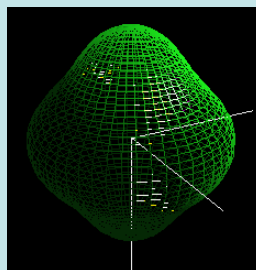
R_0



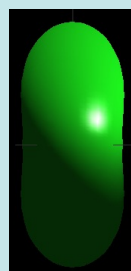
$R_0, R_1 < 0$



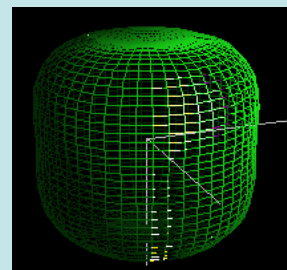
$R_0, R_1 > 0$



$R_0, R_6 > 0$

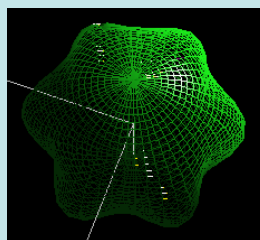


$R_0,$
 R_2 and $R_6 > 0$

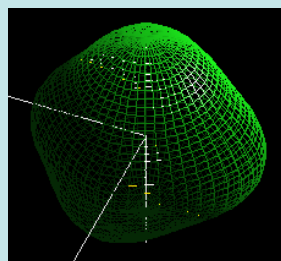


$R_0, R_6 < 0$

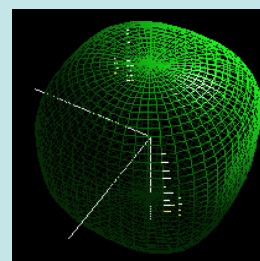
$6/m$



$R_0, R_4 > 0$



$R_0, R_1 > 0$



$R_0, R_1 < 0$

$m3m$

Combined Analysis approach

Extracted Intensities

WIMV, E-WIMV
Harmonics, components, ADC

Orientation Distribution Function

Rietveld

Structure
+
Microstructure
+
phase %

Popa-Balzar,
sin²ψ

Residual stresses
Strain Distribution Function

Specular Reflectivity

Roughness,
electron Density
& EDP,
Thickness

pole figures
inverse pole figures

Structural parameters
atomic positions, substitutions, vibrations
cell parameters

Multiphased, layered samples:
Thickness,
Anisotropic Sizes
and μ -strains (*Popa*),
Stacking faults (*Warren*),
Distributions, Turbostratism (*Ufer*)

Phase ratio (amorphous + crystalline)
Le Bail *Rietveld*

Fresnel,
Matrix (Parrat),
DWBA

Voigt,
Reuss,
Geometric
mean

Le Bail

Grinding to powderise another dilemma !

Grinding: removes angular relationship, adds correlations

Texture:

- not measured
- removed ? hope to get a perfect powder

Strains, defaults, anisotropy ... :

- some removed, some added

Same sample ?

Rare samples ?

Minimum experimental requirements

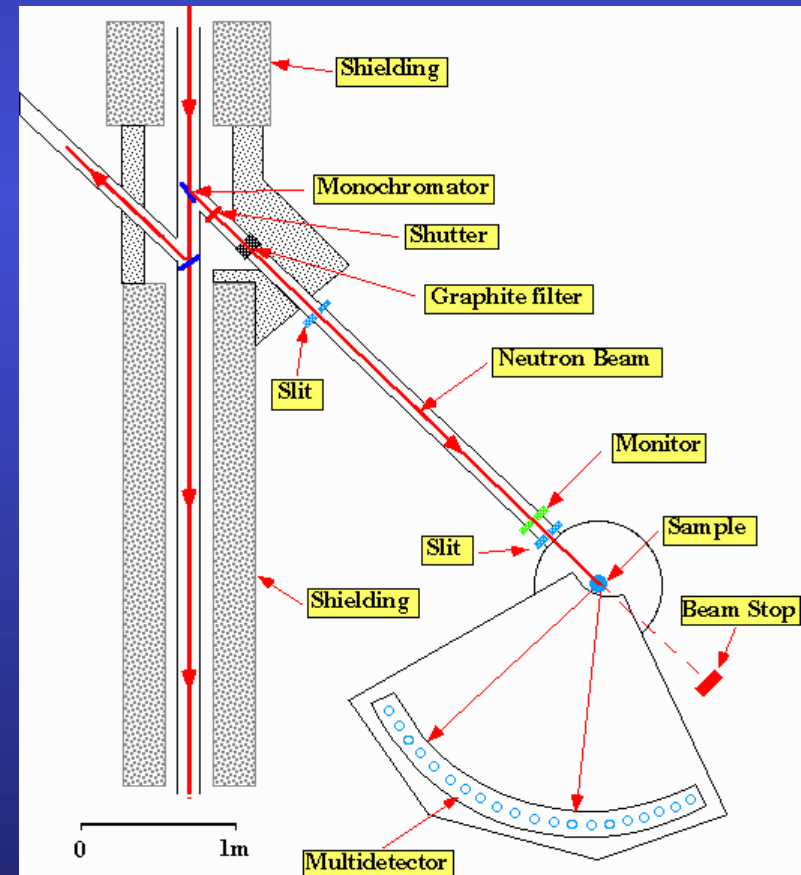
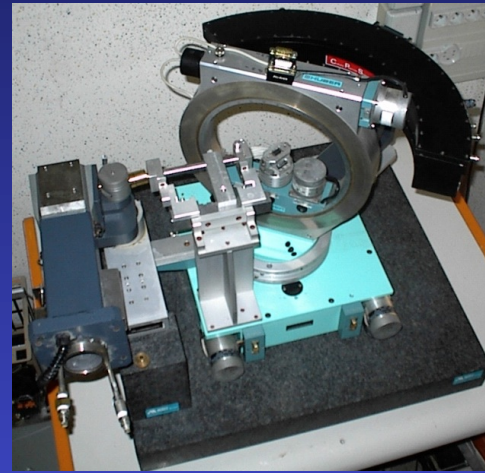
1D or 2D Detector + 4-circle diffractometer
(X-rays and neutrons)
CRISMAT, ILL

+

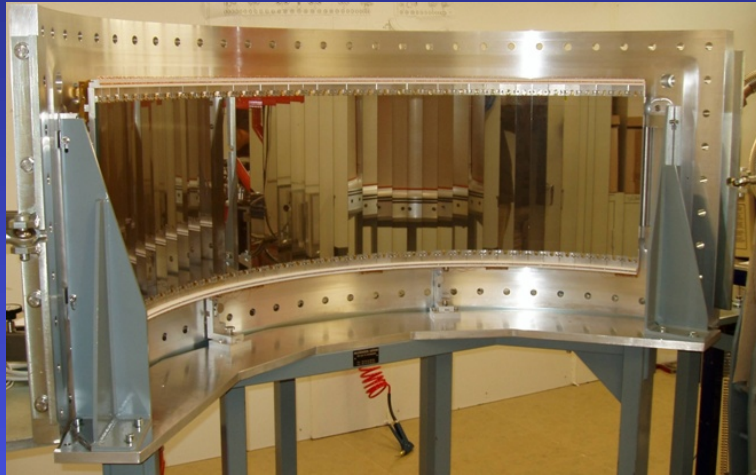
~1000 experiments (2θ diagrams)
in as many sample orientations

+

Instrument calibration
(peaks widths and shapes,
misalignments, defocusing ...)



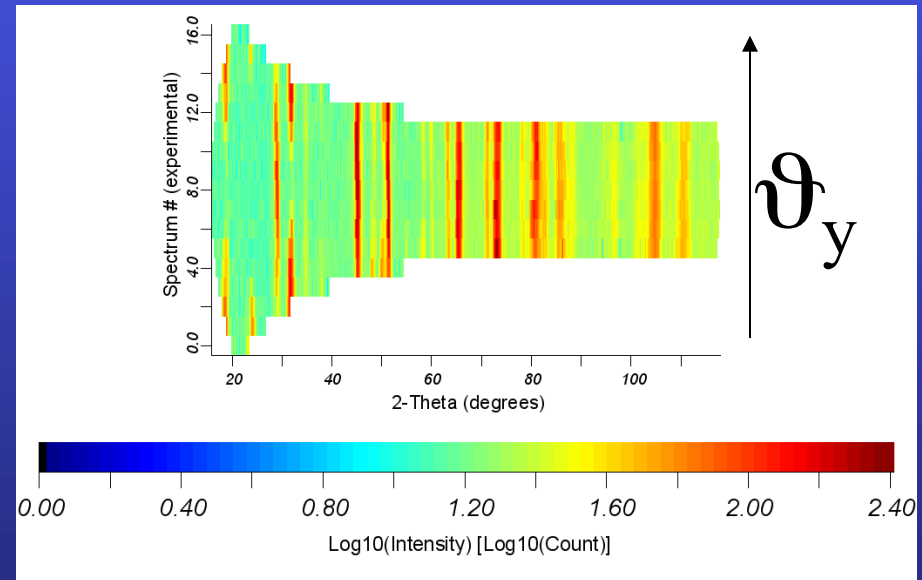
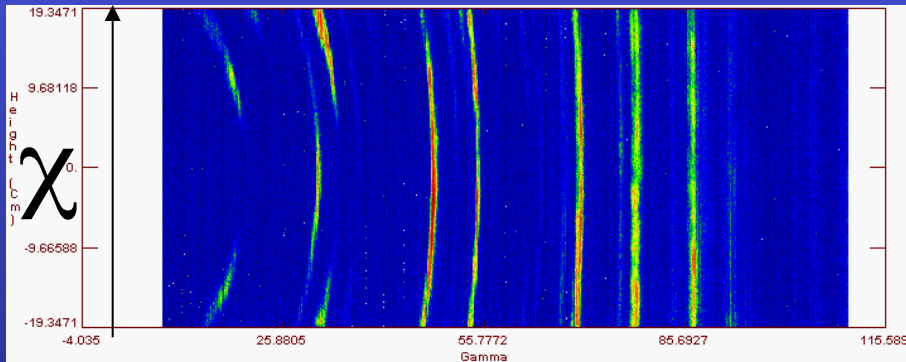
2D Curved Area Position Sensitive Detector



D19 - ILL

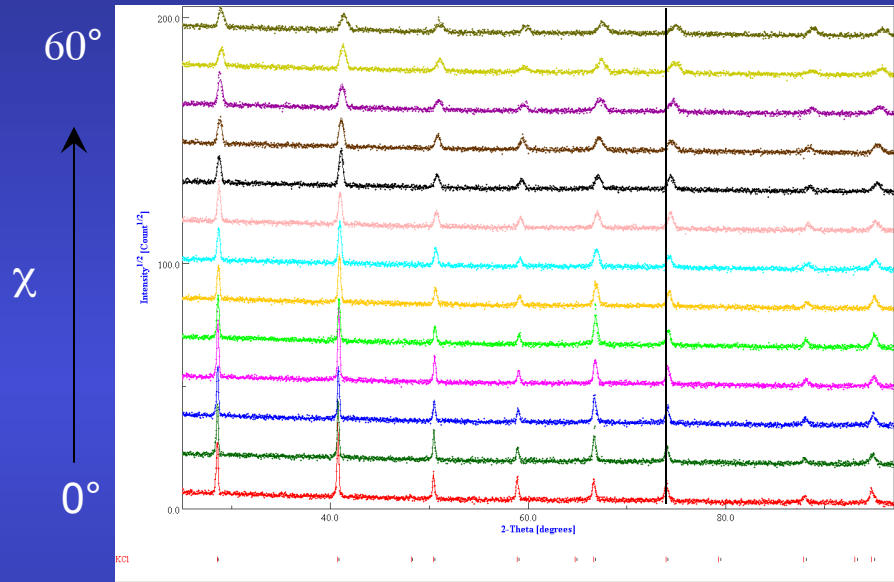
+

~100 experiments (2D Debye-Scherrer diagrams)
in as many sample orientations

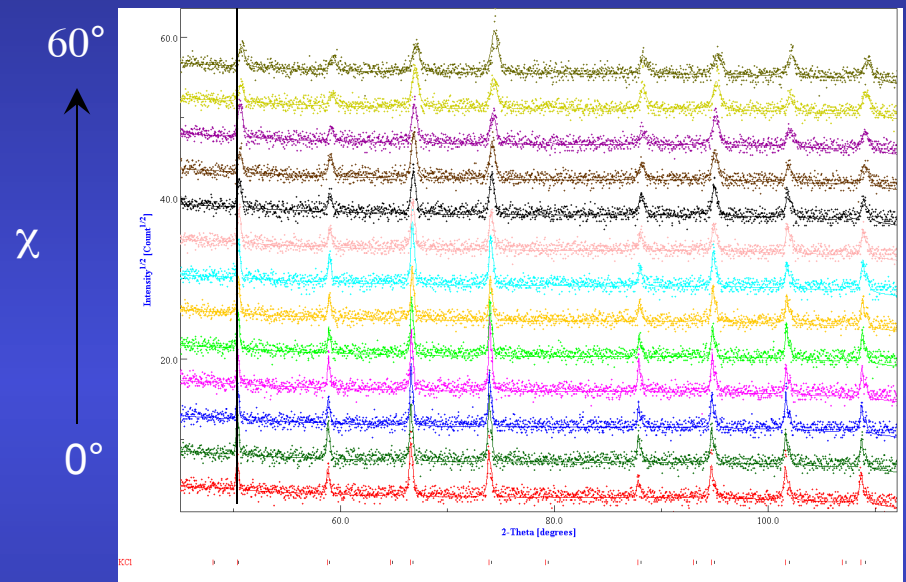


Calibration

$\omega = 20^\circ$



$\omega = 40^\circ$



KCl, LaB₆ ...



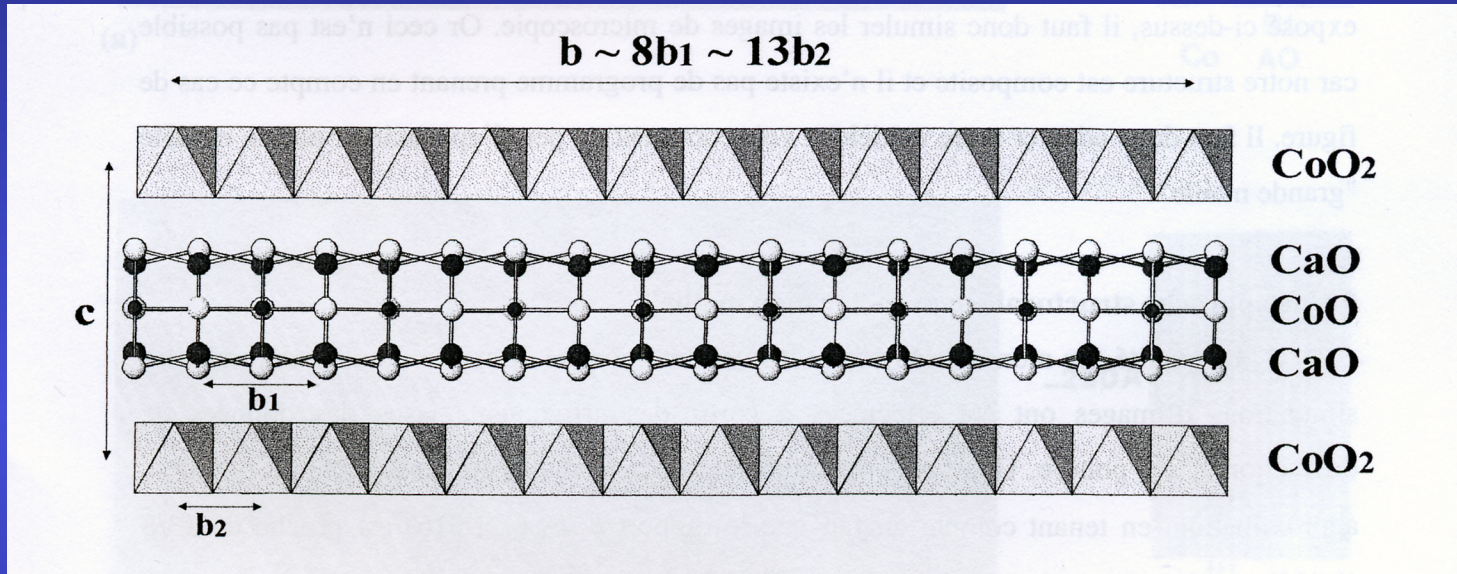
FWHM (ω , χ , 2θ ...)
2 θ shift
gaussianity
asymmetry
misalignments ...

Minimization algorithms

- Can be fully used in the method (everywhere)
- **Marquardt Least Squares** (based on steepest decrease and Gauss-Newton)
 - Efficient, best with few parameters, near the solution
- **Evolutionary computation** (or genetic algorithm)
 - Slow, not efficient, requires a lot of resources
 - Unlimited number of parameters
 - Can start far from the solution
- **Simulated annealing** (the solution proceed like a random walk, but the walking step decreases as temperature decreases)
 - In between the Marquardt and evolutionary algorithms
- **Simplex** (generates $n+1$ starting solutions as vertices of a polygon, n number of parameters, and contract/expand the polygon around the minima)
 - Slow on convergence
 - Remains close to the solution, but explore more minima with respect to the Marquardt

Ca₃Co₄O₉ thermoelectrics

Ca₃Co₄O₉: Misfit lamellar and modulated Structure, with high thermopower



Two monoclinic sub-systems:

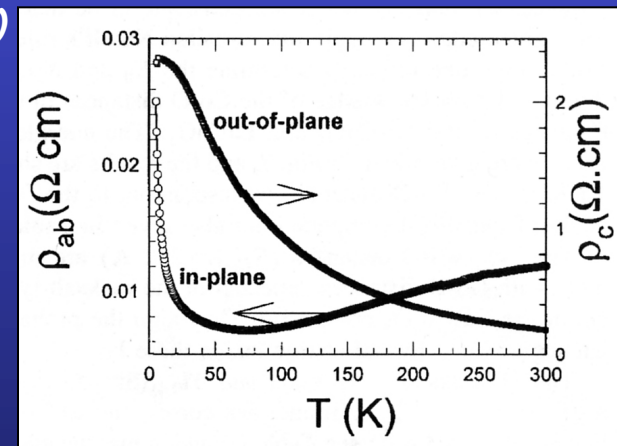
S1 with $a \sim 4.8\text{\AA}$, $b_1 \sim 4.5\text{\AA}$, $c \sim 10.8\text{\AA}$ et $\beta \sim 98^\circ$ (NaCl-type)

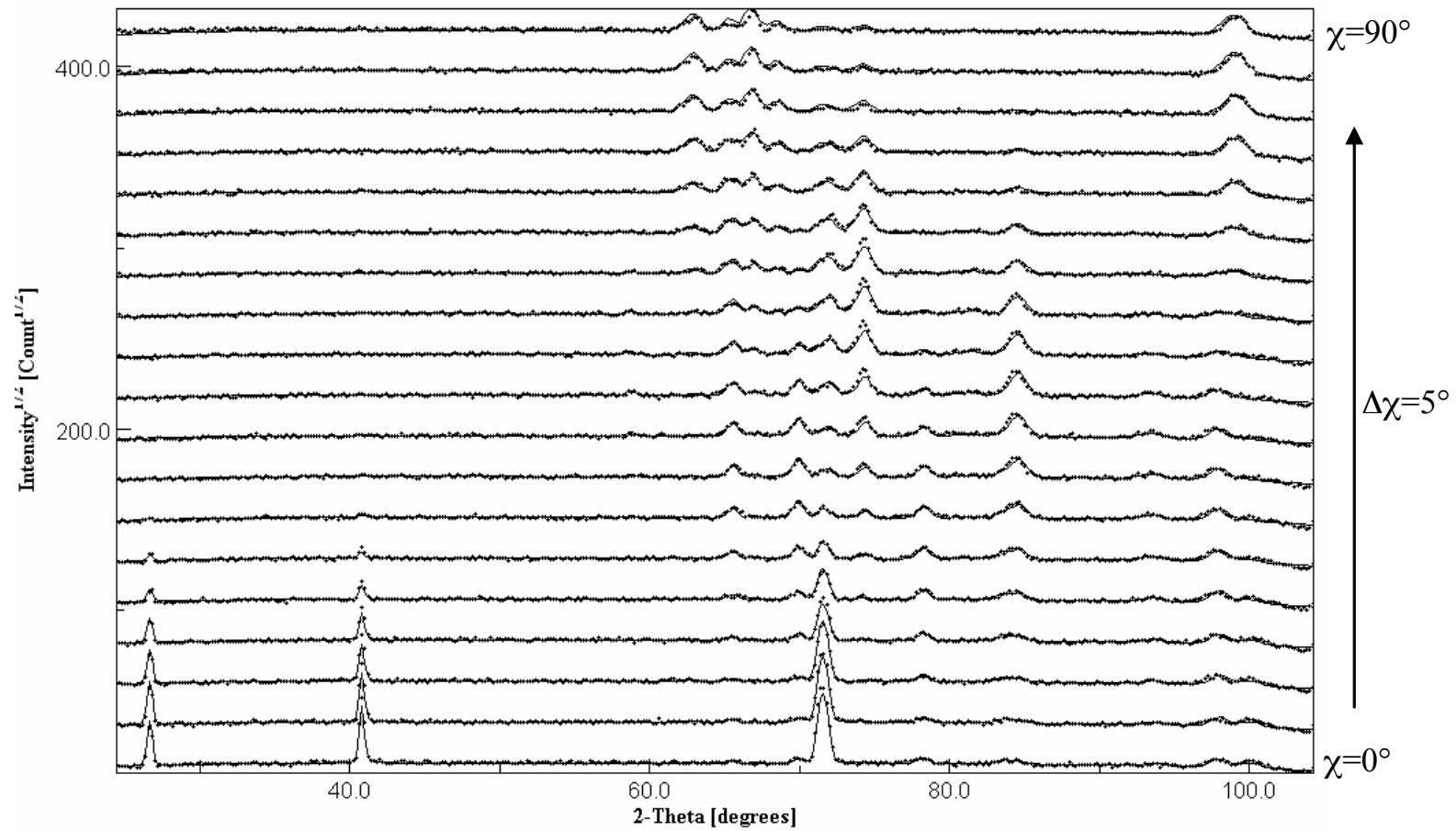
S2 with $a \sim 4.8\text{\AA}$, $b_2 \sim 2.8\text{\AA}$, $c \sim 10.8\text{\AA}$ et $\beta \sim 98^\circ$ (CdI₂-type)

$$\Gamma = \sigma_{ab} / \sigma_c \sim 10$$



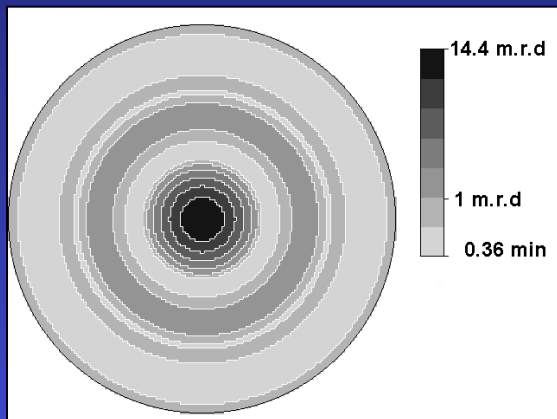
Texture



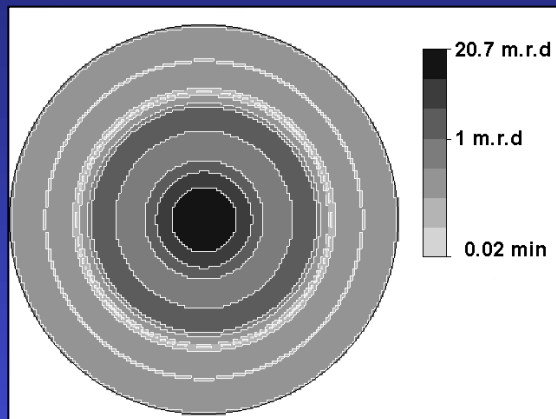


RP=19.7%, Rw=11.9%

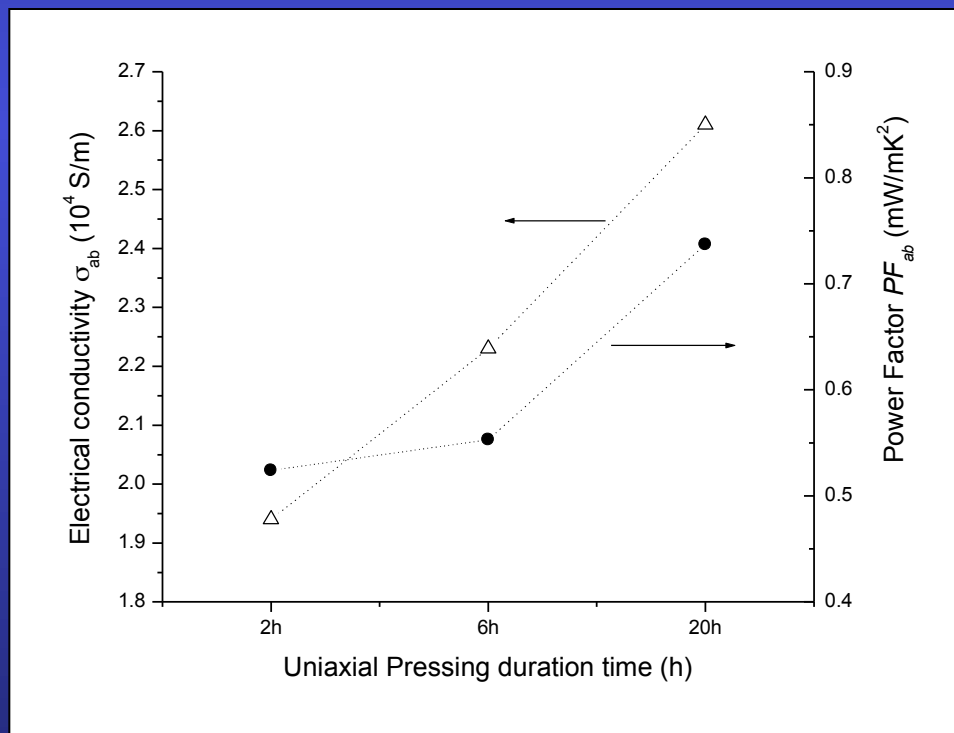
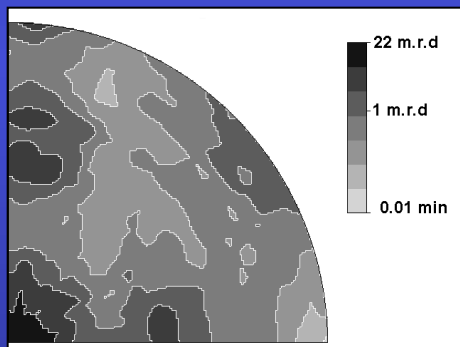
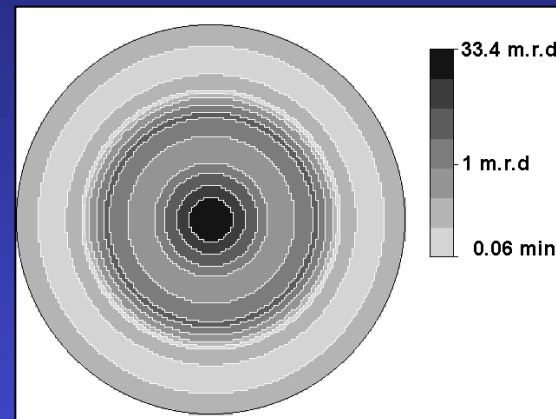
9.8 MPa for 2 h



19.6 MPa for 6 h



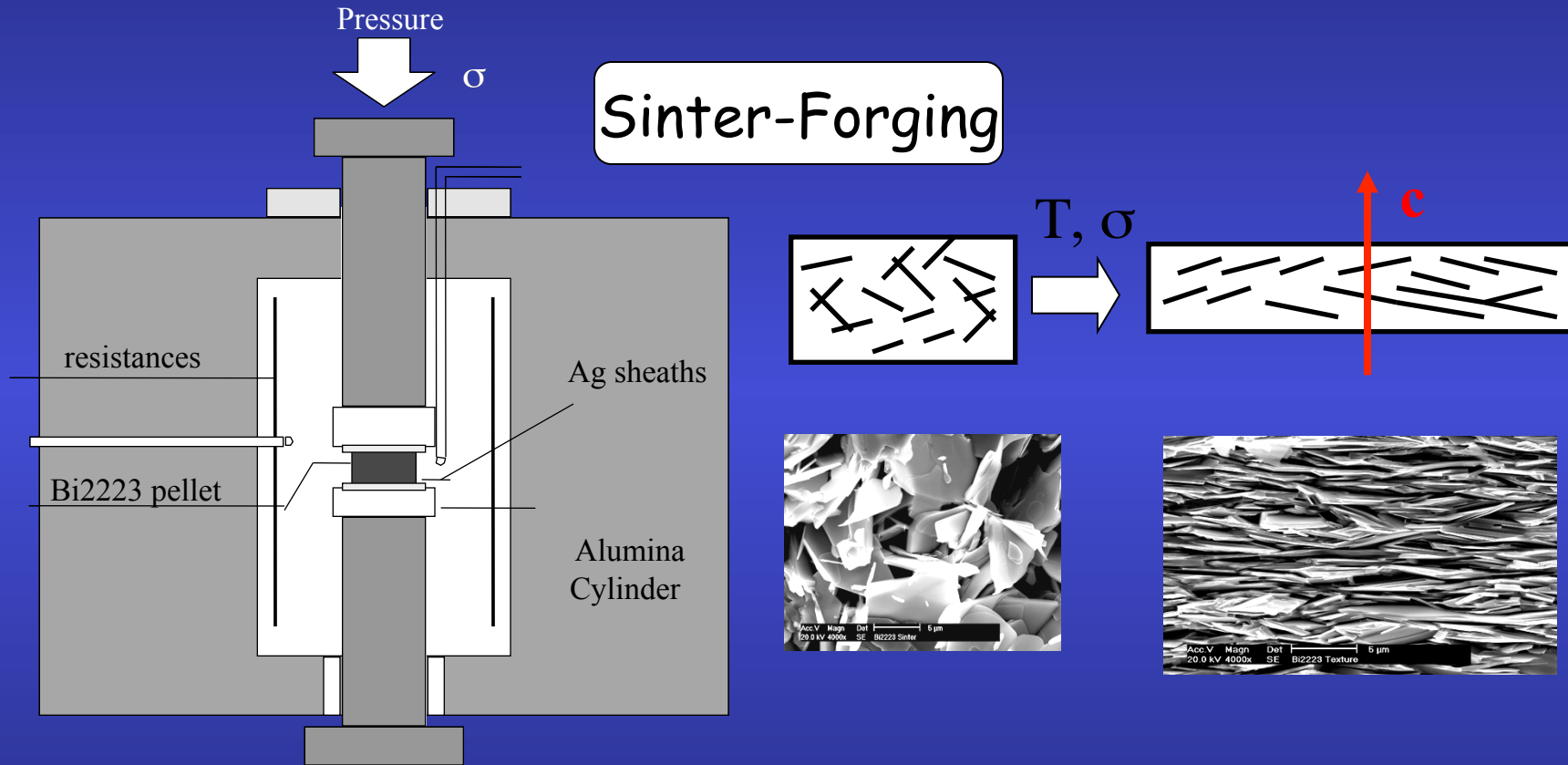
19.6 MPa for 20 h



Templated Growth Method

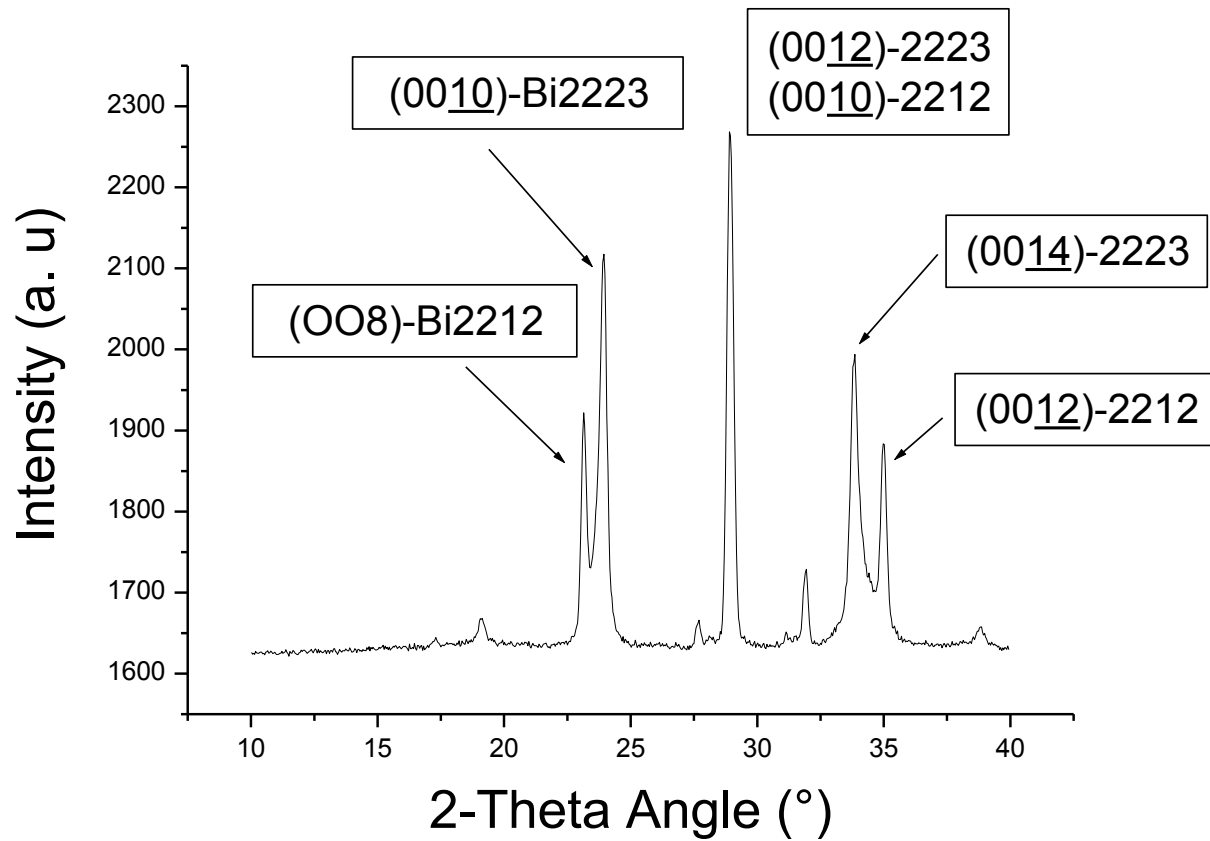
Bi2223 compounds

E. Guilmeau, PhD

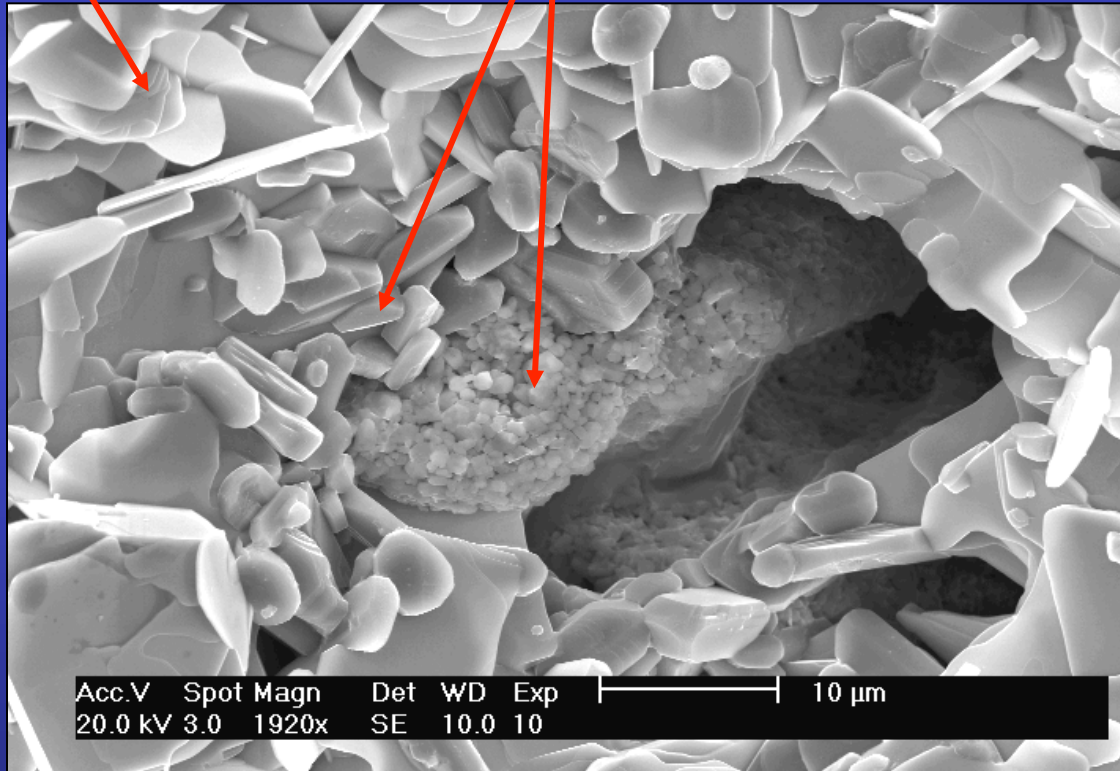


Grain alignment \Rightarrow $\nearrow J_c$

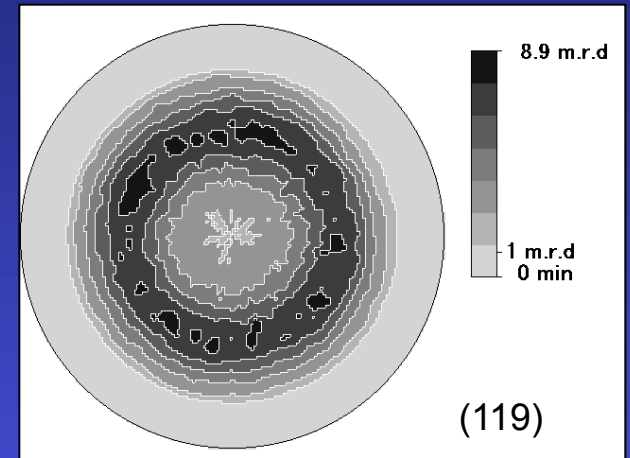
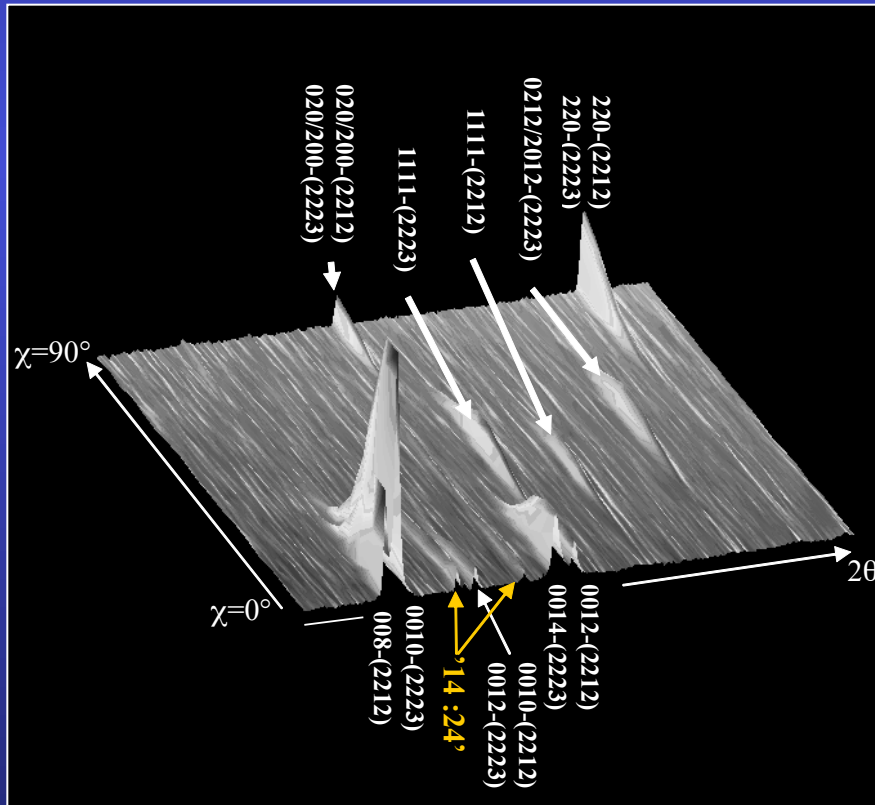
(00ℓ) Texture



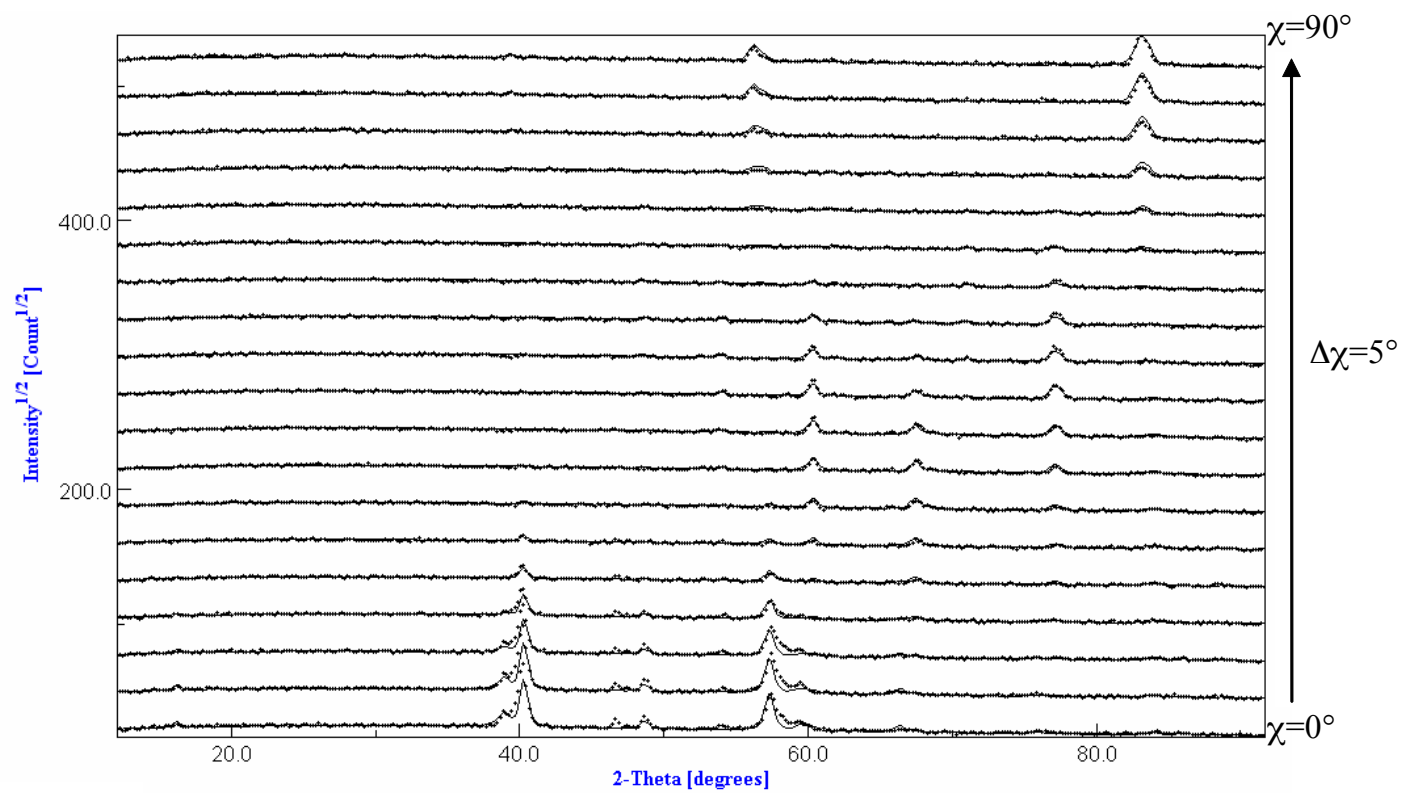
Bi2212 + Secondary phases \longrightarrow Bi2223



Combined Analysis



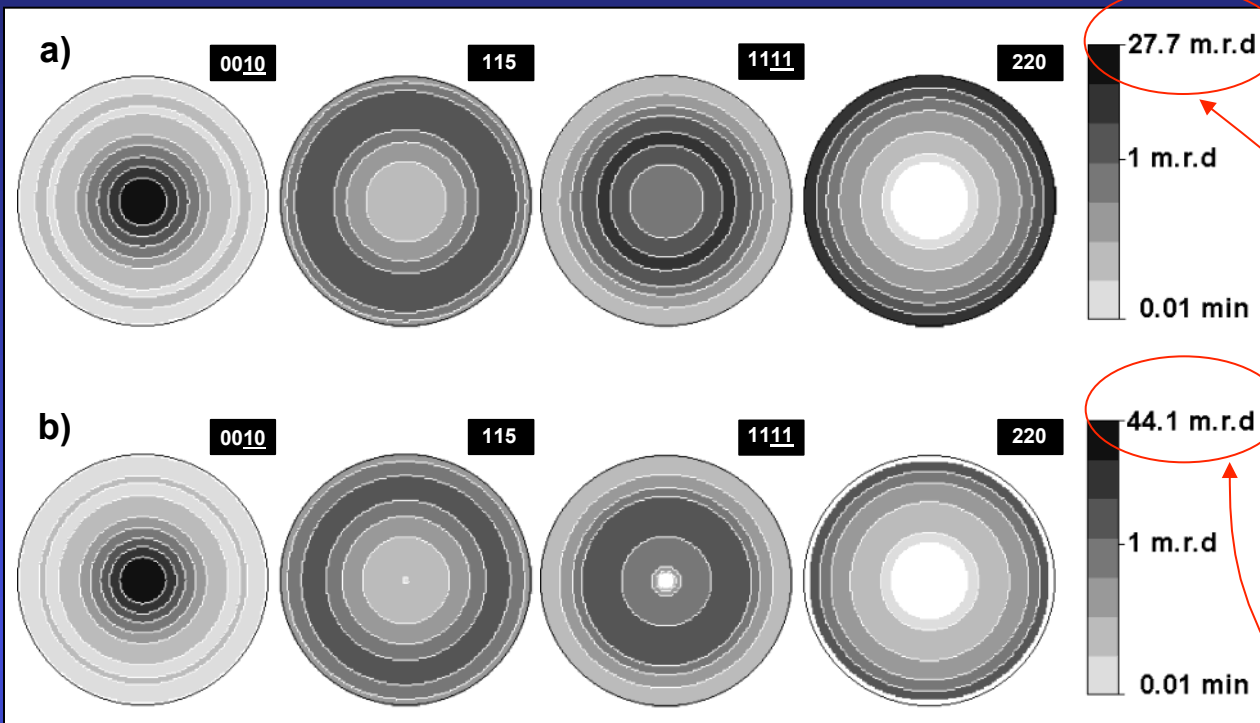
- Neutrons
- Sample: $\sim 70 \text{ mm}^3$
- 2θ patterns for $\chi=0^\circ$ to 90°
- No φ rotation (fibre texture).



2223
2212



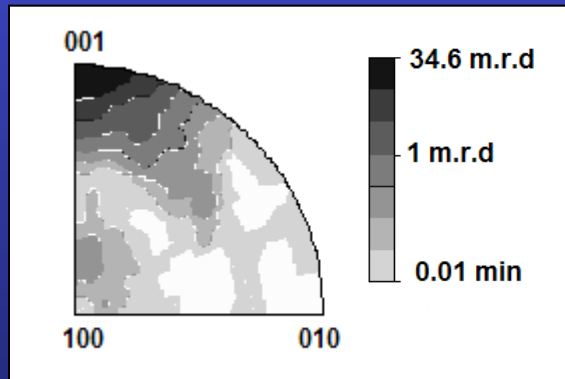
$R_w=9.12$
 $RP=16.24$



*Recalculated
(WIMV)*

*Extracted
(Le Bail)*

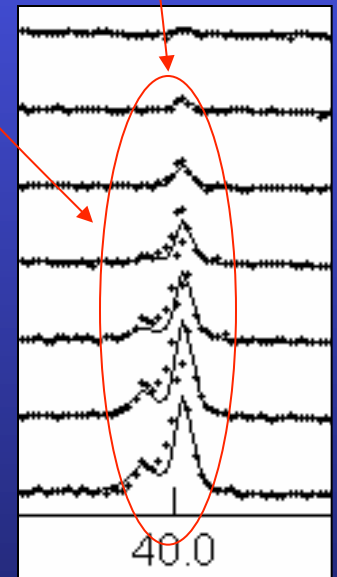
Logarithmic density scale, equal area projection



Logarithmic density scale, equal area projection

Stacking faults and/or intergrowth on the c-axis
 → New periodicities and peaks characterized with intermediate c parameters.

However, no algorithm is included to solve intergrowths in the combined approach.



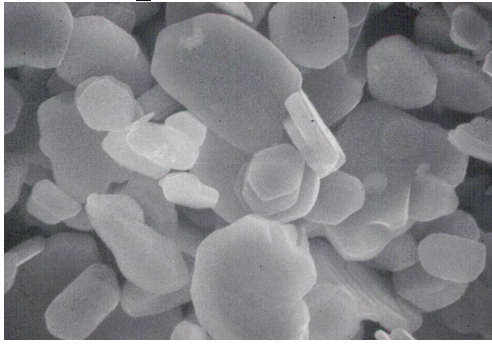
40.0

Effect of the sinter-forging treatment on the texture development, crystal growth, transport properties

Sinter-forging dwell time (h)	Orientation Distribution Max (m.r.d.)		% Bi2223	Cell parameters (Å)		Crystallite size Bi2223 (nm)	Rb (%)	Rw (%)	Rexp (%)	RP0 (%)	RP1 (%)	J_c (A/cm ²)
	Bi2212	Bi2223		Bi2223	Bi2212							
20	21.8	20.7	59.9±1.3	a=5.419(3) b=5.391(3) c=37.168(3)	a=5.414(3) b=5.393(3) c=30.800(3)	205±7	7.56	11.1	4.55	17.74	10.56	12500
50	24.1	24.4	72.9±2.9	a=5.419(3) b=5.408(3) c=37.192(3)	a=5.416(3) b=5.396(3) c=30.806(3)	273±10	7.54	11.37	4.58	17.05	11.04	15000
100	31.5	25.2	84.4±4.6	a=5.410(3) b=5.405(3) c=37.144(3)	a=5.412(3) b=5.403(3) c=30.752(3)	303±10	5.4	8.04	3.69	13.54	9.31	19000
150	65.4	27.2	87.0±4.1	a=5.417(3) b=5.403(3) c=37.199(3)	a=5.413(3) b=5.407(3) c=30.792(3)	383±13	6.13	9.12	4.8	16.24	12.25	20000

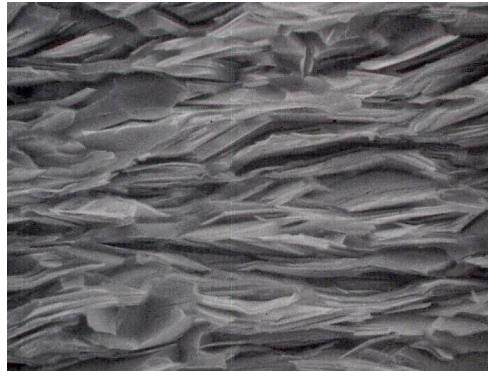


powder



10 μm

Textured bulk



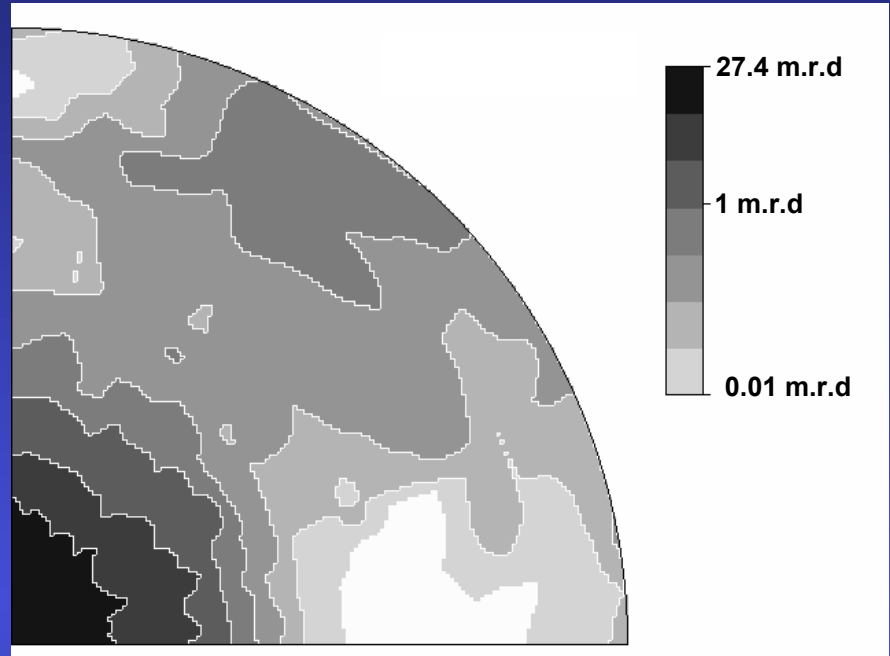
10 μm

*Magnetic alignment
and
Templated Growth
method*

Analysis:

- neutrons
- 3D Supercell: $a=4.8309\text{\AA}$, $b\sim 8b1\sim 13b2\sim 36.4902\text{\AA}$, $c=10.8353\text{\AA}$, $\beta=98.13^\circ$
174 atoms/cell
- Sample : 0.6 cm^3

Logarithmic density scale, equal area projection



Magnetic Alignment



- *magnetic alignment really efficient to obtain strong textures*
- *combined analysis of modulated structures possible*

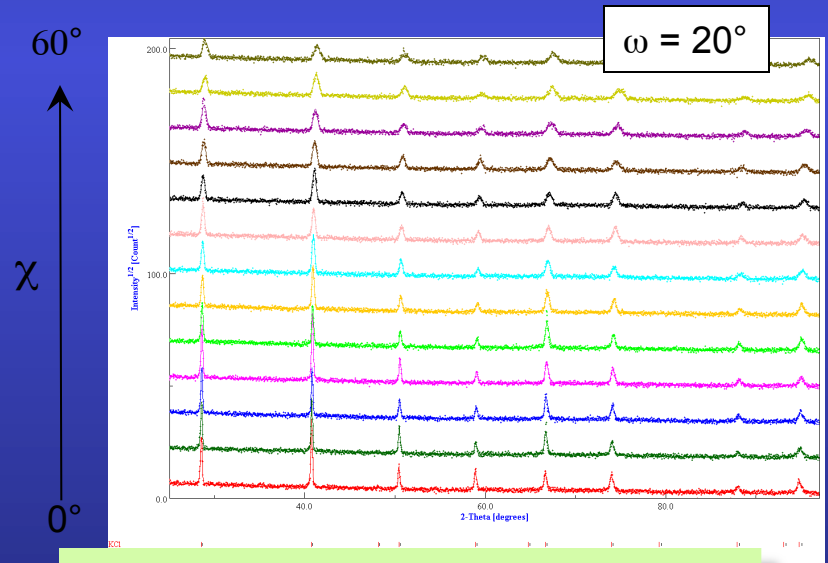
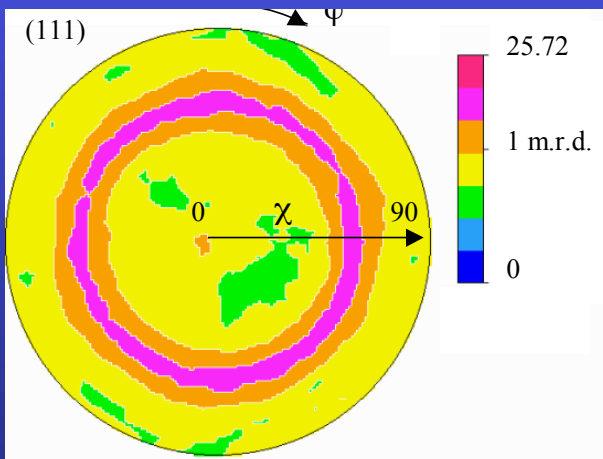
Ferroelectric PCT films

J. Ricote, Madrid

thin films:

$(\text{Ca}_{0.24}\text{Pb}_{0.76})\text{TiO}_3$ sol-gel synthesised solutions deposited by spin coating on a substrate of $\text{Pt}/\text{TiO}_2/\text{Si}$, with and without a treatment at 650°C for 30 min.

All films are crystallised at 700°C for 50 s by Rapid Thermal Processing (RTP; $30^\circ\text{C}/\text{s}$). A series is also recrystallised at 650°C for 1 to 3 h.



Refinement of individual spectra

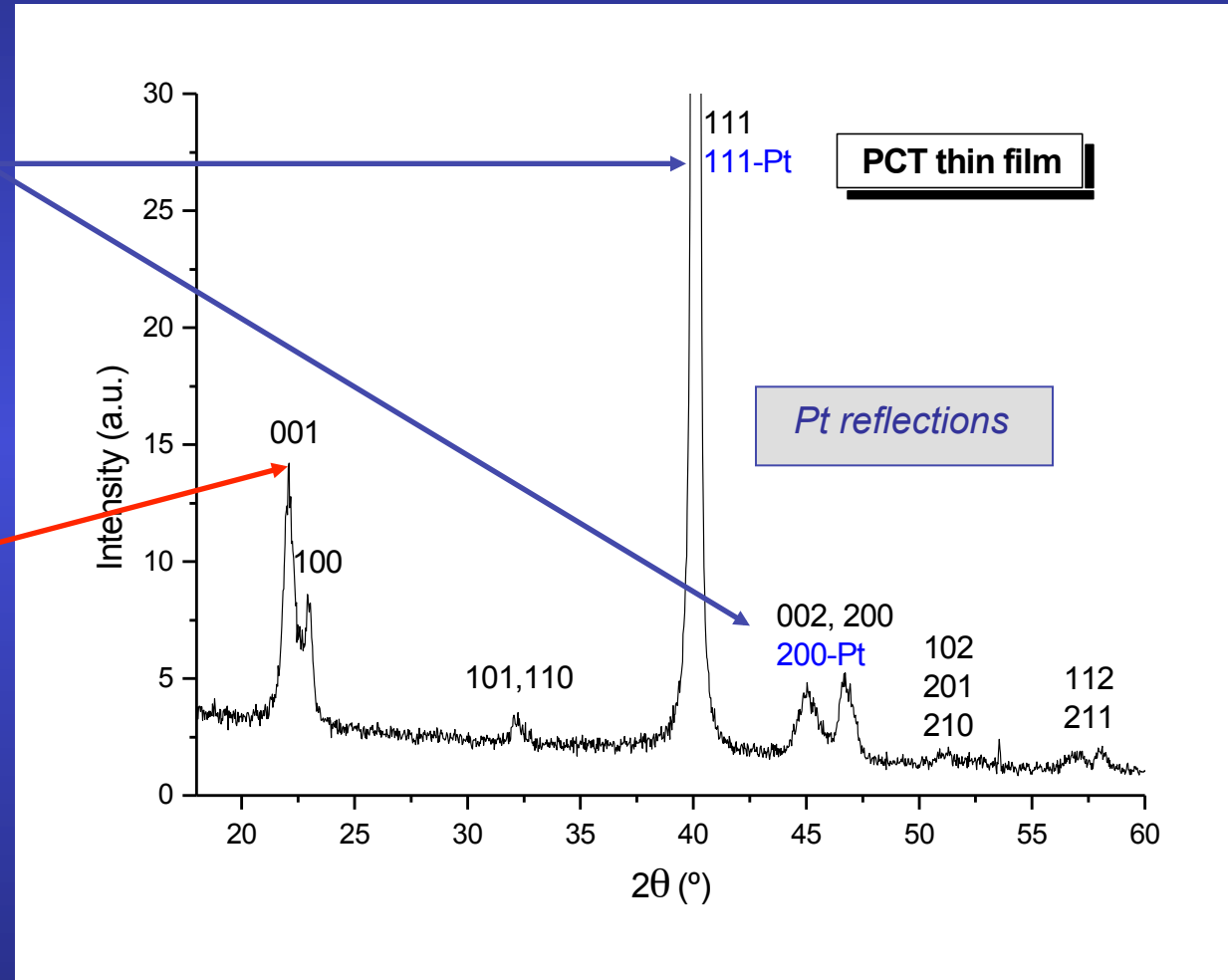
Limitations of the simple Quantitative Texture Analysis

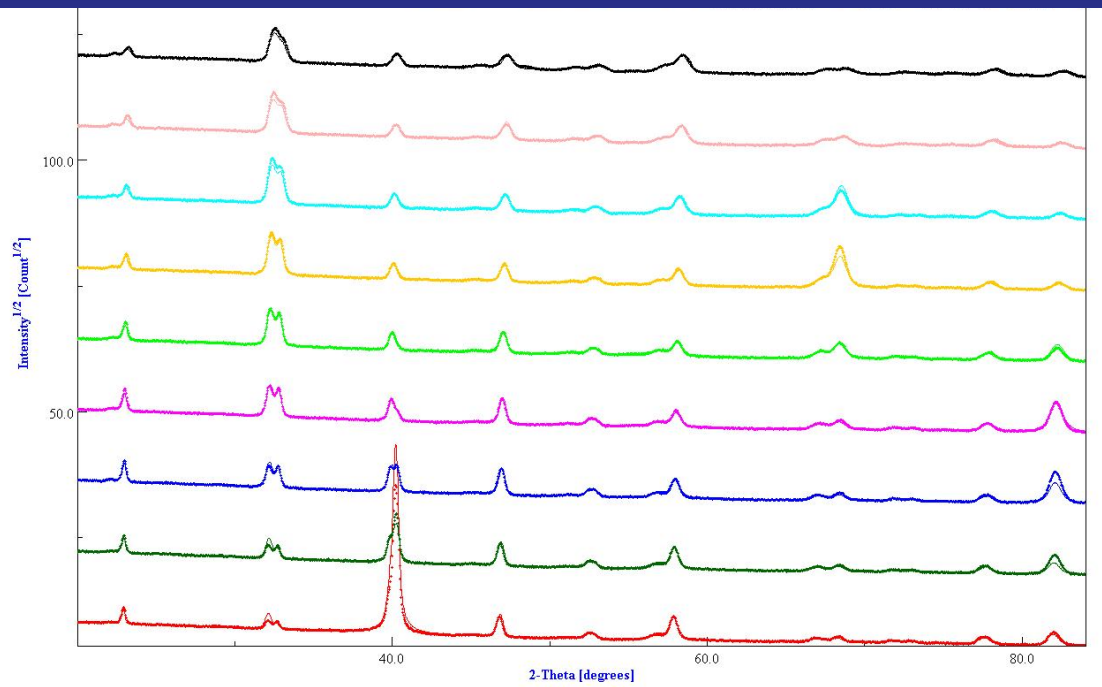
Structural parameters are difficult to obtain due to:

Substrate influence:

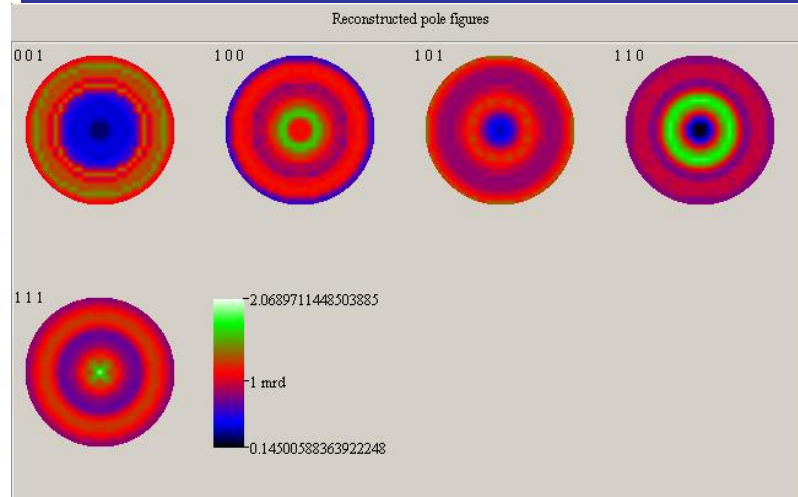
overlapping of reflections from the film and the substrate

TEXTURE effects:
peaks that do not appear at low χ angles

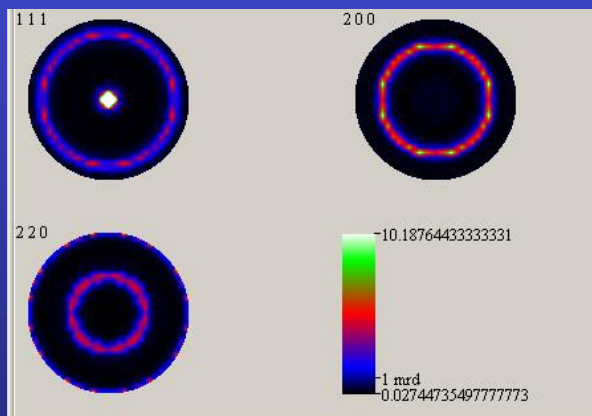




PCT



Pt

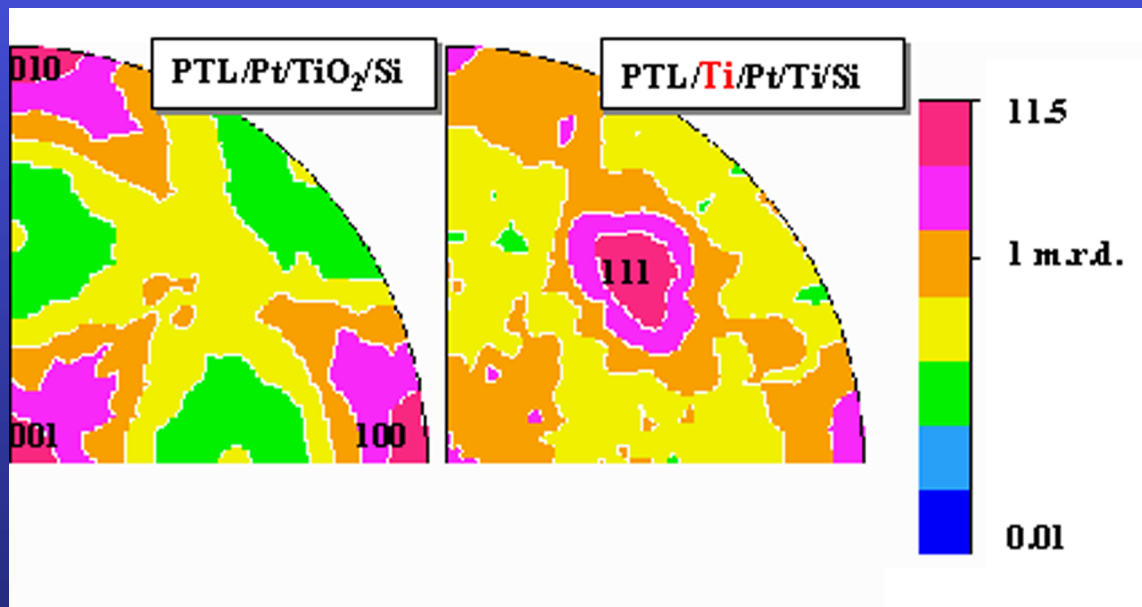


$a = 3.9108(1) \text{ \AA}$
 $T = 457(3) \text{ \AA}$
 $t_{\text{iso}} = 458(3) \text{ \AA}$
 $\epsilon' = 0.0032(1) \text{ rms}$

$a = 3.9156(1) \text{ \AA}$
 $c = 4.0497(3) \text{ \AA}$
 $T = 2525(13) \text{ \AA}$
 $t_{\text{iso}} = 390(7) \text{ \AA}$
 $\epsilon = 0.0067(1) \text{ rms}$

$R_W = 13\%$; $R_B = 12\%$; $R_{\text{exp}} = 22\%$.(Rietveld)
 $R_W = 5\%$; $R_B = 6\%$ (E-WIMV)

Atom	Occupancy	x	y	z
Pb	0.76	0.0	0.0	0.0
Ca	0.24	0.0	0.0	0.0
Ti	1.0	0.5	0.5	0.477(2)
O1	1.0	0.5	0.5	0.060(2)
O2	1.0	0.0	0.5	0.631(1)



Structural parameters

Pt layer

	a (Å)	thickness (nm)	R factors (%)
non-treated substrate			
Pt	3.9108(1)	45.7(3)	$R_W=13, R_B=12, R_{exp}=22$
annealed substrate			
Pt	3.9100(4)	46.4(3)	$R_W=8, R_B=14, R_{exp}=21$
Pt (Recryst. 1h)	3.9114(2)	47.8(3)	$R_W=9, R_B=20, R_{exp}=21$
Pt (Recryst. 2h)	3.9068(1)	46.9(3)	$R_W=9, R_B=14, R_{exp}=22$
Pt (Recryst. 3h)	3.9141(4)	47.5(9)	$R_W=27, R_B=12, R_{exp}=21$

Annealing of the substrate does not introduce significant variations on the structure of the Pt layer

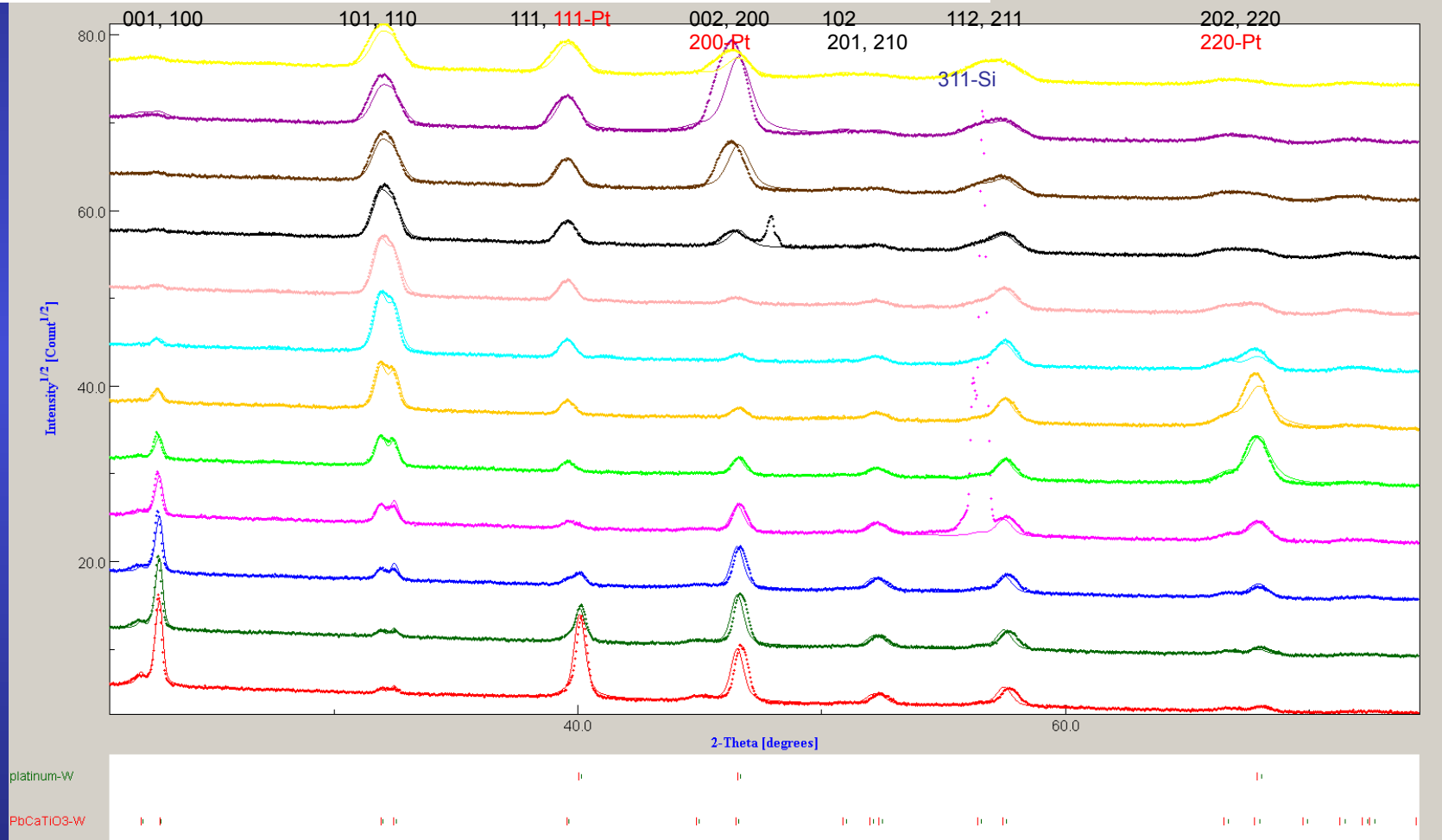
PTC film

	a (Å)	c (Å)	thickness (nm)
on non-treated substrate			
PCT	3.9156(1)	4.0497(6)	272.5(13)
on annealed substrate			
PCT	3.8920(6)	4.0187(8)	279.0(9)
PCT (Recryst. 1h)	3.8929(2)	4.0230(4)	266.1(11)
PCT (Recryst. 2h)	3.8982(2)	4.0227(4)	258.4(9)
PCT (Recryst. 3h)	3.9001(4)	4.0228(11)	253.6(29)

Recrystallisation reduces the stress on the film, and, increases the lattice parameters

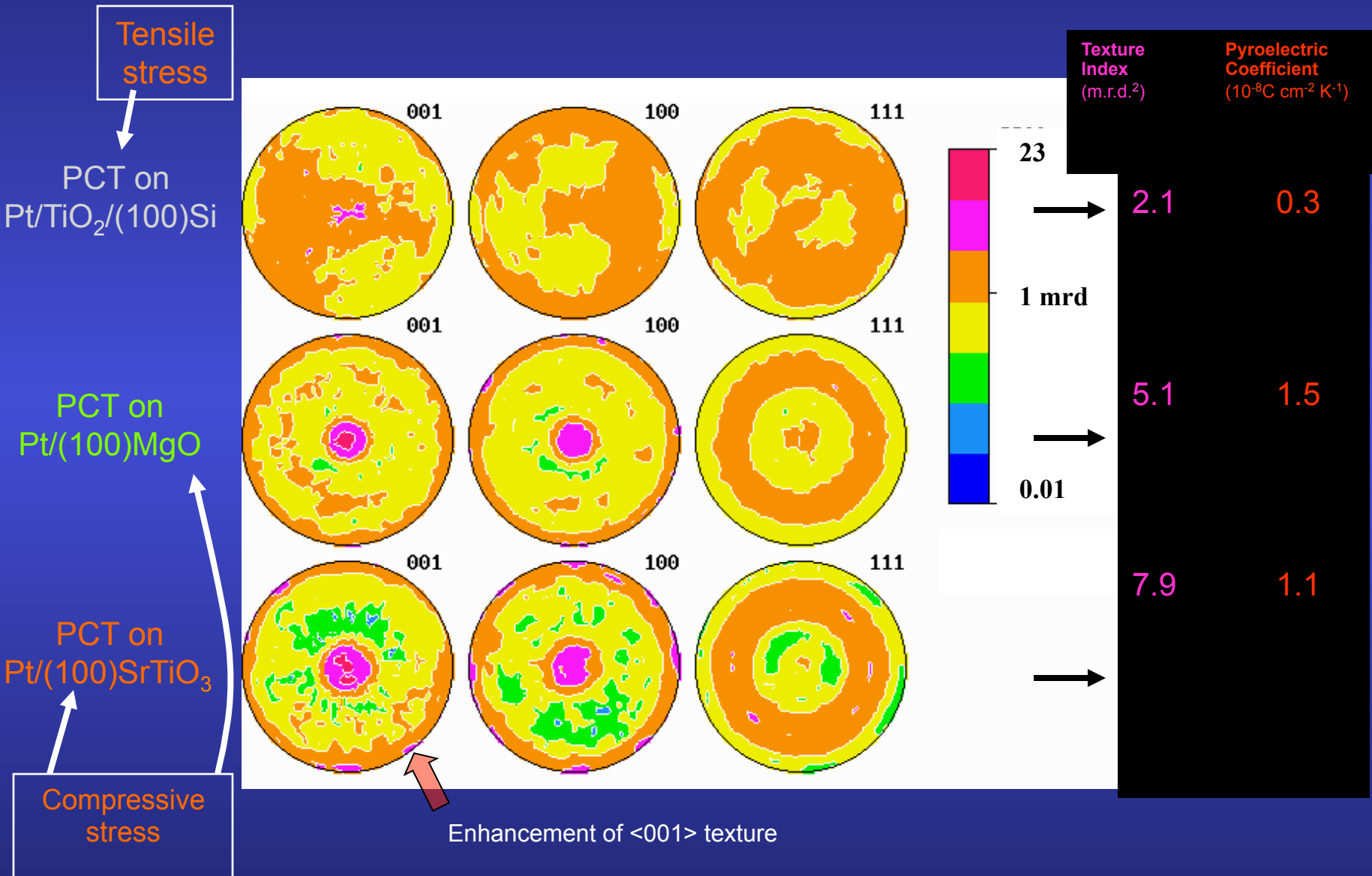
Structural, microstructural and texture quantitative characterisation of ferroelectric thin films by the combined method

Analysis of the X-ray diffraction diagrams of a PCT film on Pt/TiO₂/Si



$R_W = 13\%$; $R_B = 12\%$; $R_{exp} = 22\%$.(Rietveld)
 $R_W = 5\%$; $R_B = 6\%$ (E-WIMV)

Substrate influence on Residual Stress and Texture

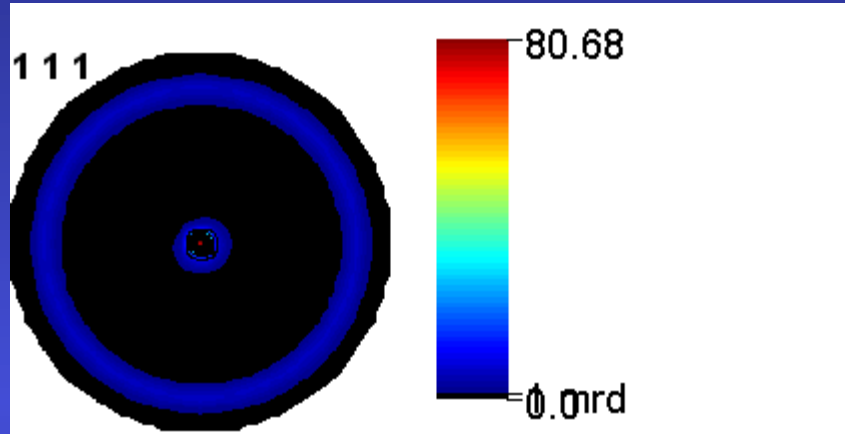


Compliance coefficients [10 ⁻³ GPa ⁻¹]	PbTiO ₃ single crystal (data set A)	Film random orientation	PCT-Si <001> contrib.≈17%	PLT <001> contrib.≈49%	PCT-Mg <001> contrib.≈68%
S ₁₁	6.5	10.1	10.5	10.0	9.7
S ₂₂	6.5	10.0	10.5	10.0	9.7
S ₃₃	33.3	9.8	9.0	10.3	11.3
S ₄₄	14.5	13.2	12.8	12.9	13.1
S ₅₅	14.5	13.2	12.8	13.0	13.1
S ₆₆	9.6	13.4	14.0	13.5	12.7
S ₁₂	-0.35	-3.3	-3.5	-3.2	-3.0
S ₂₁	-0.35	-3.3	-3.5	-3.2	-3.0
S ₁₃	-7.1	-3.2	-3.1	-3.4	-3.6
S ₃₁	-7.1	-3.2	-3.1	-3.4	-3.6
S ₂₃	-7.1	-3.2	-3.1	-3.4	-3.6
S ₃₂	-7.1	-3.2	-3.1	-3.4	-3.6
S ₃₃ /S ₁₁	5.1	0.97	0.86	1.03	1.16
S ₁₃ /S ₁₂	20.3	0.97	0.89	1.06	1.20

Geometric mean average + biaxial stress state

Ferroelectric PMN-PT films

J. Ricote, DMF-Madrid



Pt

$$a = 3.91172(1) \text{ \AA}$$

$$T = 583(5) \text{ \AA}$$

$$t_{\text{iso}} = 960(1) \text{ \AA}$$

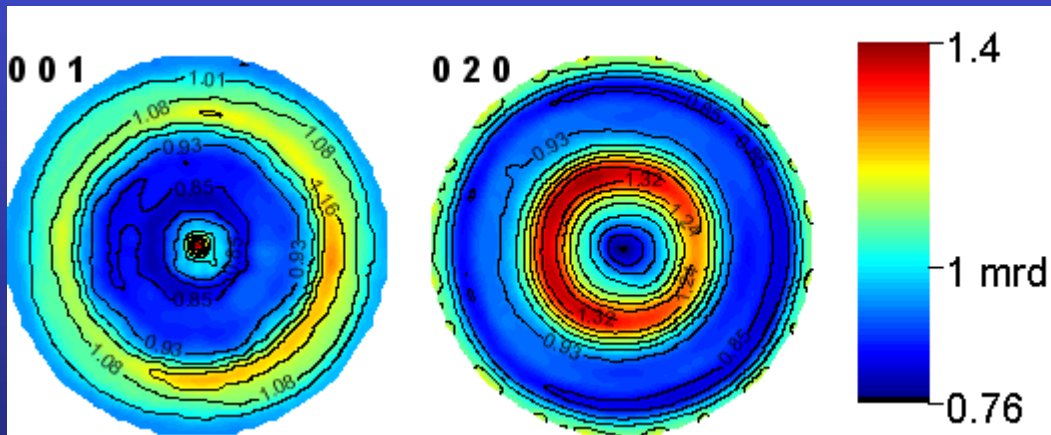
$$\varepsilon = 0.0032(1) \text{ rms}$$

$$\sigma_{11} = 0.639(1) \text{ GPa}$$

$$\sigma_{22} = 0.651(1) \text{ GPa}$$

$$\sigma_{12} = -0.009(1) \text{ GPa}$$

$\text{Pb}_{0.7}(\text{Mg}_{1/3}\text{Nb}_{2/3})\text{O}_3\text{-Pb}_{0.3}\text{TiO}_3 / \text{TiO}_2 / \text{Pt} / \text{Si-(100)}$



$$a = 5.67858(9) \text{ \AA}$$

$$b = 5.69038(9) \text{ \AA}$$

$$c = 3.99558(4) \text{ \AA}$$

$$\beta = 90.392(1) \text{ \AA}$$

$$T = 1322(9) \text{ \AA}$$

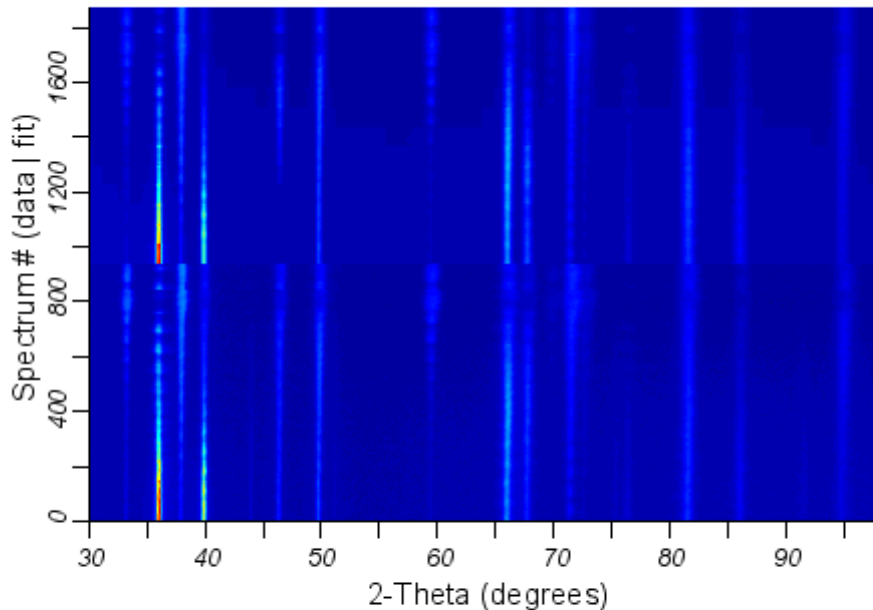
$$t_{\text{iso}} = 1338(2) \text{ \AA}$$

$$\varepsilon = 0.0067(1) \text{ rms}$$

AIN/Pt/TiO_x/Al₂O₃/Ni-Co-Cr-Al

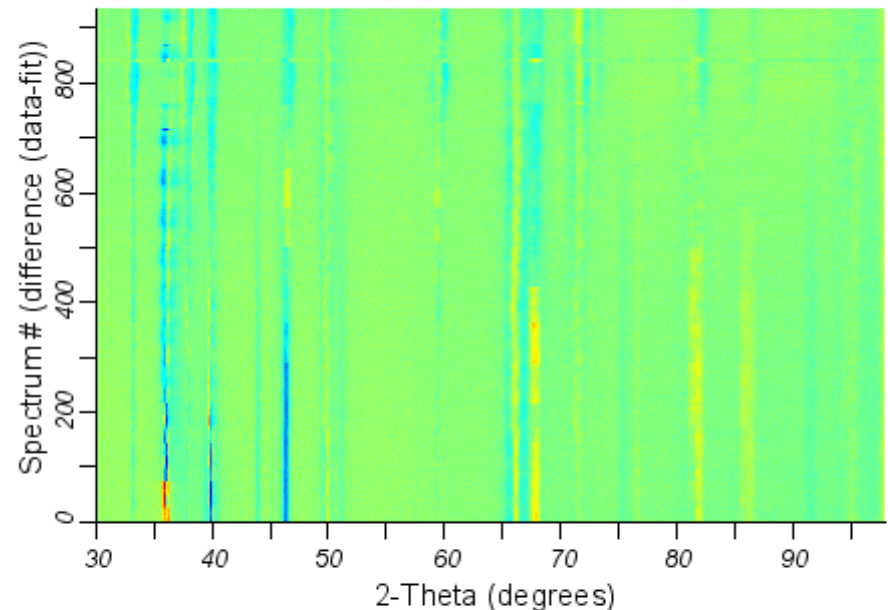
2D Multiplot for Data 05_37P64

measured data and fit



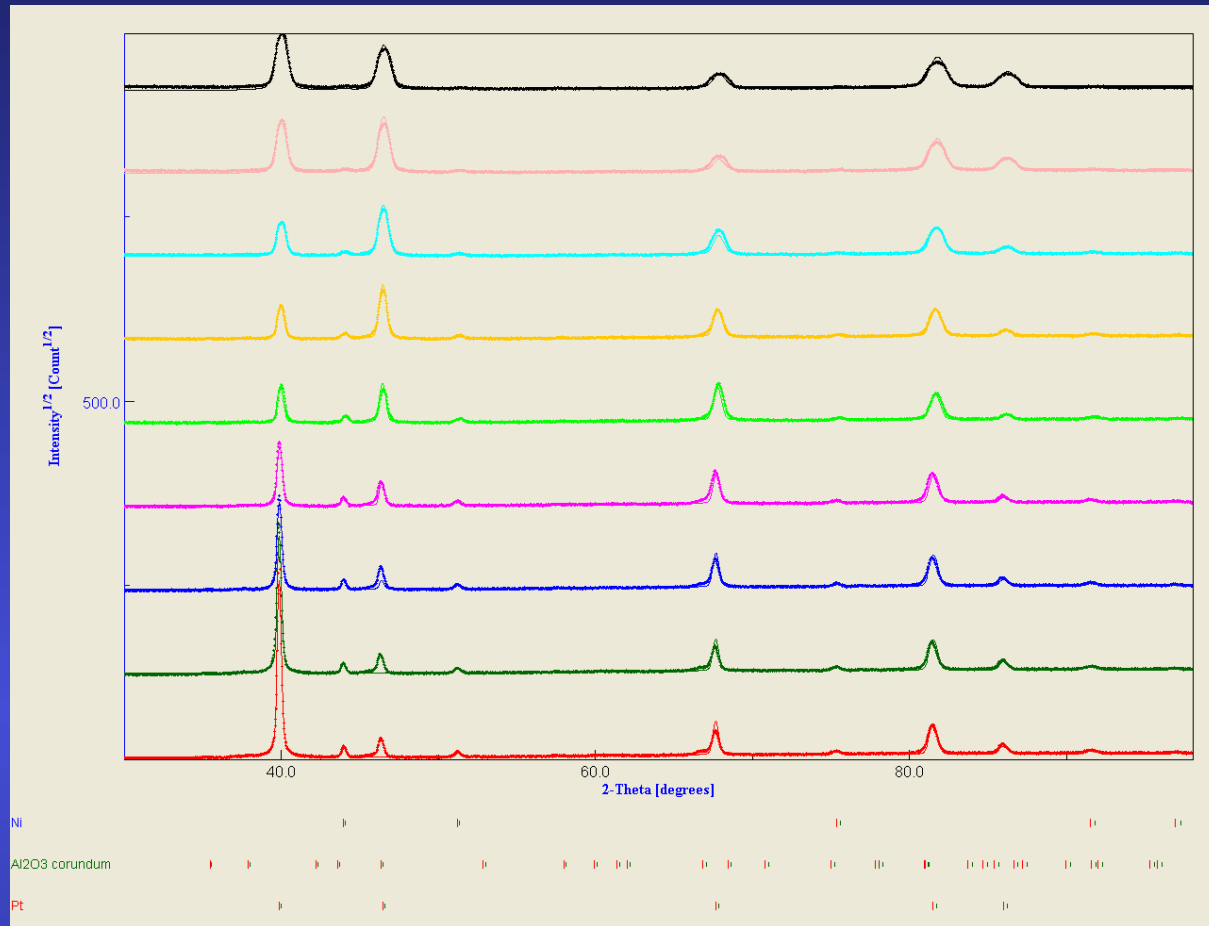
2D difference plot for Data 05_37P64

difference data - fit

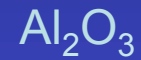


Rw (%) = 24.120445
Rexp (%) = 5.8517213

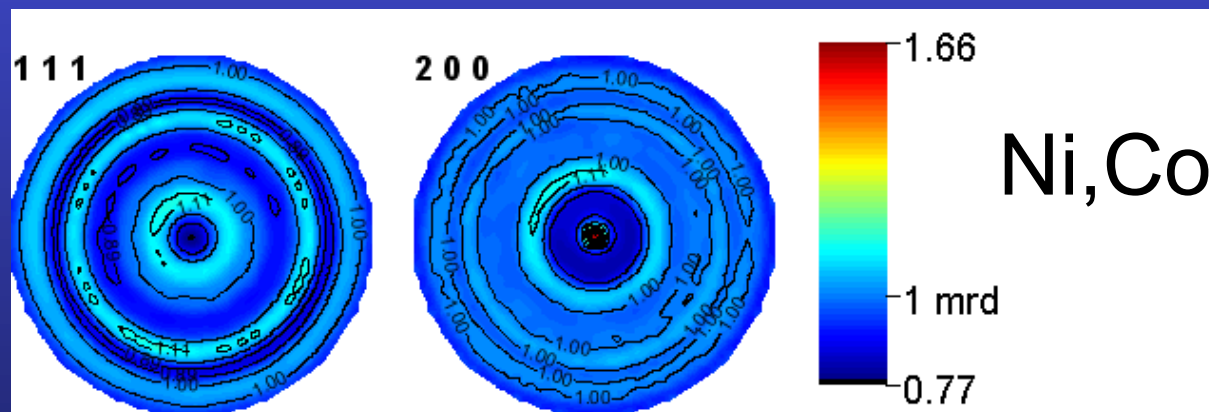
T(AIN) = 14270(3) nm
T(Pt) = 430(3) nm



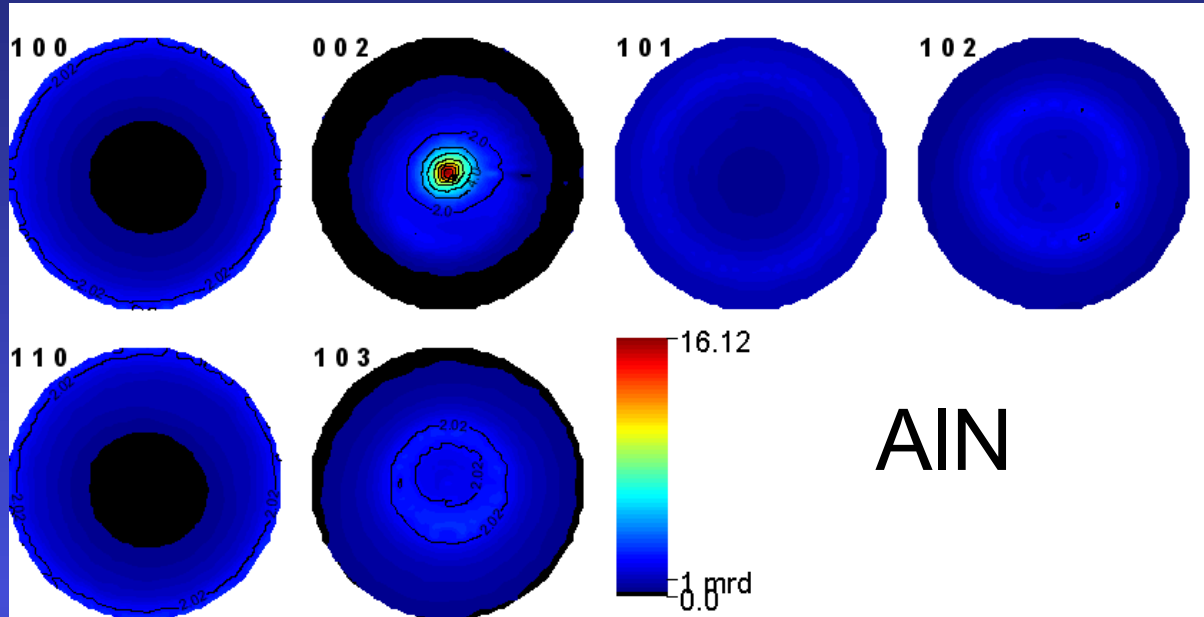
(χ, φ) randomly
selected diagrams



$a = 4.7562(6) \text{ \AA}$
 $c = 12.875(3) \text{ \AA}$
 $T = 7790(31) \text{ nm}$
 $\langle t \rangle = 150(2) \text{ \AA}$
 $\langle \varepsilon \rangle = 0.008(3)$



$a = 3.569377(5) \text{ \AA}$
 $\langle t \rangle = 7600(1900) \text{ \AA}$
 $\langle \varepsilon \rangle = 0.00236(3)$
 $\sigma_{11} = -328(8) \text{ MPa}$
 $\sigma_{22} = -411(9) \text{ MPa}$



Rw (%) = 4.1

$a = 3.11203(1) \text{ \AA}$

$c = 4.98252(1) \text{ \AA}$

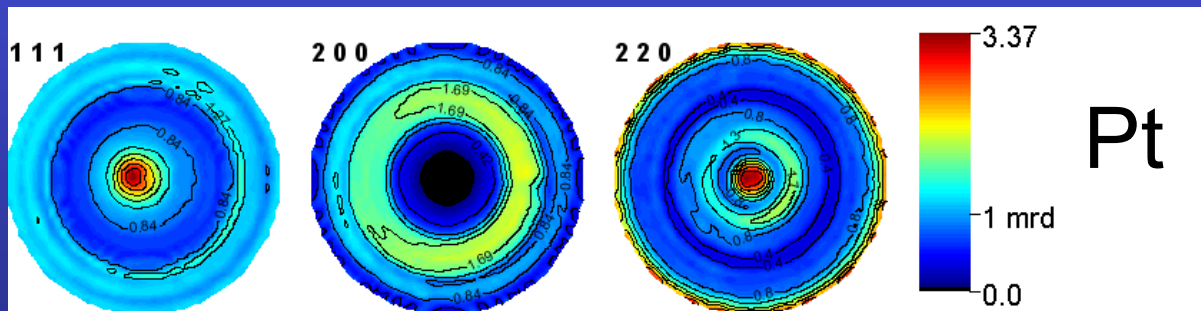
$T = 14270(3) \text{ nm}$

$\langle t \rangle = 2404(8) \text{ \AA}$

$\langle \varepsilon \rangle = 0.001853(2)$

$\sigma_{11} = -1019(2) \text{ MPa}$

$\sigma_{22} = -845(2) \text{ MPa}$



Rw (%) = 33.3

$a = 3.91198(1) \text{ \AA}$

$T = 1204(3) \text{ nm}$

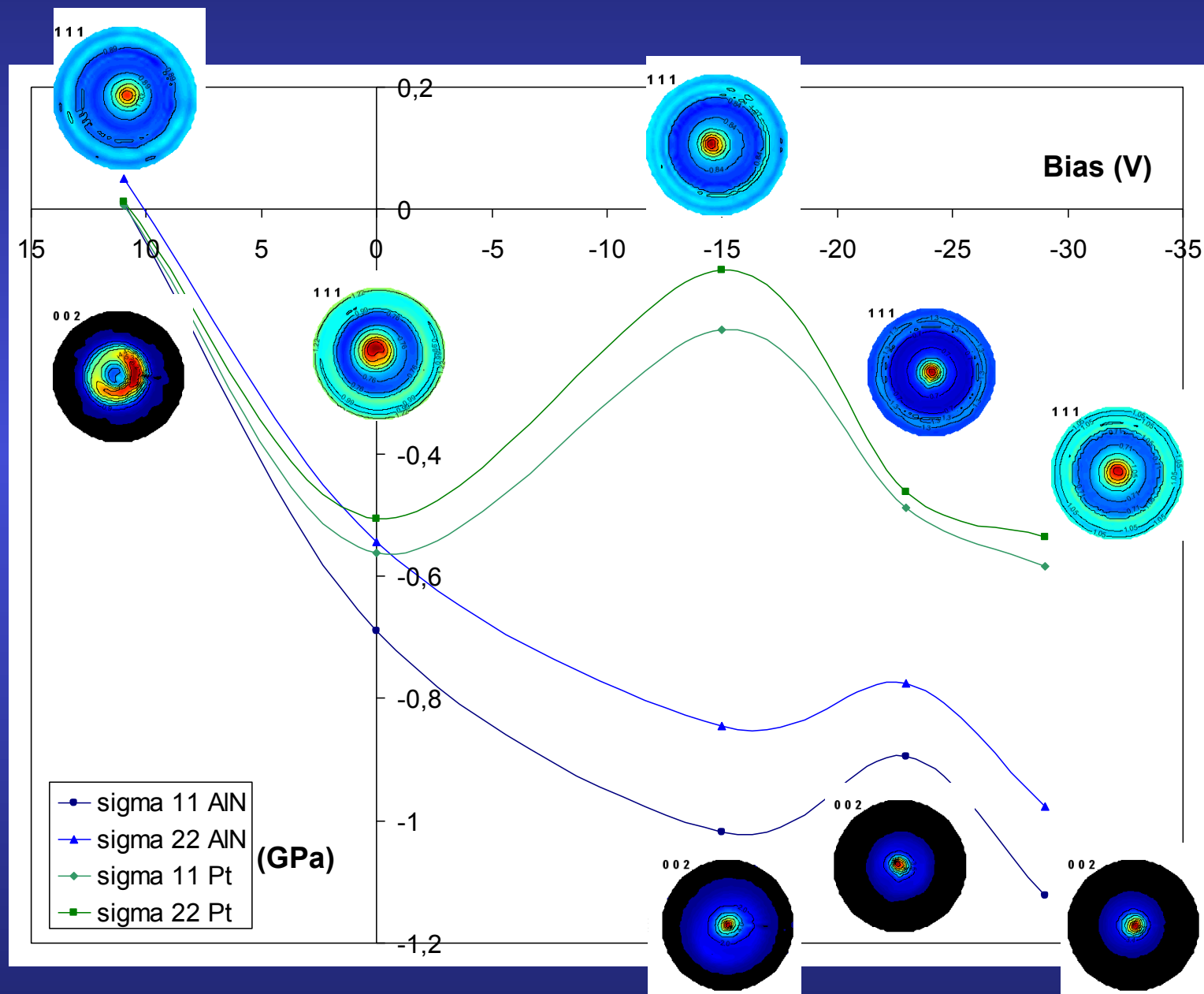
$\langle t \rangle = 2173(10) \text{ \AA}$

$\langle \varepsilon \rangle = 0.002410(3)$

$\sigma_{11} = -196.5(8)$

$\sigma_{22} = -99.6(6)$

Substrate bias vs stress-texture evolution



Si nanocrystalline thin films

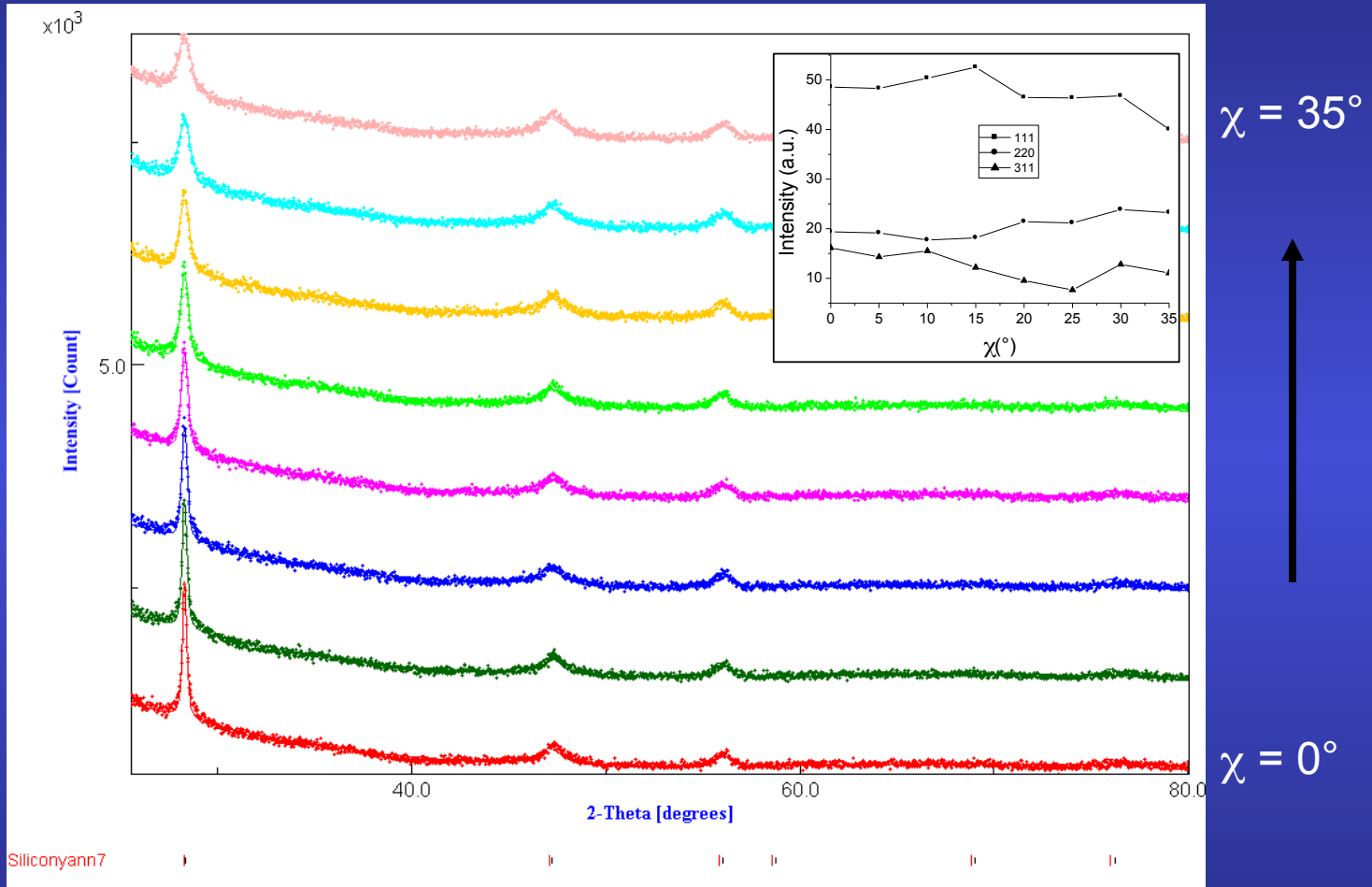
M. Morales, Caen

Silicon thin films deposition by reactive magnetron sputtering:

- ⇒ power density $2\text{W}/\text{cm}^2$
- ⇒ total pressure: $p_{\text{total}} = 10^{-1}$ Torr
- ⇒ plasma mixture: H_2 / Ar , $p_{\text{H}_2} / p_{\text{total}} = 80 \%$
- ⇒ temperature: 200°C
- ⇒ substrates: amorphous SiO_2 (a- SiO_2)
(100)-Si single-crystals
- ⇒ target-substrate distance (d)
 - a- SiO_2 substrates: $d = 4, 6, 7, 8, 10, 12$ cm
films A, B, C, D, E, F
 - (100)-Si: $d = 6, 12$ cm
films G, H

Aim: quantum confinement, photoluminescence properties

Typical refinement

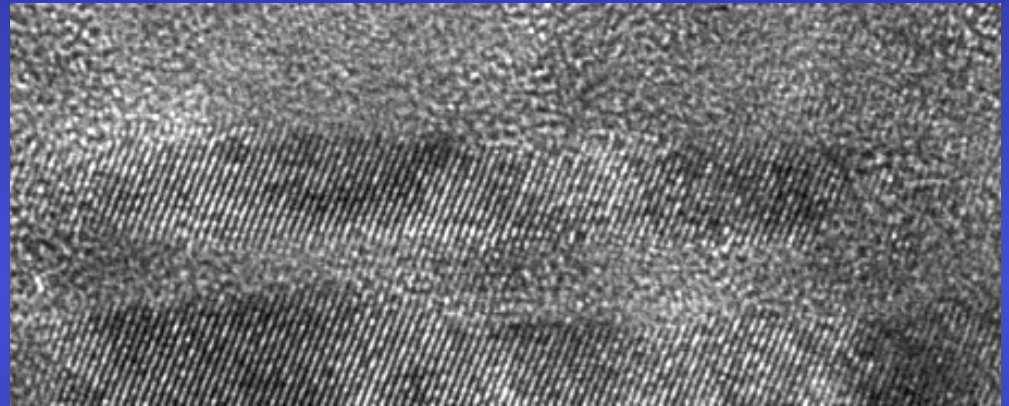
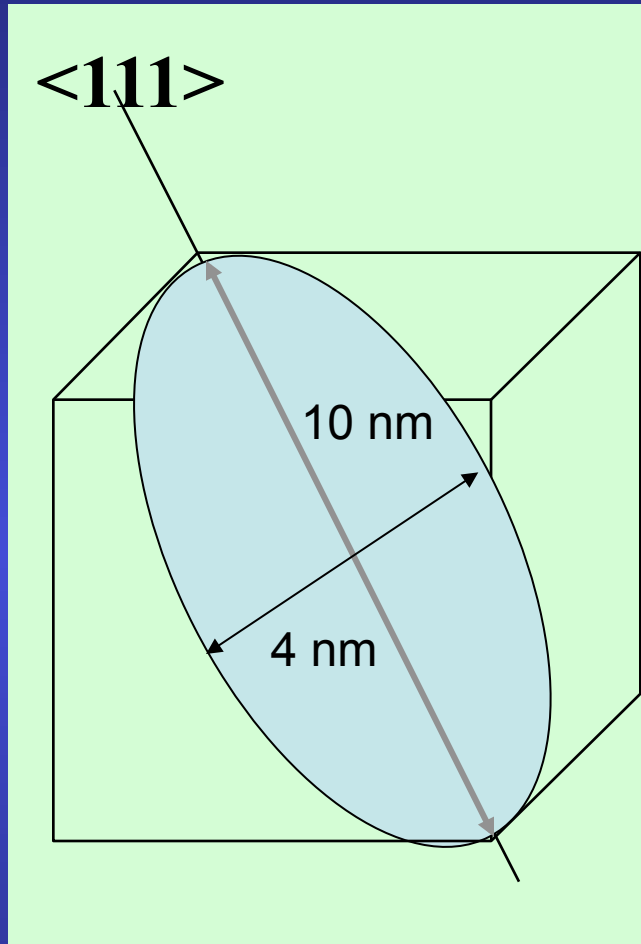


broad, anisotropic diffracted lines, textured samples

Refinement Results

Sample	d (cm)	a (Å)	RX thickness (nm)	Anisotropic sizes (Å)			Texture parameters			Reliability factors (%)			
				<111>	<220>	<311>	Maximum (m.r.d.)	minimum (m.r.d.)	Texture index F ² (m.r.d ²)	RP ₀	R _w	R _B	R _{exp}
A	4	5.4466 (3)	—	94	20	27	1.95	0.4	1.12	1.72	4.0	3.7	3.5
B	6	5.4439 (2)	711 (50)	101	20	22	1.39	0.79	1.01	0.71	4.9	4.3	4.2
C	7	5.4346 (4)	519 (60)	99	40	52	1.72	0.66	1.05	0.78	4.3	4.0	3.9
D	8	5.4461 (2)	1447 (66)	100	22	33	1.57	0.63	1.04	0.90	5.5	4.6	4.5
E	10	5.4462 (2)	1360 (80)	98	20	25	1.22	0.82	1.01	0.56	5.0	3.9	4.0
F	12	5.4452 (3)	1110 (57)	85	22	26	1.59	0.45	1.05	1.08	4.2	3.5	3.7
G	6	5.4387 (3)	1307 (50)	89	22	28	1.84	0.71	1.01	1.57	5.2	4.7	4.2
H	12	5.4434 (2)	1214 (18)	88	22	24	2.77	0.50	1.12	2.97	5.0	4.5	4.3

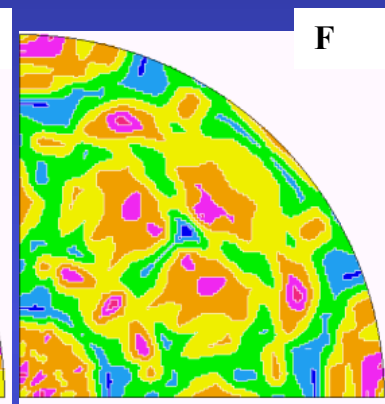
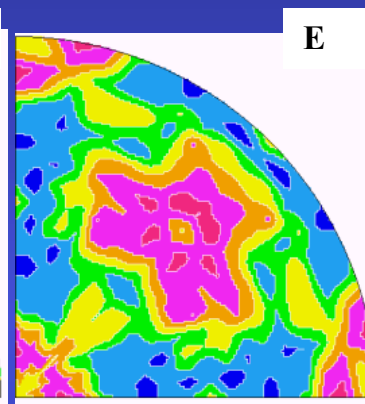
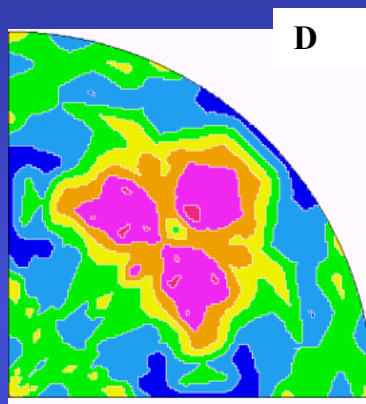
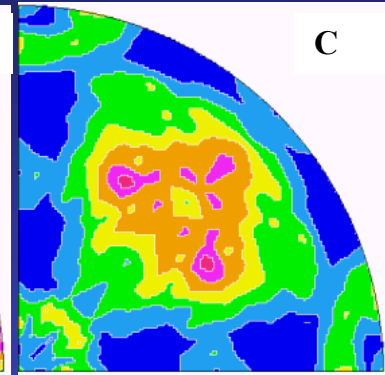
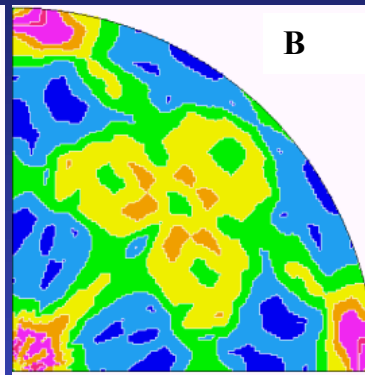
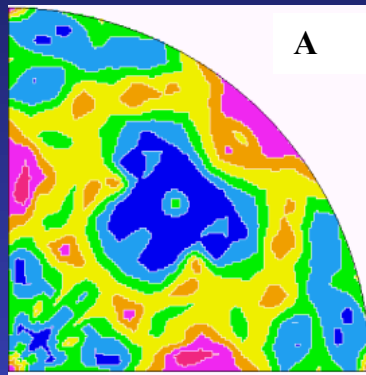
Mean anisotropic shape



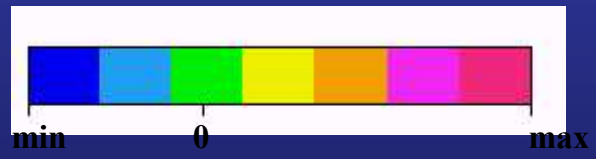
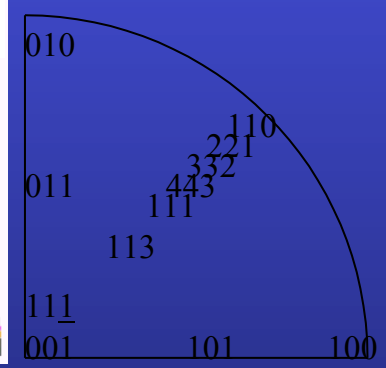
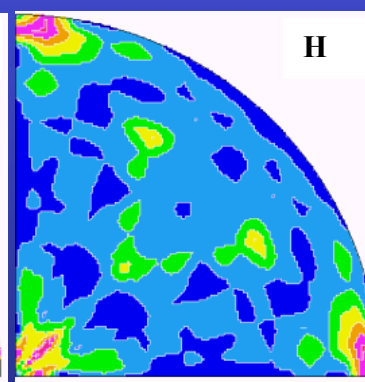
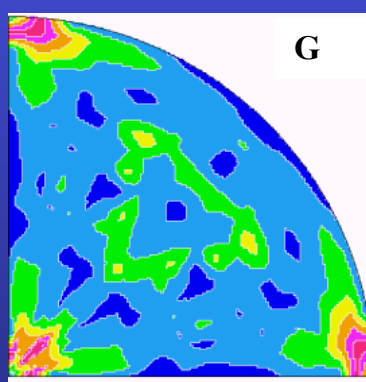
Schematic of the mean crystallite shape for Sample D represented in a cubic cell, as refined using the Popa approach and exhibiting a strong elongation along $\langle 111 \rangle$, and TEM image

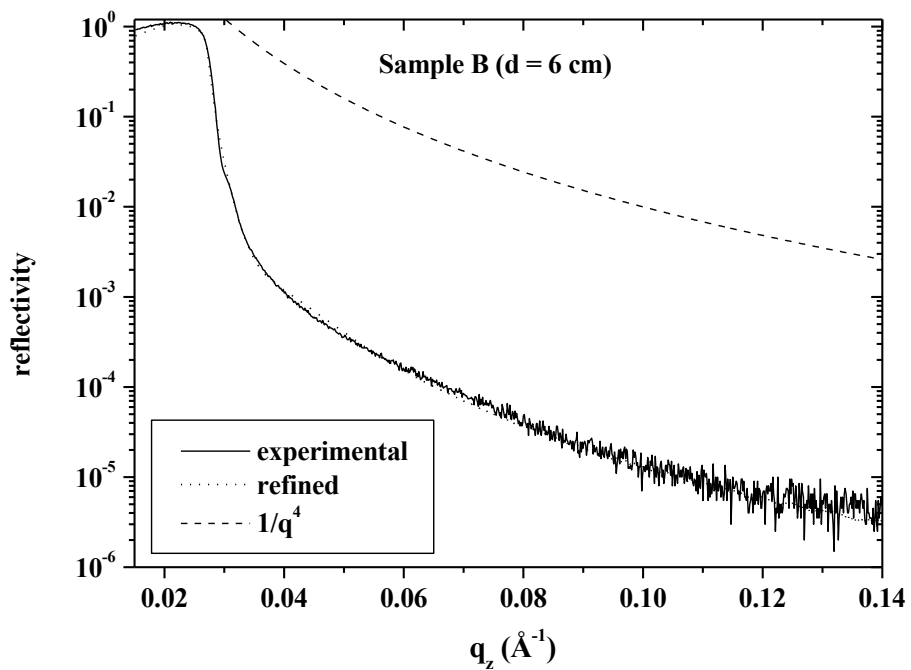
001 Inverse Pole Figures

a-SiO₂



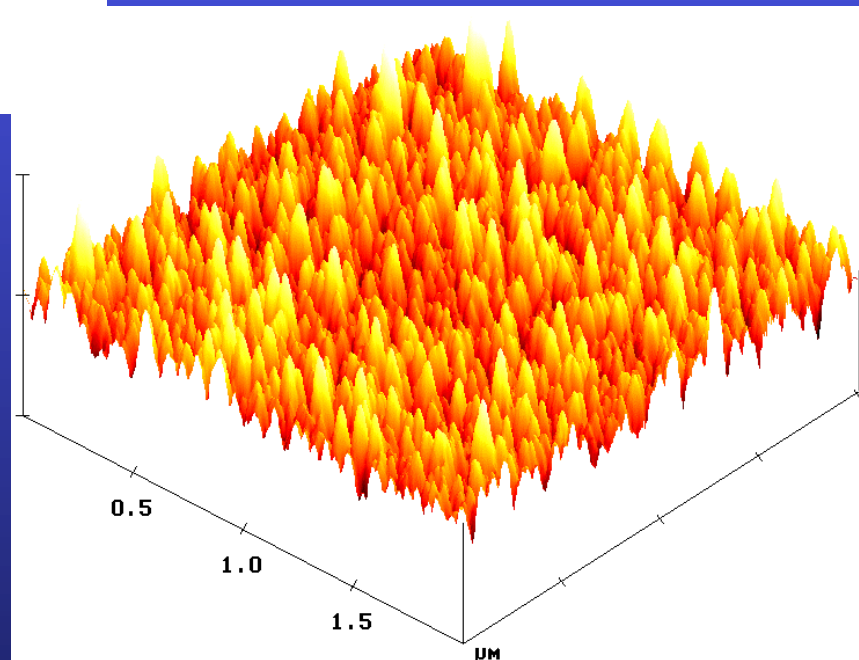
(100)-Si

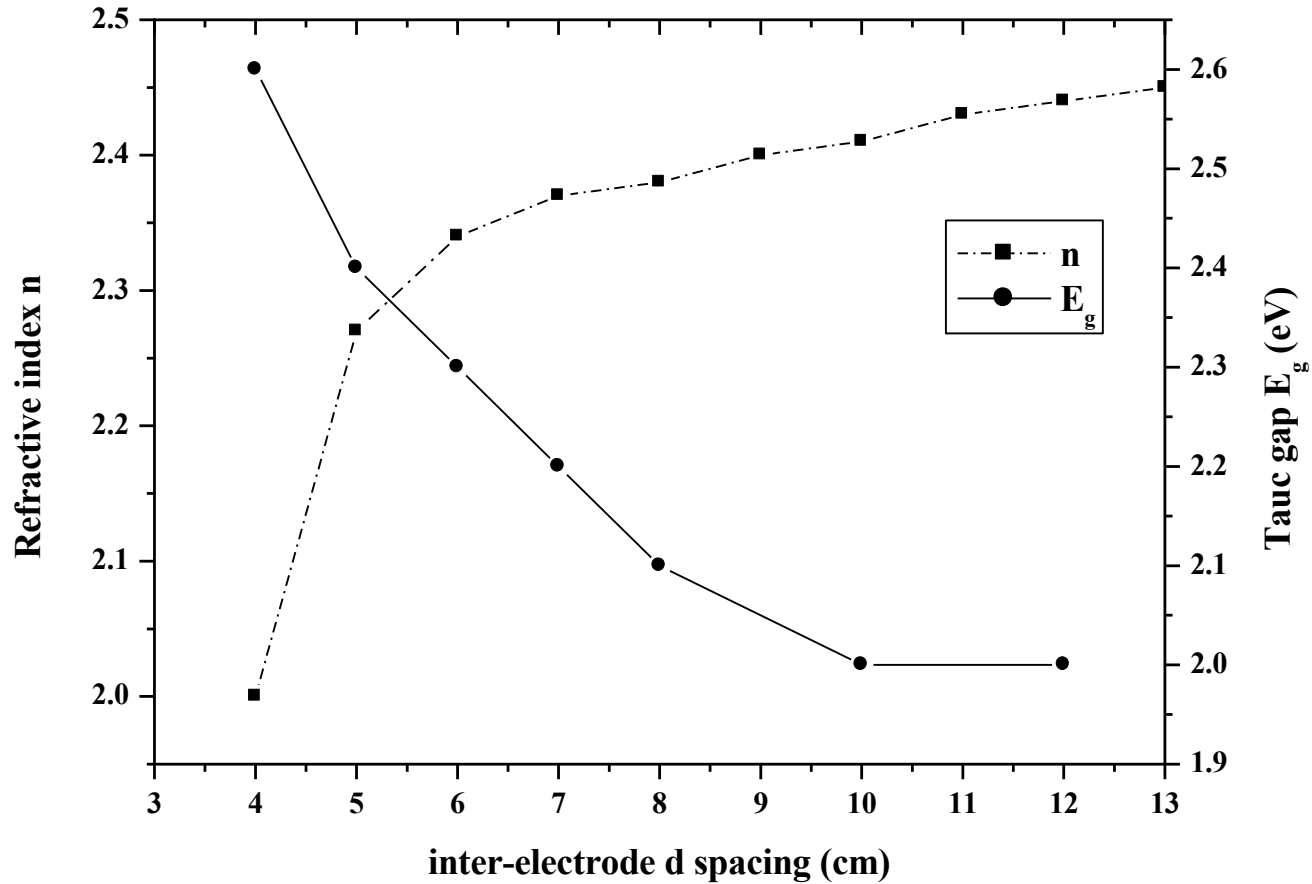




XRR:
Roughness
governed

AFM:
homogeneous
roughness





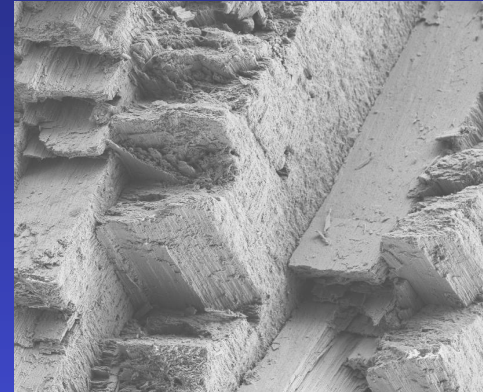
↪ Refractive index linked to film porosities:
 Larger target-sample distances: increased compacity due to lower
 nanopowder filling

Aragonitic layers in mollusc shells

Gastropods

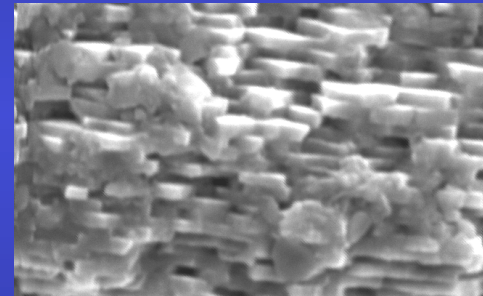
*Crossed
lamellar layers*

Charonia lampas lampas (triton or trumpet cousin)



*Columnar
Nacre*

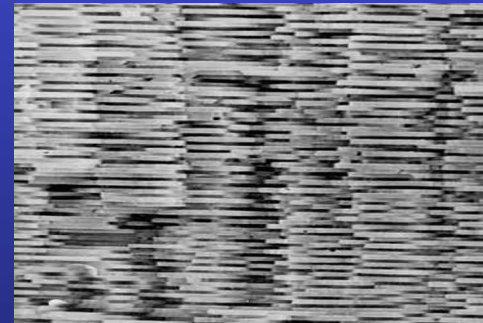
Haliotis tuberculata (common abalone)

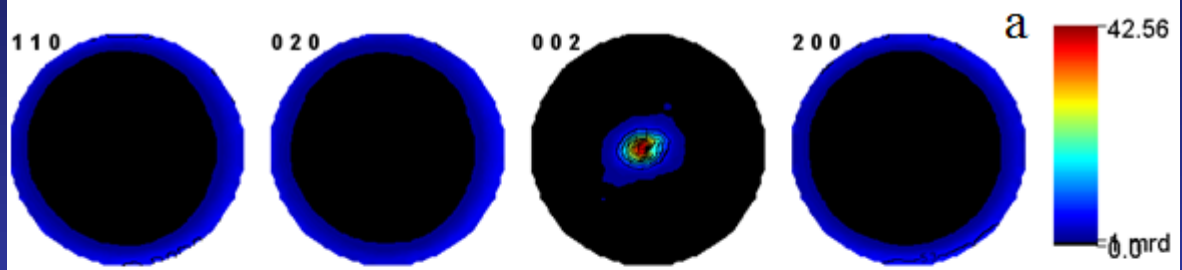


Bivalves

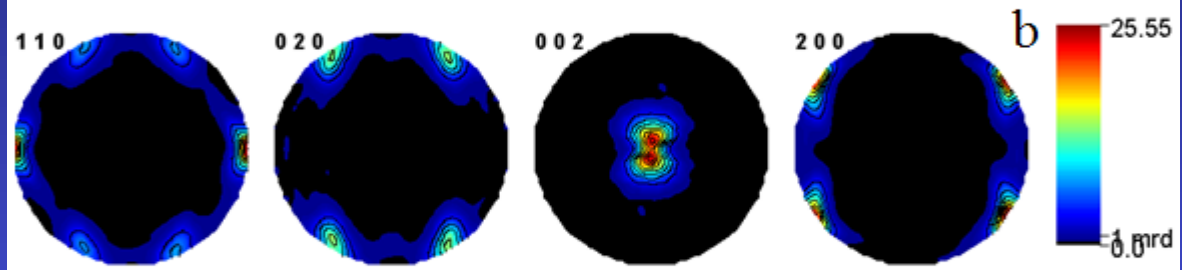
Sheet Nacre

Pinctada maxima (Mother of pearl oyster)

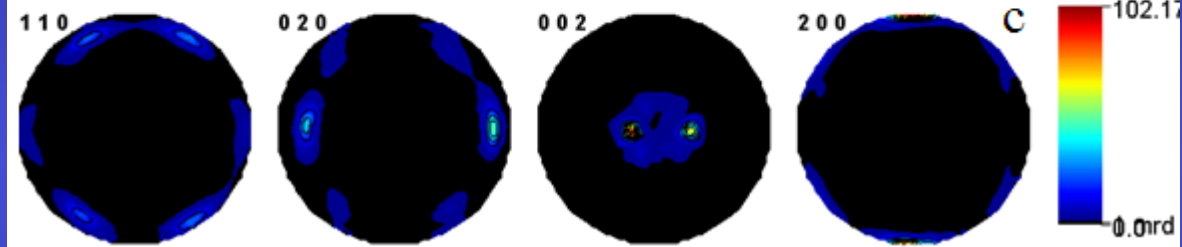




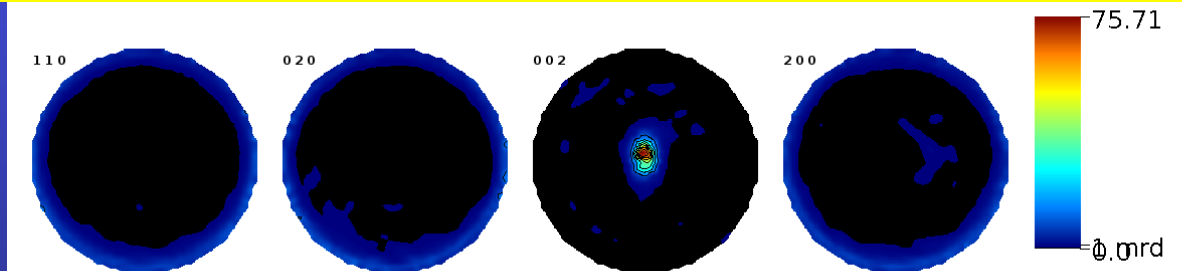
Outer CL
43 mrd²



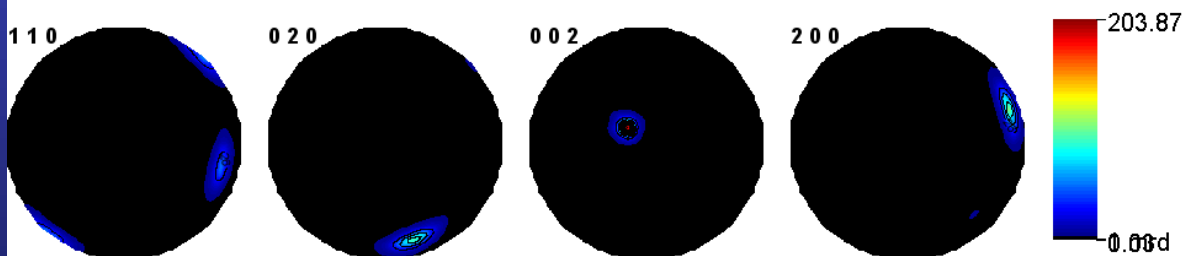
Inter Radial CL
47 mrd²



Inner Com CL
721 mrd²



Inner Columnar Nacre
211 mrd²



Inner Sheet Nacre
1100 mrd²

Unit-cell distortions

	OCL	<i>Charonia</i> IRCL	ICCL	<i>Pinctada</i> ISN	<i>Haliotis</i> ICN
a (Å)	4,98563(7)	4,97538(4)	4,9813(1)	4,97071(4)	4.9480(2)
b (Å)	8,0103(1)	7,98848(8)	7,9679(1)	7,96629(6)	7.9427(6)
c (Å)	5,74626(3)	5,74961(2)	5,76261(5)	5,74804(2)	5.7443(6)
$\Delta a/a$	0,0047	0,0026	0,0038	0.0017	-0.0029
$\Delta b/b$	0,0053	0,0026	0,0000	-0.0002	-0.0032
$\Delta c/c$	0,0004	0,0010	0,0033	0.0007	0.0007
$\Delta V/V$ (%)	1,05	0,62	0,71	0.22	-0.60

Anisotropic cell distortion - depends on the layer

Only nacres exhibit (a,b) contraction

Due to inter- and intra-crystalline molecules

Distortions and anisotropies larger than pure intra- effect (Pokroy et al. 2007)

Elastic stiffnesses

Single crystal	160	37.3 87.2	1.7 15.7 84.8	41.2	25.6	42.7
ICCL	96.5	31.6 139	13.7 9.5 87.8	29.8	36.6	40.2
RCL	130.1	32.6 103.3	10.3 14.1 84.5	36.3	31.1	40.5
OCL	111.1	32.9 119	13.2 11.8 84.8	32.8	34.6	40.9

Structural distortions in aragonitic biogenic ceramic composites

**Aplanarity of carbonate groups in
 CaCO_3**

$$\Delta Z_{\text{C-O1}} = c(z_{\text{C}} - z_{\text{O1}})$$

Calcite

*Biogenic
aragonite*

*Mineral
aragonite*

0 \AA

Intermediate ?

0.05744 \AA

Atomic Structures

		Geological reference	<i>Charonia lampas</i> OCL	<i>Charonia lampas</i> IRCL	<i>Charonia lampas</i> ICCL	<i>Strombus decorus</i> mixture	<i>Pinctada maxima</i> ISN
Ca	y	0.41500	0.41418(5)	0.414071(4)	0.41276(9)	0.4135(7)	0.41479 (3)
	z	0.75970	0.75939(3)	0.76057(2)	0.75818(8)	0.7601(8)	0.75939 (2)
C	y	0.76220	0.7628(2)	0.76341(2)	0.7356(4)	0.7607(4)	0.7676 (1)
	z	-0.08620	-0.0920(1)	-0.08702(9)	-0.0833(2)	-0.0851(7)	-0.0831 (1)
O1	y	0.92250	0.9115(2)	0.9238(1)	0.8957(3)	0.9228(4)	0.9134 (1)
	z	-0.09620	-0.09205(8)	-0.09456(6)	-0.1018(2)	-0.0905(9)	-0.09255 (7)
O2	x	0.47360	0.4768(1)	0.4754(1)	0.4864(3)	0.4763(6)	0.4678 (1)
	y	0.68100	0.6826(1)	0.68332(9)	0.6834(2)	0.6833(3)	0.68176 (7)
	z	-0.08620	-0.08368(6)	-0.08473(5)	-0.0926(1)	-0.0863(7)	-0.09060 (4)
ΔZ_{C-O1} (Å)		0.05744	0.00029	0.04335	0.1066	0.031	0,054

Carbonate group aplanarity specific to a given layer

Aplanarity decreases from inner to outer shell layers (CL layers)

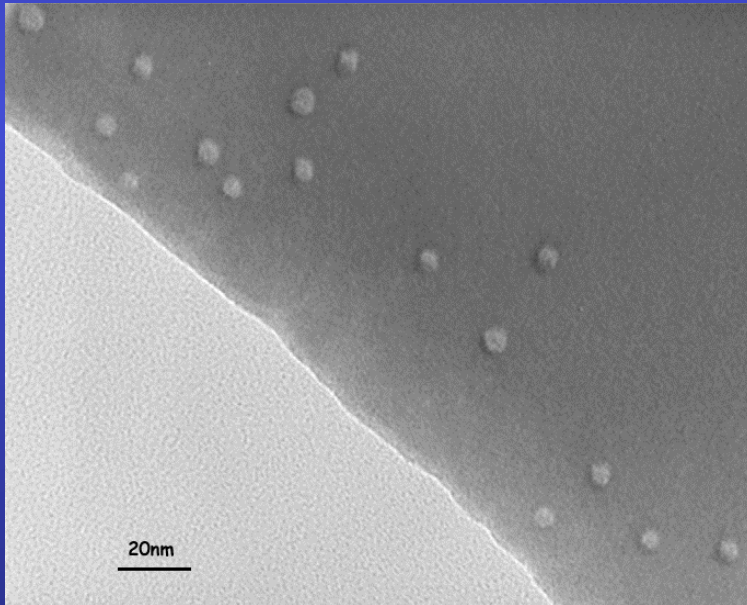
-> up to quite $\Delta Z=0$ outside (nearly the calcite value)

Average aplanarity on the whole shell = geological reference (Strombus)

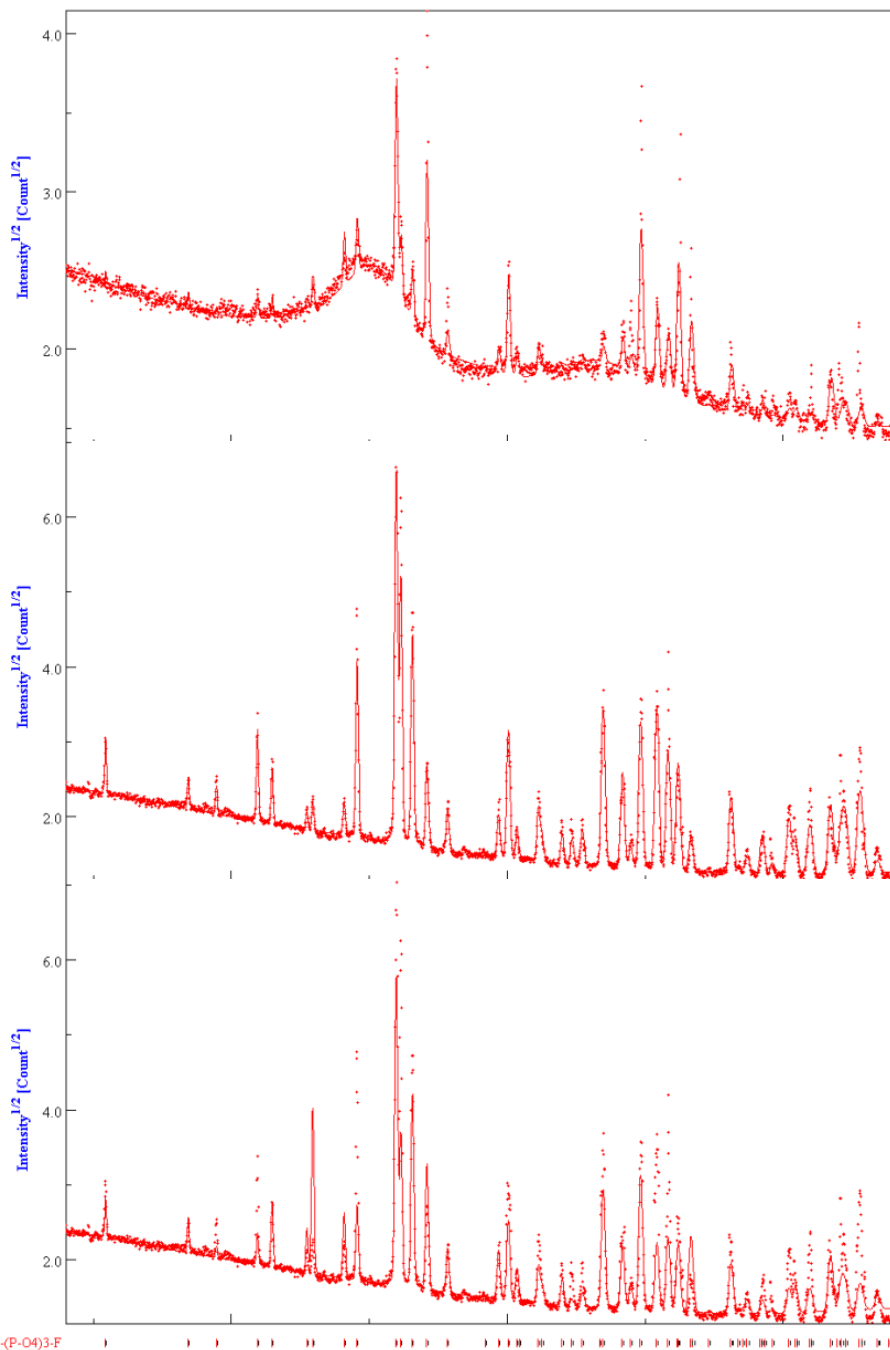
In *Haliotis nacre*: large $\Delta Z=0.08$, + strong anisotropy: less stable nacre

Irradiated FluorApatite (FAp) ceramics

Self-recrystallisation under irradiation, depending on $\text{SiO}_4 / \text{PO}_4$ ratio (FAp / Nd-Britholite) and on irradiating species



TEM of FAp
irradiated with 70
MeV, 10^{12} Kr cm^{-2}
ions



texture corrected,
 10^{13} Kr cm⁻²

Virgin, with texture
correction

Virgin, no texture
correction

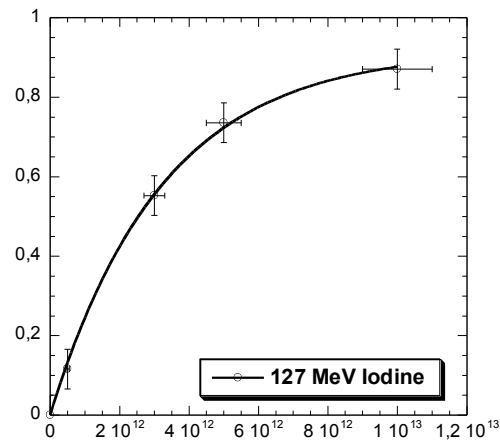
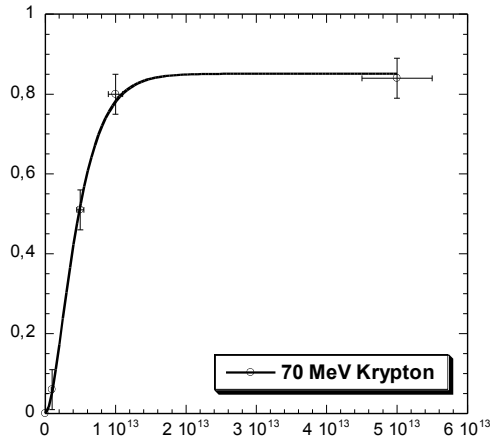
Fluence (ions.cm ⁻²)	Vc/V (%)	A (Å)	c (Å)	<t> (nm)	Δ _a /a ₀ (%)	Δ _c /c ₀ (%)	R _w (%)	R _B (%)
0	100	9.3365(3)	6,8560(5)	294(22)	-	-	14.6	9.1
Kr								
10 ¹¹	100	-	-	-	-	-		
10 ¹²	100	-	-	-	-	-		
5.10 ¹²	49(1)	9.3775(9)	6.8912(8)	294(20)	0.44	0.53	24	15
10 ¹³	20(1)	9.4236(5)	6.9105(5)	291(20)	0.94	0.82	9.9	6
5.10 ¹³	14(1)	9.3160(4)	6.8402(5)	294(22)	-0.21	-0.22	10.5	5.9
I								
10 ¹¹	-	-	-	-	-	-		
5.10 ¹¹	86(2)	9.3603(3)	6.8790(5)	90(10)	0.26	0.35	23.9	15.1
10 ¹²	-	-	-	-	-	-		
3.10 ¹²	47(2)	9.3645(3)	6.8840(5)	91(6)	0.30	0.42	13.3	9
5.10 ¹²	29.2(5)	9.3765(5)	6.8881(6)	77(11)	0.44	0.48	10.4	7.3
10 ¹³	13.2(2)	9.3719(4)	6.8857(6)	82(9)	0.38	0.45	6.7	4.9

Single impact model associated to crystal size reduction

Cell parameters and volume increase, then relax

Amorphisation / recrystallisation competition: single or double impact

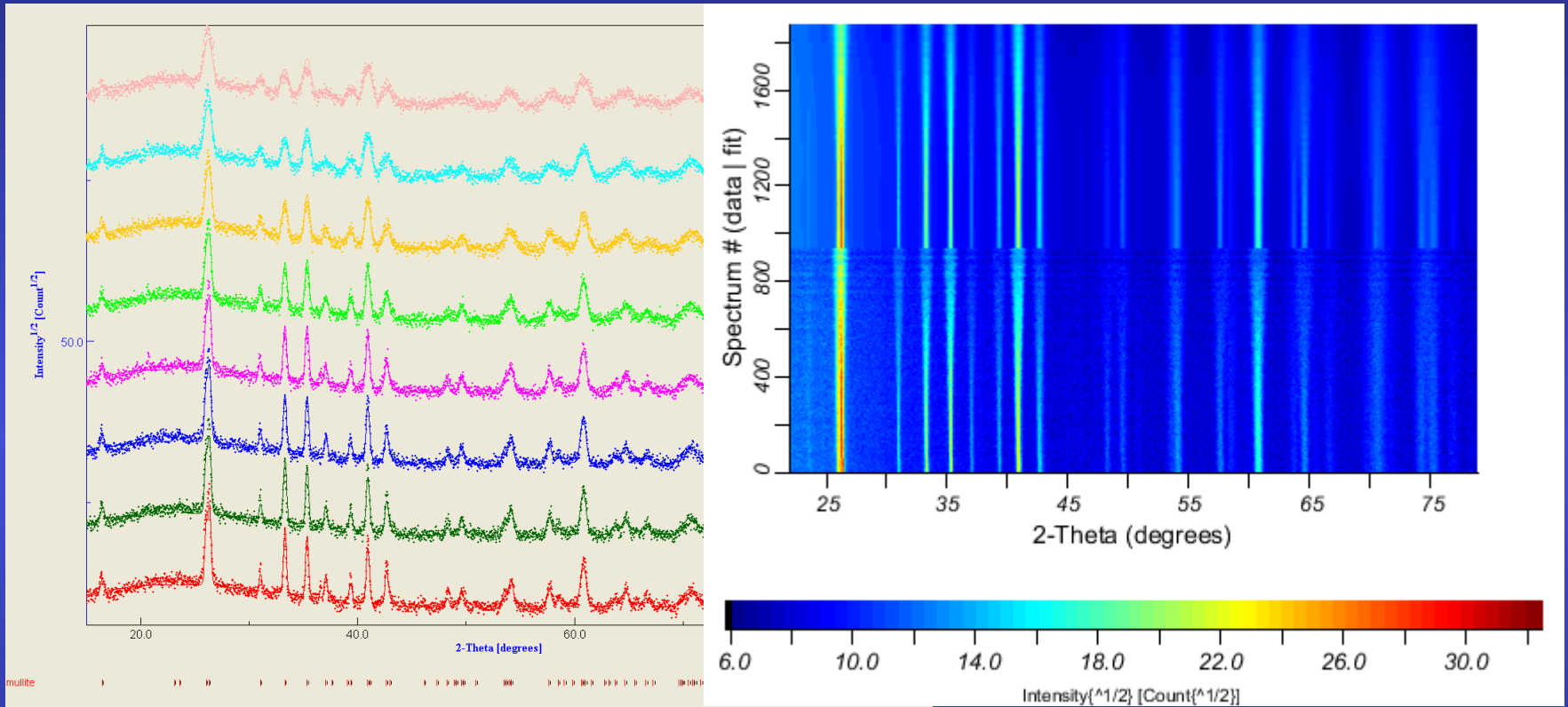
Amorphous/crystalline volume fraction (damaged fraction $F_d = V_a / V$) as determined by x-ray diffraction



B

Fitting parameters	Krypton		Iodine
	Single impact $F_d = B(1 - \exp(-A\phi t))$	Double impact $F_d = B(1 - (1 + A\phi t)\exp(-A\phi t))$	Single impact $F_d = B(1 - \exp(-A\phi t))$
$A = \pi R^2$ (cm ²)	$1.85 \pm 0.15 \cdot 10^{-13}$	$4.1 \pm 0.15 \cdot 10^{-13}$	$3.3 \pm 0.15 \cdot 10^{-13}$
Radius R (nm)	2.4 ± 0.2	3.6	3.2
B (Max.damage rate)	0.87	0.85 ± 0.2	0.92 ± 0.2
χ^2	0.013	0.0006	0.0004

Mullite-silica composites

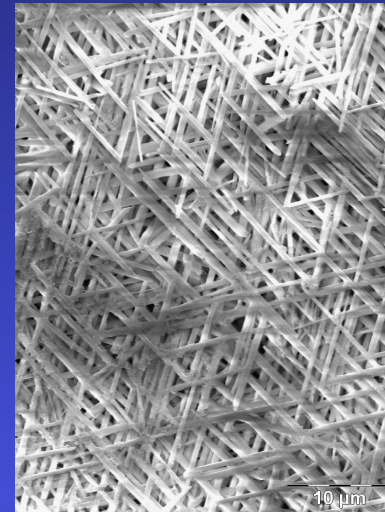
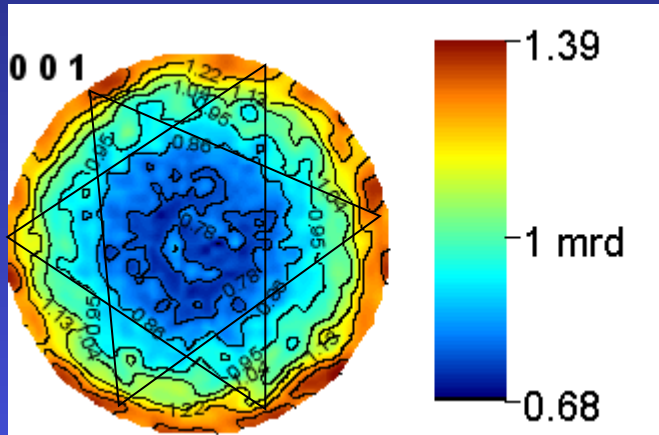


ODF: $R_w = 4.87 \%$, $R_B = 4.01 \%$

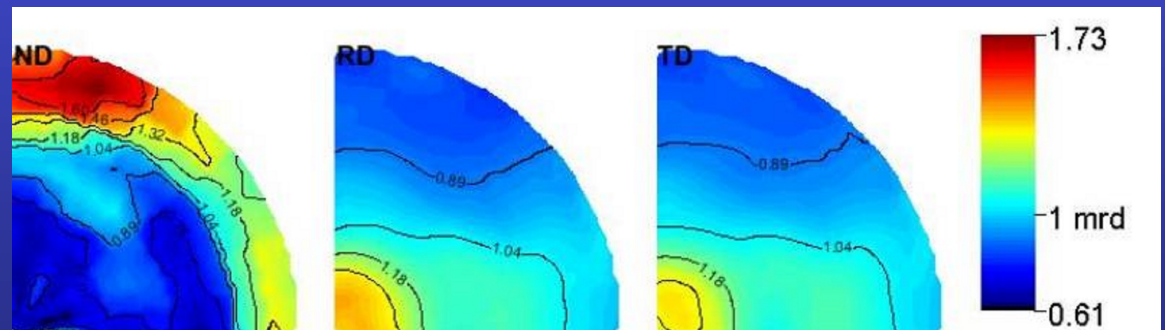
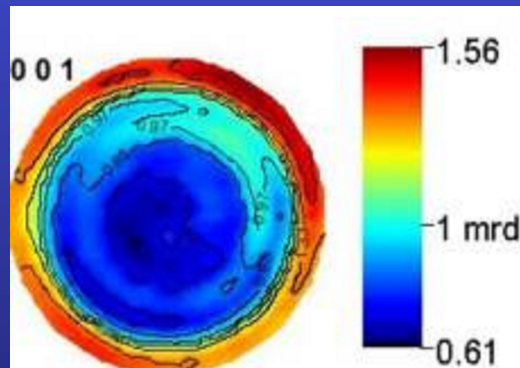
Rietveld: $R_w = 12.90 \%$, GoF = 1.77

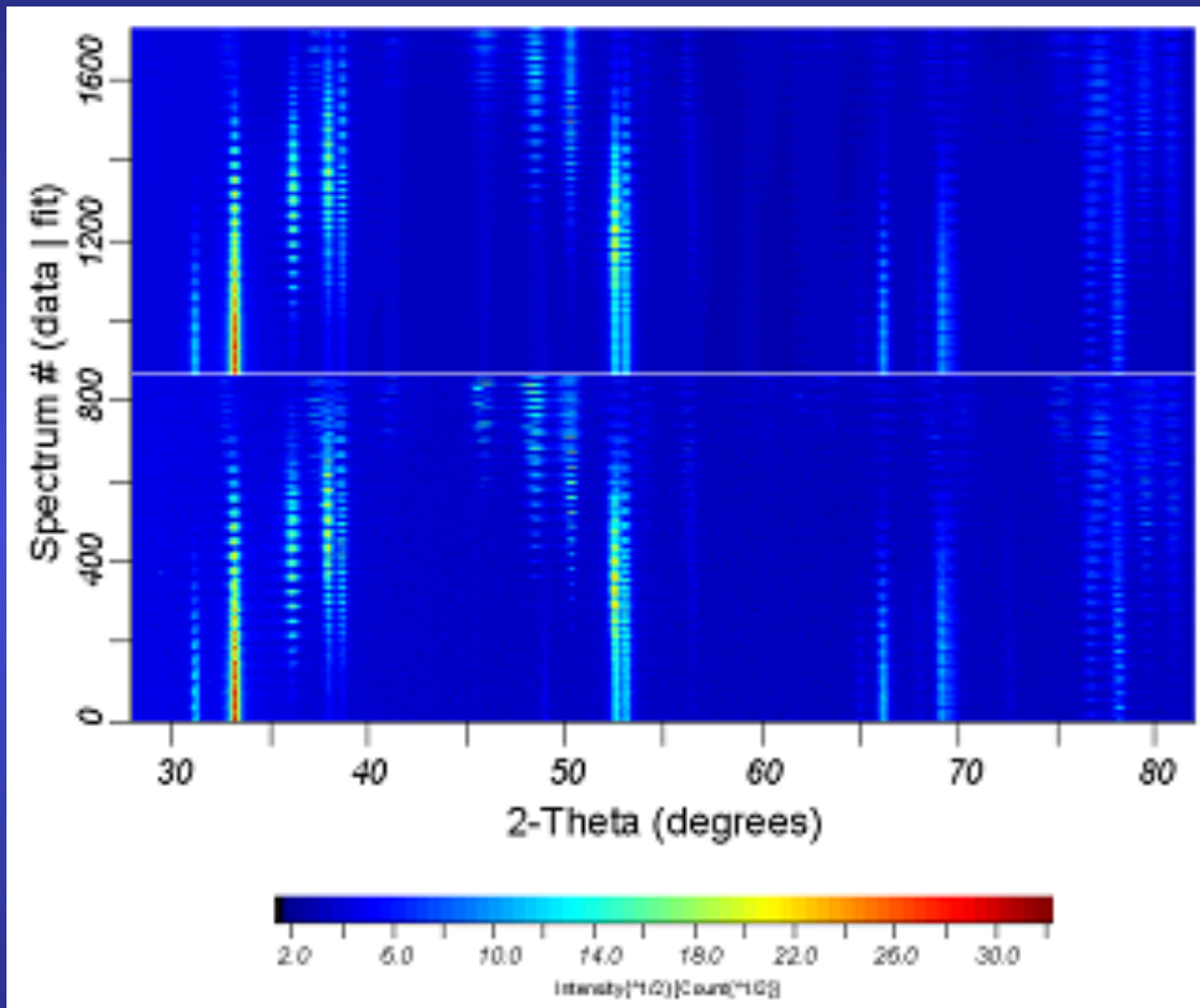
Mullite: $a = 7.56486(5) \text{ \AA}$; $b = 7.71048(5) \text{ \AA}$; $c = 2.89059(1) \text{ \AA}$

Uniaxially pressed



Centrifugated



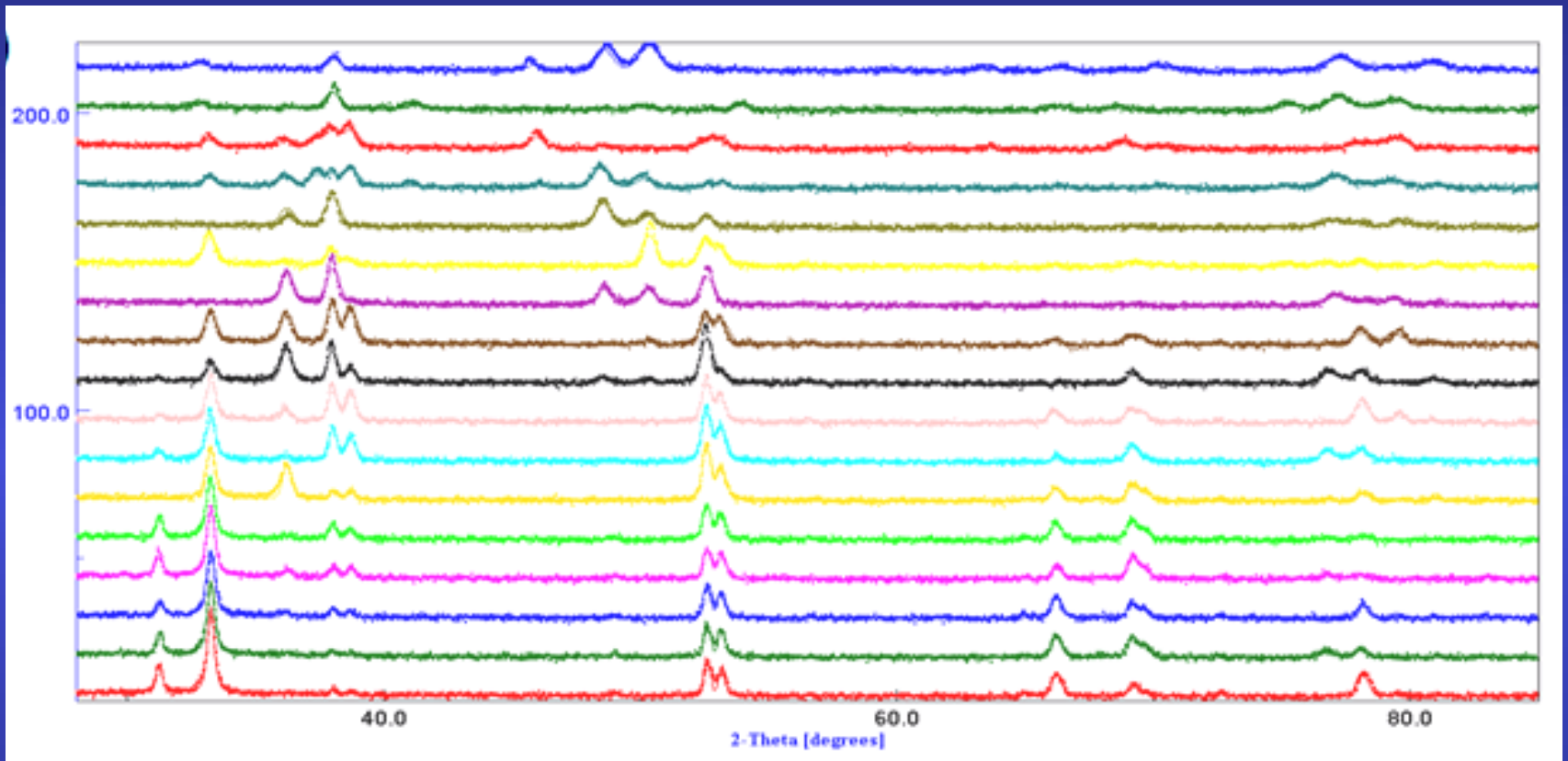


refined

experiments

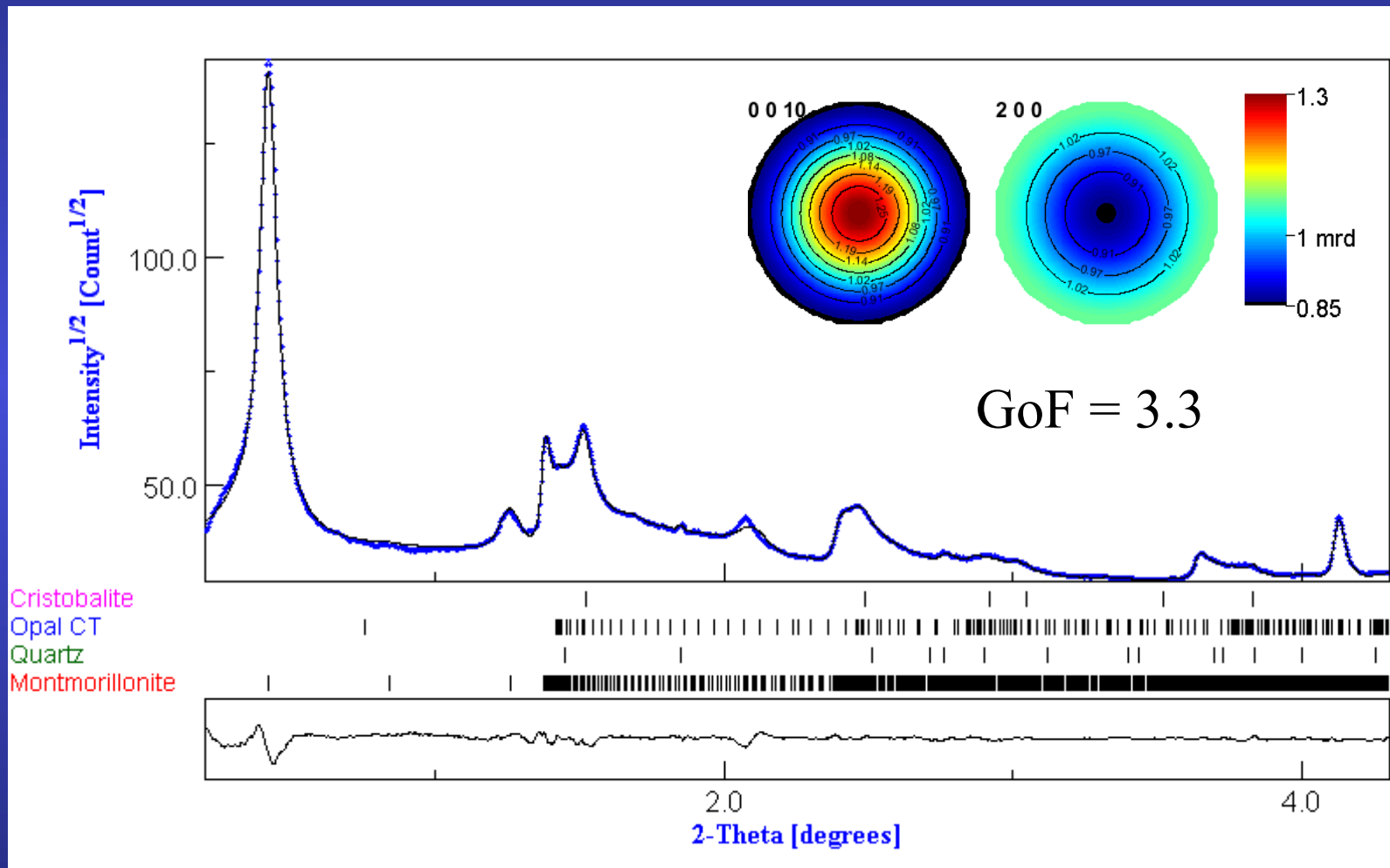
GoF:1,72
R _w : 28,0%
R _{exp} :21,3%

for all (χ, φ) sample orientations

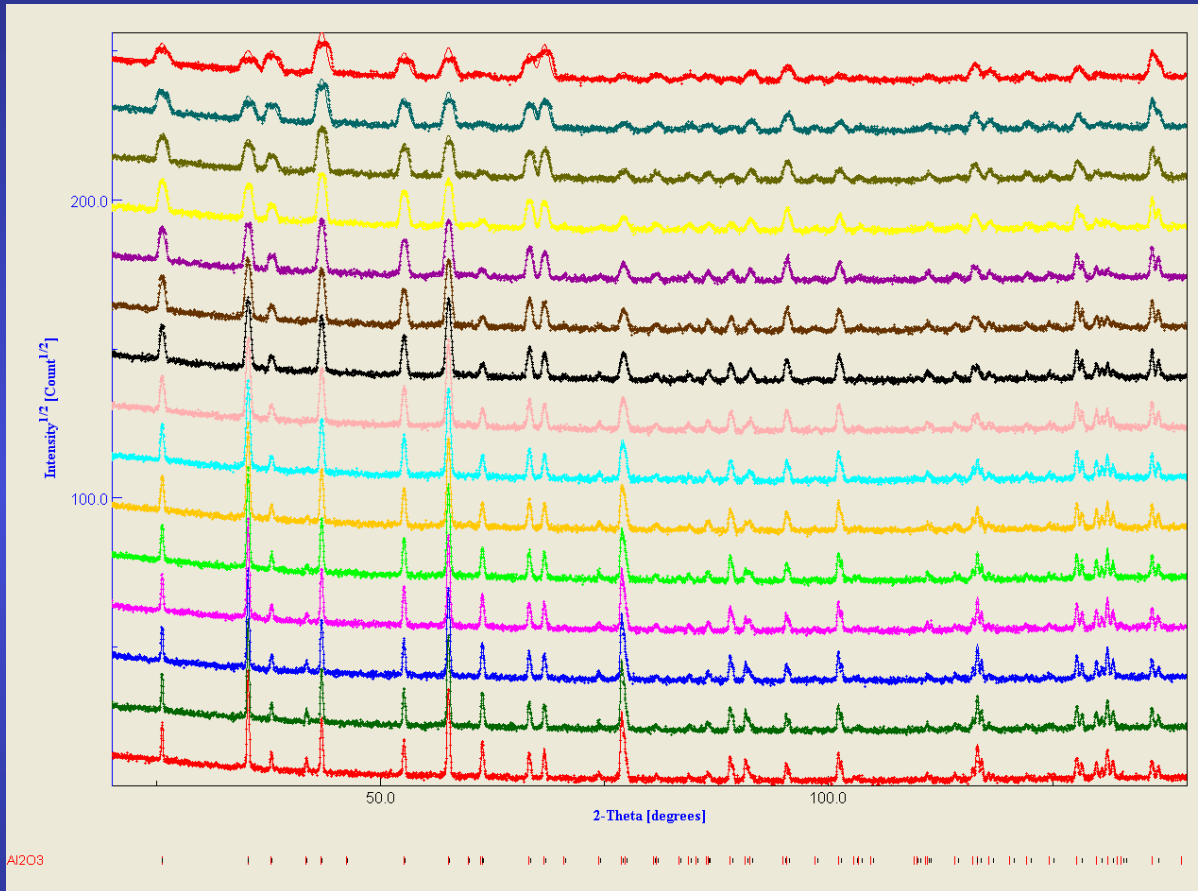


IRC layer of *Charonia lampas lampas* for selected (χ, φ) sample orientations

Turbostratic phyllosilicate aggregates



Al_2O_3 « standard » powder



2 θ -scans:

GoF = 1.92

$R_W = 15.60 \%$

$R_B = 11.94 \%$

θ -2 θ -scans:

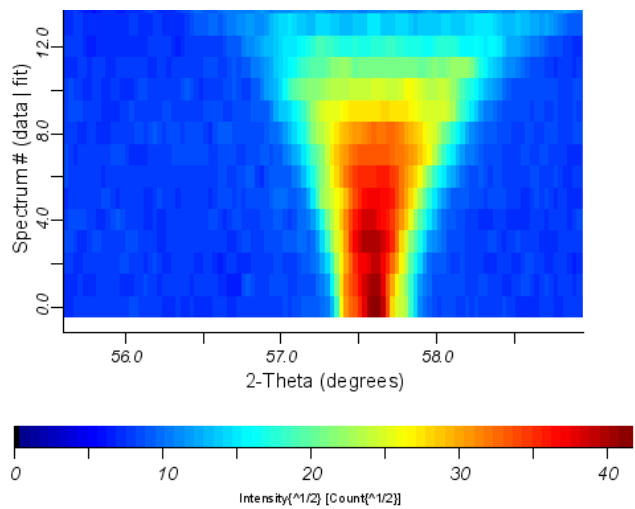
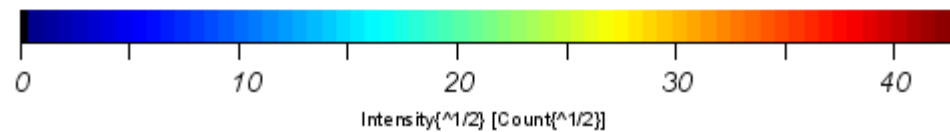
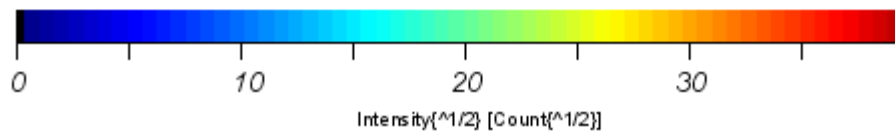
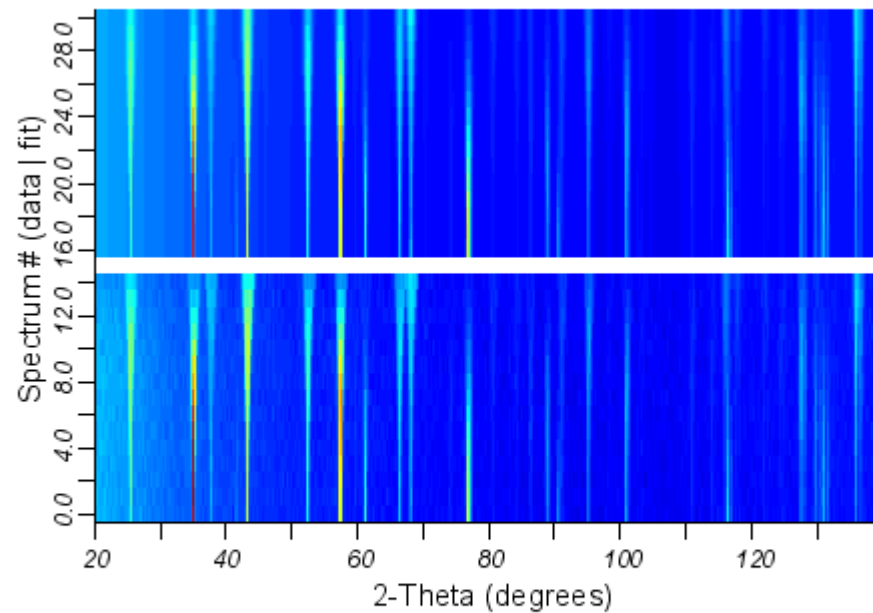
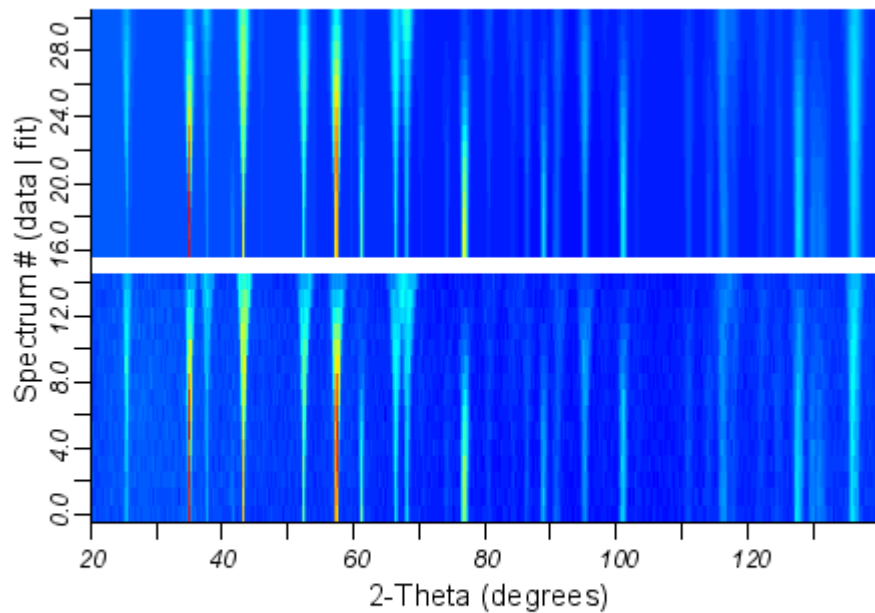
GoF = 1.86

$R_W = 16.11 \%$

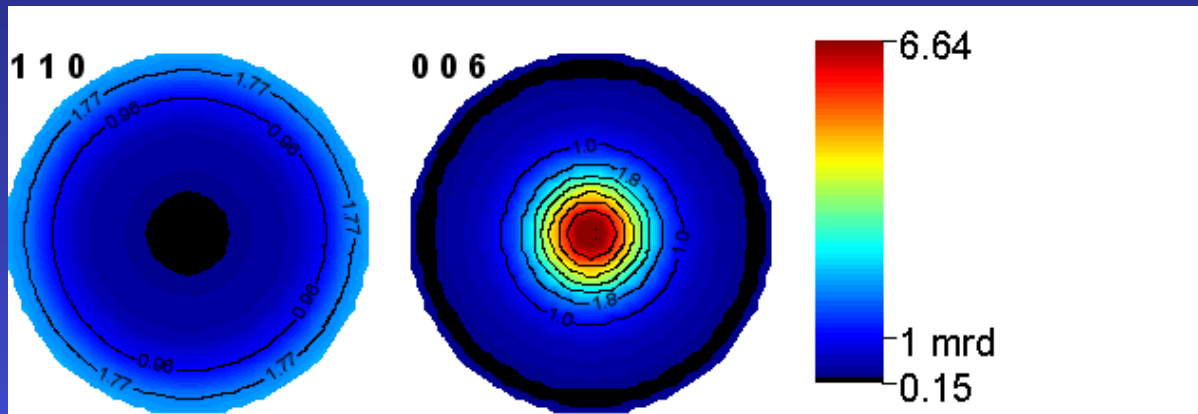
$R_B = 12.40 \%$

15 diagrams x 5 mn (fibre texture): 1.25 h

936 diagrams x 5 mn (non symmetric texture): 3.25 days



-70 microns x shift in χ
And texture !!



$$R_W (\%) = 9.23$$

$$R_B (\%) = 7.40$$

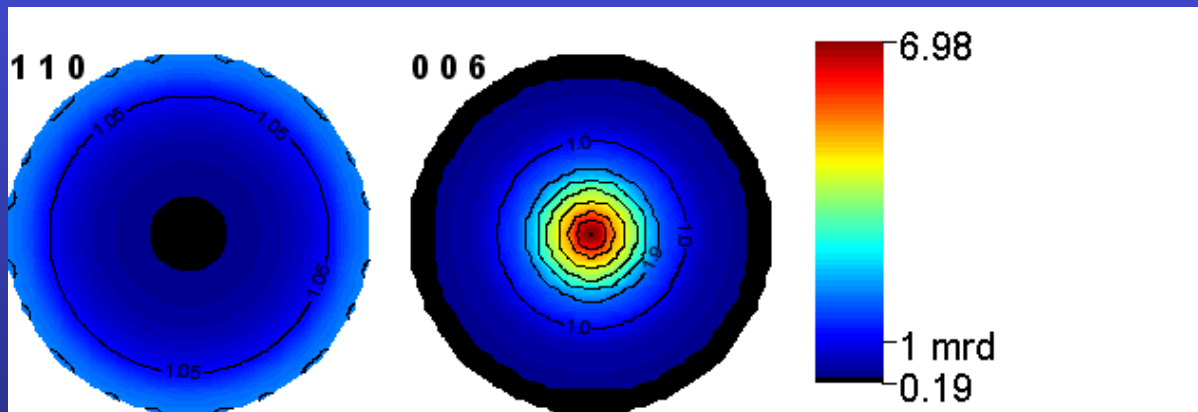
$$a = 4.75611(6) \text{ \AA}$$

$$c = 12.9806(1) \text{ \AA}$$

$$z_{Al} = 0.35266(3) \text{ \AA}$$

$$x_O = 0.6923(2) \text{ \AA}$$

Cyclic-fibre texture assumed



$$R_W (\%) = 7.14$$

$$R_B (\%) = 5.64$$

$$a = 4.75874(3) \text{ \AA}$$

$$c = 12.99373(7) \text{ \AA}$$

$$z_{Al} = 0.35225(2) \text{ \AA}$$

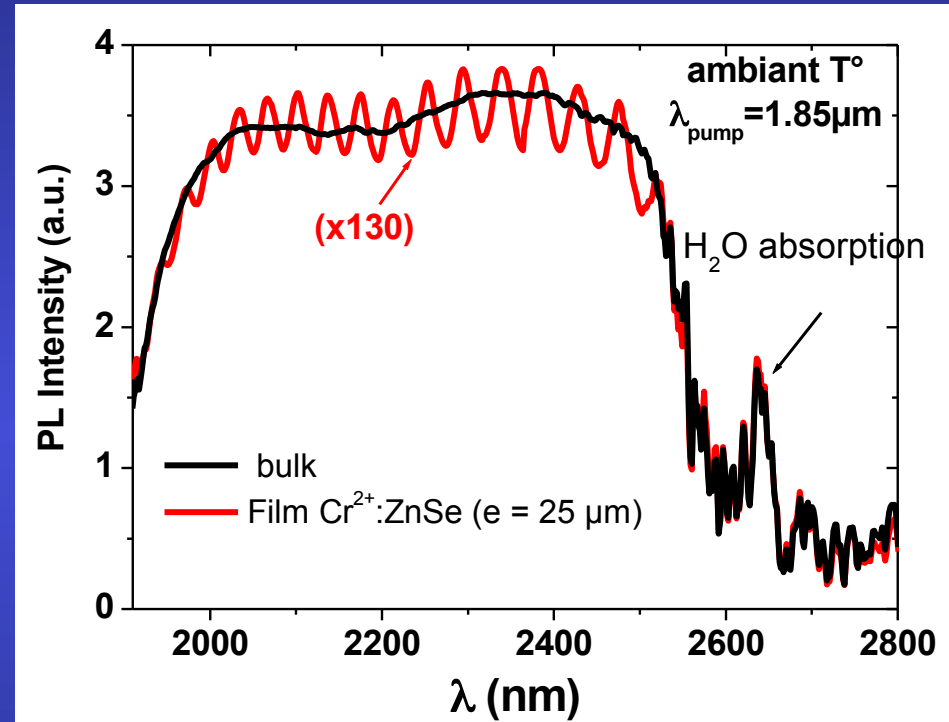
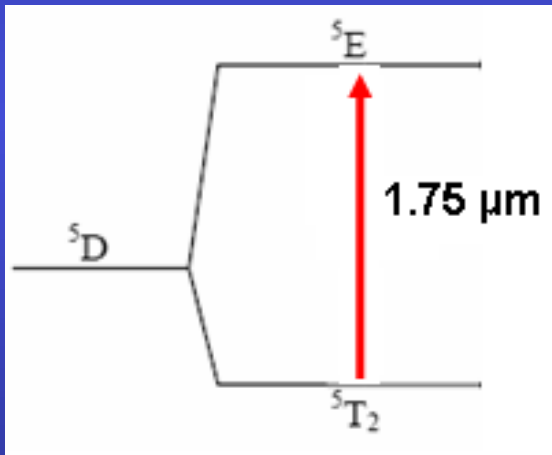
$$x_O = 0.6943(2) \text{ \AA}$$

ZnSe:Cr²⁺ films

N. Vivet, PhD

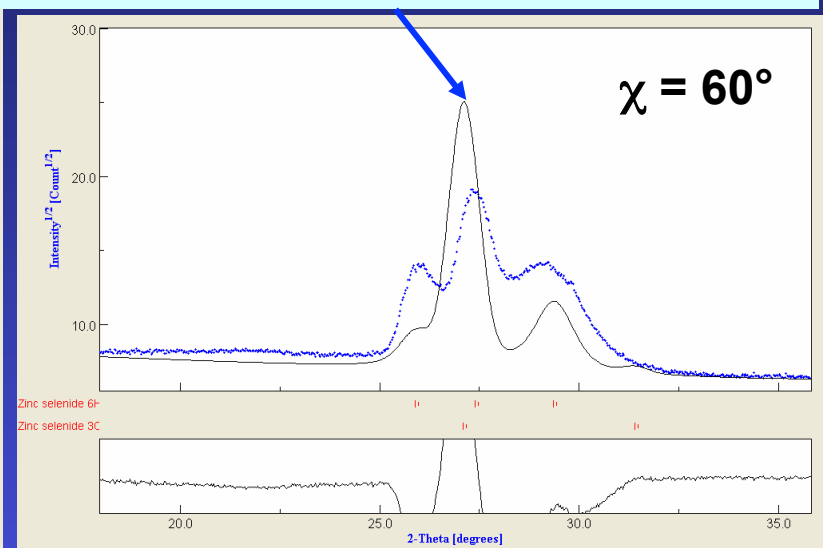
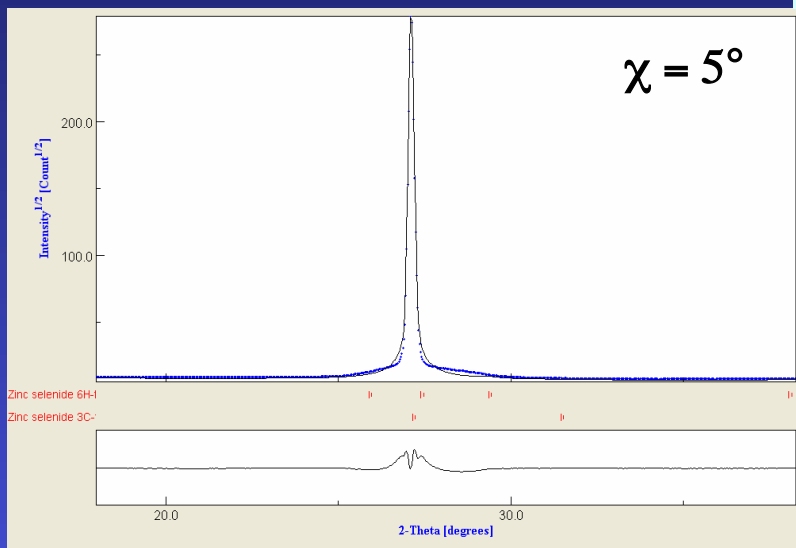
conditions:

- ◆ $20 \leq T_d \leq 385^\circ\text{C}$
- ◆ $P_{\text{RF}} = 50\text{-}200\text{W}$
- ◆ $P_{\text{Ar}} = 0.5\text{ Pa and } 2\text{ Pa}$
- ◆ $d = 7\text{ and } 10\text{ cm}$

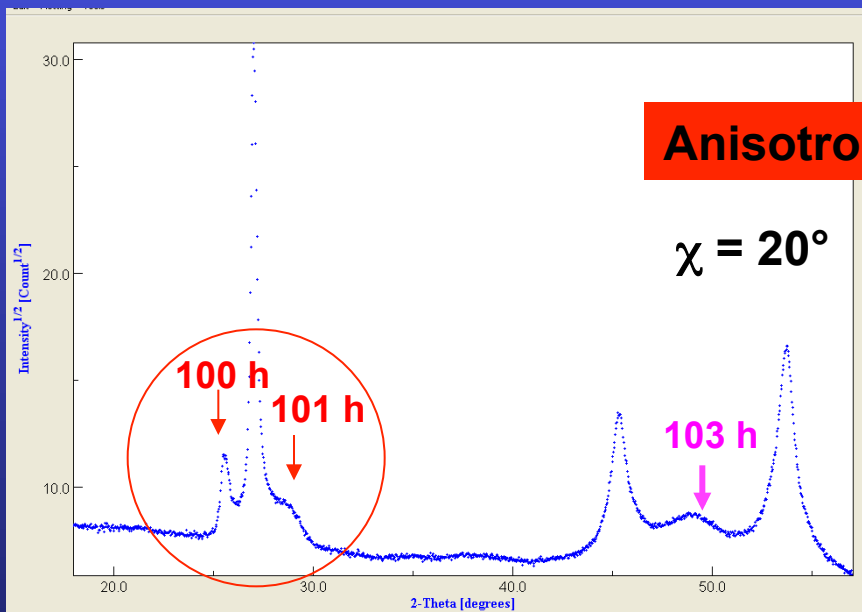


- ◆ Large emission band centred at 2200nm: $^5\text{E} \rightarrow ^5\text{T}_2$ transition (Cr²⁺)
- ◆ Single crystals and thin films: similar spectra

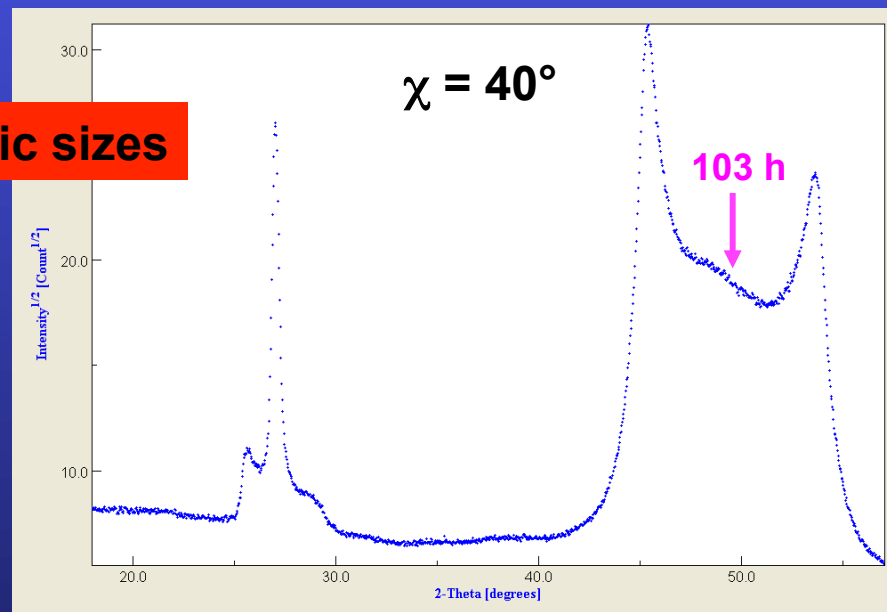
111 Peak shifts



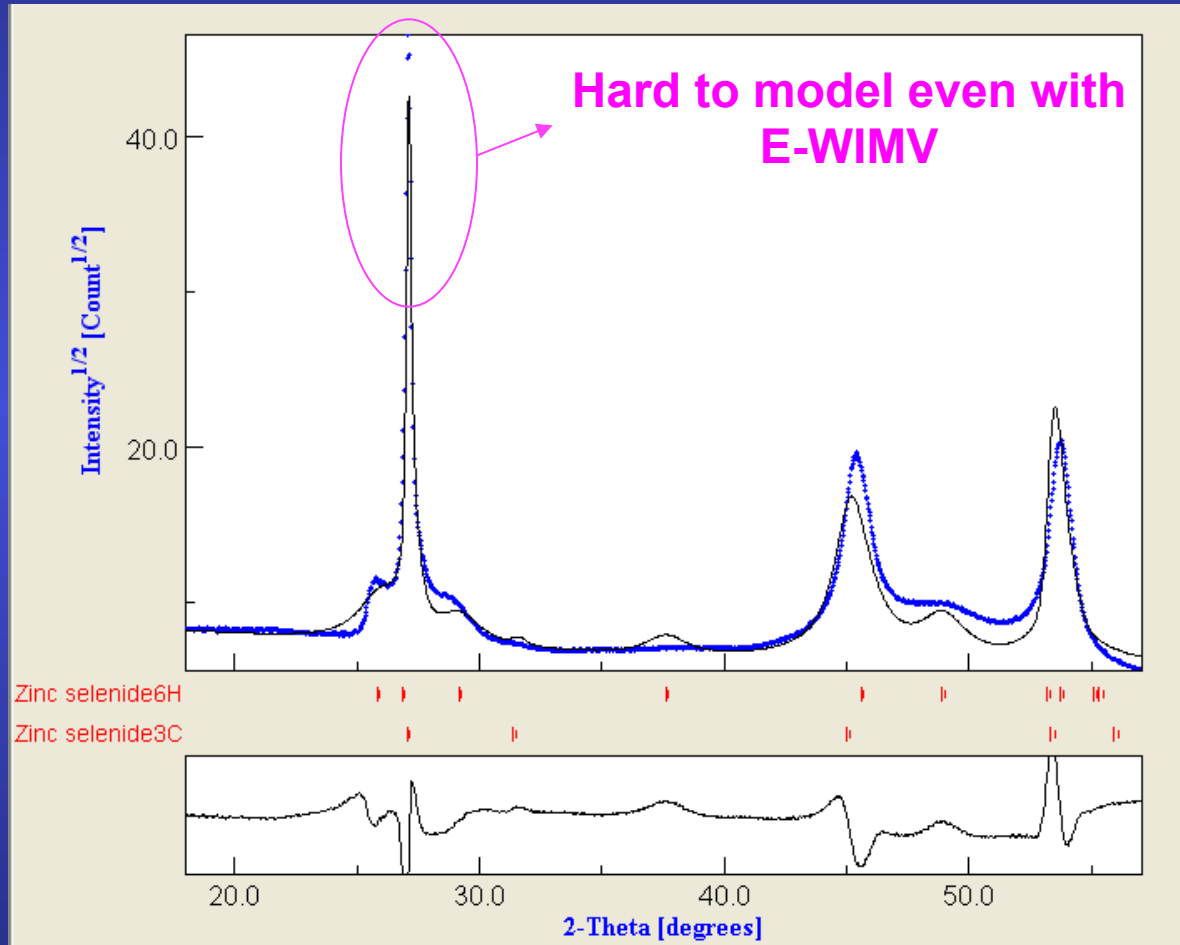
Residual stresses and/or stacking faults



Anisotropic sizes



Fibre Texture + 2 polytypes (6H and 3C) + anisotropic sizes + residual stresses and/or stacking faults + layering



Sum diagram: $\omega = 13.65^\circ$, $P_{RF} = 200W$

Independent measurements

Different wavelengths and rays

Reflectivity: thickness, roughness, electron density profiles

X-ray Fluorescence: composition

Spectroscopies: local structures (PDF, FTIR, Mossbauer ...), eventually anisotropic (P-EXAFS, ESR, Raman ...), Element profiles (SIMS, RBS ...) ...

Physical models: magnetisation, conductivity ...

Specular reflectivity: $\mathbf{q}=(0,0,z)$

- Fresnel:

$$R(\mathbf{q}) = \left| \frac{q_z - \sqrt{q_z^2 - q_c^2 + \frac{32i\pi^2\beta}{\lambda^2}}}{q_z + \sqrt{q_z^2 - q_c^2 + \frac{32i\pi^2\beta}{\lambda^2}}} \right|^2 \delta q_x \delta q_y$$

- matrix:

$$R^{flat} = \frac{r_{0,1}^2 + r_{1,2}^2 + 2r_{0,1}r_{1,2} \cos 2k_{z,1}h}{1 + r_{0,1}^2 r_{1,2}^2 + 2r_{0,1}r_{1,2} \cos 2k_{z,1}h}$$

- Born approximation:
Electron Density Profile

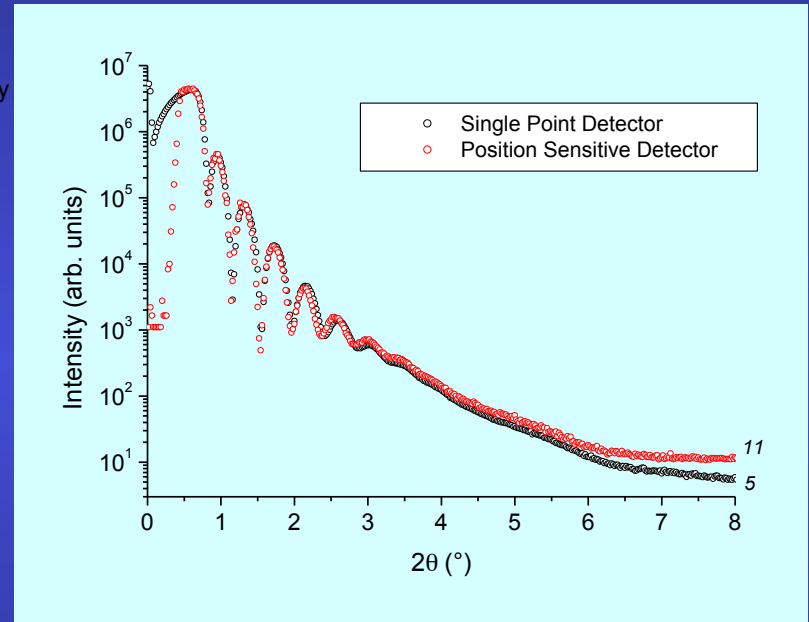
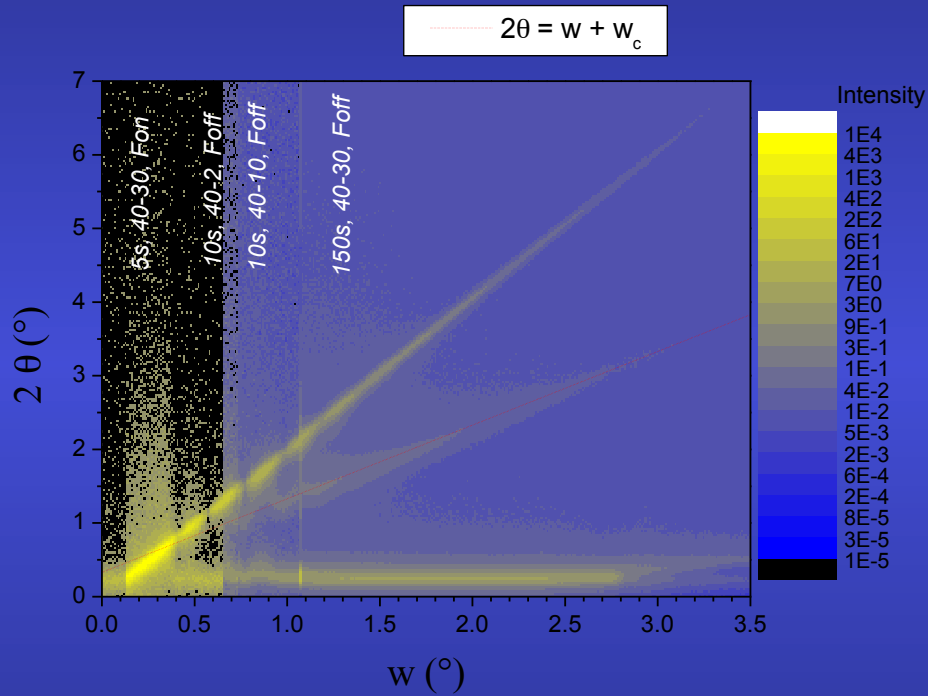
$$R(q_z) = r \cdot r^* = R_F(q_z) \left| \frac{1}{\rho_s} \int_{-\infty}^{+\infty} \frac{d\rho(z)}{dz} e^{iq_z z} dz \right|^2$$

- Roughness:

$$R^{rough}(q_z) = R(q_z) \exp(-q_{z,0} q_{z,1} \sigma^2) \quad \text{Low-angles (reflectivity)}$$

$$S_R = 1 - p \exp(-q) + p \exp\left(\frac{-q}{\sin \theta}\right) \quad \text{high-angle (Suortti)}$$

CPS scans



Useful for having bot specular and off-specular signals in one scan

Conclusions

- a) Texture affects phase ratio and structure determination
- b) Microstructure (crystallite size) affects texture (go to a)
- c) Stresses shift peaks then affects structure and texture determination
- d) Combined analysis may be a solution, unless you can destroy your sample or are not interested in macroscopic anisotropy ...
- e) If you think you can destroy it, perhaps think twice
- f) more information is always needed: local probes ...
- g) Combined Analysis (D. Chateigner Ed), Wiley-ISTE 2010